

Georgia State University

ScholarWorks @ Georgia State University

Biology Theses

Department of Biology

12-14-2021

Stressful Situations: Investigating Cell Death Pathways in Protozoal Parasite *Crithidia fasciculata*

Andrew Ho

Follow this and additional works at: https://scholarworks.gsu.edu/biology_theses

Recommended Citation

Ho, Andrew, "Stressful Situations: Investigating Cell Death Pathways in Protozoal Parasite *Crithidia fasciculata*." Thesis, Georgia State University, 2021.

doi: <https://doi.org/10.57709/26634859>

This Thesis is brought to you for free and open access by the Department of Biology at ScholarWorks @ Georgia State University. It has been accepted for inclusion in Biology Theses by an authorized administrator of ScholarWorks @ Georgia State University. For more information, please contact scholarworks@gsu.edu.

STRESSFUL SITUATIONS: INVESTIGATING CELL DEATH PATHWAYS IN
PROTOZOAL PARASITE *CRITHIDIA FASCICULATA*

by

ANDREW HO

Under the Direction of Paul N Ulrich, PhD

A Thesis Submitted in Partial Fulfillment of the Requirements for the Degree of

Master of Science

in the College of Arts and Sciences

Georgia State University

2021

ABSTRACT

Protozoa of the Class Kinetoplastida include clinically-relevant pathogens such as *Leishmania* and *Trypanosoma*. Although specific mechanisms or biological significance of programmed cell death (PCD) have yet to be established in these organisms, morphological and biochemical characteristics similar to mammalian PCD have been observed when triggered by various stressors. *Crithidia fasciculata* is a trypanosomatid that does not infect humans and is a model for studying cell death pathways. This study identifies orthologous proteins potentially involved in PCD in *C. fasciculata* and clinically-relevant species. Oxidative stress, thermal stress, rotenone, and starvation were used to induce PCD-like processes. Morphological and nuclear features were assessed by fluorescent microscopy with annexin-V, Hoechst, and propidium iodide. Oncosis-like and apoptosis-like features emerged following cellular stress. Additionally, monodansylcadaverine staining of vacuoles suggests autophagic processes occur. The results establish that cell death pathways in *C. fasciculata* share features with but are distinct from mammalian PCD.

INDEX WORDS: trypanosomatids, programmed cell death, apoptosis, autophagy, oncosis

Copyright by
Andrew Ho
2021

STRESSFUL SITUATIONS: INVESTIGATING CELL DEATH PATHWAYS IN
PROTOZOAL PARASITE *CRITHIDIA FASCICULATA*

by

ANDREW HO

Committee Chair: Paul Ulrich

Committee: Eric Gilbert

Liana Artinian

Electronic Version Approved:

Office of Graduate Services

College of Arts and Sciences

Georgia State University

December 2021

DEDICATION

For my mom, who never seems to run out of love. Con yêu mẹ nhiều lắm.

ACKNOWLEDGEMENTS

First and foremost, my greatest thank you is to Dr. Paul Ulrich, my mentor and PI of many years now. Without his dedication to advancing research opportunities in undergraduates, I would not have joined his molecular parasitology CURE as an undergraduate nor developed the profound interest in scientific research that I have today. He has been a pillar of inspiration, walking me through trivialities, both in the lab and out, and through every case of impostor syndrome. His dedication as a mentor has helped me become a better student, professional, teacher, scientist, and person.

I would also like to thank my thesis committee members, Dr. Eric Gilbert and Dr. Liana Artinian, for their expert opinion and advice in the development of my thesis project. Dr. Gilbert graciously allowed me into his lab during my undergraduate career and has been incredibly kind and supportive through my scientific career. Additionally, I would thank Dr. Jenny Yang for her brief time as a mentor and committee member.

Thank you to members of the Aneja Lab, Dr. Ritu Aneja, Shriya, and Chakri, for the experience, growth, and lessons during my first semester as a master's student.

Thank you to Dr. Mariya Campbell, my 4905 TA, research mentor, and professional inspiration during my undergraduate years. Her advice, nature, and lessons continue to push me to be a better scientist.

Thank you to the Department of Biology at Georgia State University, from the administrative office to the maintenance and sanitation crew to the NSC stockroom attendants, for fostering a productive home for research.

Thank you to Bill and Melinda Gates for initiating the Gates Millennium Scholarship (GMS) Program and the GMS program for granting me the opportunity to pursue higher education and research without worrying about financial support.

There are not enough words to thank my mother, family, and friends who have kept me sane, believed in me unconditionally, and supported me through the thick and thin. To Linda and Huong, my forever girls, thank you for unwavering friendship. To my Semester at Sea friends Kevin, Vienna, and Emily for their constant support. Finally, a thank you to Bryant, my best friend and #1 supporter, who has never stopped believing me, even when I don't believe in myself.

TABLE OF CONTENTS

ACKNOWLEDGEMENTS		V
LIST OF TABLES		X
LIST OF FIGURES		XI
LIST OF ABBREVIATIONS		XIV
1 INTRODUCTION		1
1.1 Trypanosomatids		1
<i>1.1.1 Trypanosomatids, a global burden</i>		<i>1</i>
<i>1.1.2 Trypanosomatid biology</i>		<i>4</i>
<i>1.1.3 Crithidia fasciculata as a model organism</i>		<i>5</i>
1.2 Regulated Cell death		6
<i>1.2.1 Autophagy</i>		<i>7</i>
<i>1.2.2 Necroptosis</i>		<i>8</i>
<i>1.2.3 Apoptosis</i>		<i>9</i>
<i>1.2.4 Ferroptosis</i>		<i>10</i>
<i>1.2.5 Paraptosis</i>		<i>11</i>
<i>1.2.6 Oxeiptosis</i>		<i>11</i>
<i>1.2.7 Pyroptosis</i>		<i>12</i>
<i>1.2.8 Parthanatos</i>		<i>12</i>
1.3 Cell Death in Trypanosomatids		13

2	RATIONALE	16
2.1	Hypothesis.....	16
2.2	Specific Aims	16
2.2.1	<i>Identify trypanosomatid homologs of potential proteins involved in cell death ..</i>	<i>16</i>
2.2.2	<i>Determine methods to induce and measure cell death in C. fasciculata</i>	<i>17</i>
2.2.3	<i>Characterize cellular morphology during cell death</i>	<i>17</i>
2.2.4	<i>Characterize nuclear changes during cell death.....</i>	<i>18</i>
3	METHODS	19
3.1	Reagents	19
3.2	Parasite culture.....	19
3.3	Bioinformatics analysis.....	20
3.4	Stress treatments	20
3.4.1	<i>Thermal stress.....</i>	<i>21</i>
3.4.2	<i>Starvation.....</i>	<i>21</i>
3.4.3	<i>Oxidative stress</i>	<i>21</i>
3.4.4	<i>Rotenone</i>	<i>22</i>
3.5	Staining and Microscopy	22
3.5.1	<i>Slide preparation</i>	<i>22</i>
3.5.2	<i>Staining parameters</i>	<i>22</i>
3.5.3	<i>Data collection.....</i>	<i>23</i>

3.6	Assessing morphology	23
3.7	DNA fragmentation assay	24
3.8	Statistical analysis	26
4	RESULTS	27
4.1	Identification of homologs associated with cell death processes.....	27
4.2	Heat stress induces cell death.....	43
4.3	Hydrogen peroxide induces cell death	45
4.4	Rotenone induces cell death	47
4.5	Starvation induces autophagic processes	49
4.6	Cell death processes involve intranuclear DNA fragmentation.....	51
4.7	Cellular stress induces nuclear morphology changes	53
4.8	Characterizing cell death by morphological changes	55
5	DISCUSSION.....	58
	REFERENCES.....	65
	APPENDICES.....	80
	Appendix A	80

LIST OF TABLES

Table 1. Genes involved in autophagy and identified trypanosomatid homologs	31
Table 2 Genes involved in necroptosis and their trypanosomatid homologs	34
Table 3 Genes involved in apoptosis and their trypanosomatid homologs	36
Table 4 Genes involved in parthanatos and their trypanosomatid homologs	39
Table 5 Genes involved in ferroptosis and their trypanosomatid homologs	40
Table 6 Genes involved in paraptosis and their trypanosomatid homologs	41
Table 7 Genes involved in pyroptosis and their trypanosomatid homologs	41
Table 8 Genes involved in oxceptosis and their trypanosomatid homologs	42
Table 9 Putative homologs identified in trypanosomatid genomes and associated functions defined in other systems.....	80

LIST OF FIGURES

- Figure 1 Trypanosomatids lack key molecules involved in necroptosis, apoptosis, paraptosis, pyroptosis, and oxeiptosis. They however have conserved genes involved in ferroptosis, autophagy, and parthanatos. Molecules involved in PCD pathways were categorized by function, members, or pathways. Presence of homologs identified by BLASTp of *C. fasciculata*, *L. major*, *T. brucei*, and *T. cruzi* genomes is indicated by highlighting. Red text indicates homology in 1-3 parasites. **Black text** indicates homology in all 4 species. Grey text indicates homology was not identified in typanosomatid genome... 28
- Figure 2 Quantification of cells thermally stressed identify standard temperatures to induce necrosis. Cells were treated at a range of temperatures for 1 hour and stained with PI. Ppercentage of PI positive cells in a sample was determined. Data is presented as arithmetic mean + S.E.M. $p \leq 0.05$ (n=3, one-way ANOVA $p < 0.05$, unpaired T-test significance $p < 0.05$) 43
- Figure 3 Thermal stress causes morphological changes and induces cell death. Representative slides from samples quantified in Figure 2 illustrating cellular response to thermal stress as characterized by uptake of propidium iodide. Scale bars represent 10 μm 44
- Figure 4 Quantification of cells oxidatively stressed present a dose-dependent response. 45
- Figure 5 Hydrogen peroxide causes morphological changes and induces cell death. Representative slides from samples quantified in figure 4 illustrating cellular response to oxidative stress as characterized by uptake of propidium iodide. Scale bars represent 10 μm 46
- Figure 6 Quantification of cells treated with rotenone present a dose-dependent response. Cells were treated at 2 different doses of rotenone for 1 day and stained with PI and percentage

of PI positive cells in a sample was determined. Data is presented as arithmetic mean + S.E.M. (n=3, one-way ANOVA significance $p < 0.05$, unpaired T-test significance $p < 0.05$).....	47
Figure 7 Rotenone causes morphological changes and induces cell death. Representative slides from samples quantified in Figure 6 illustrating cellular response to rotenone treatment as characterized by uptake of propidium iodide. Scale bars represent 10 μm	48
Figure 8 Serum depletion and nutrient starvation induces autophagic vacuole formation. Cells were either grown in regular media without FBS for 1 hour or in PBS for 7 days and stained with MDC. Arrows highlight clusters of autophagic vacuoles observed in single cells (enlarged in insets).....	50
Figure 9 Variable changes in genomic pattern occur in response to cellular stress. Cells were stressed with 10 μM rotenone (1 day), 44°C (1 day), serum starvation (3 days), or 100 mM hydrogen peroxide in accordance to established conditions. In an effort to mimic necrotic patterns as seen in mammalian systems, cells were also treated with 0.01% Triton X-100 (4 hours) and heat shock at 55°C (15 minutes). Ten micrograms of gDNA was separated on a 1% agarose gel.	52
Figure 10 Cell death can be characterized by chromatin condensation. Cells were either treated with 2 μM rotenone or at 44°C for 1 day and stained with Hoechst33342 to visualize changes in DNA and PI to confirm cell demise. While Hoechst 33342 is permeant to the nuclear and cell membrane, it only dimly stains cells at baseline (control group) but increases in brightness in cells undergoing cell death. Arrows highlight an example of a PI-positive and Hoechst 33342-positive cell in the rotenone treated group.	54

Figure 11 Distinct patterns of nuclear morphology and cell shape are observed in dying cells.

Parasites were thermally stressed for 1 hour prior to staining with annexin-V and PI.

Patterns of morphological changes were captured and categorized by (B) baseline, non-stressed, (C) nuclear fragmentation, (D) “teardropping” and ballooning, (E) DNA condensation, (F) release of intracellular contents, (G) dissolution of the nuclear bodies, and (H) membrane rupture. 57

Figure 12 *Crithidia fasciculata*’s morphological profile of cell death is evidently unique from

currently described patterns. Literature review was conducted to determine known

characteristics of the PCD pathways of interest. Negative (-), red boxes indicate lack of that particular feature. Positive (+), green boxes indicate presence of that particular

feature. Question marks (?) indicate that current understandings of this pathway have not

reviewed these features. In this study, multiple features were not investigated and

therefore not determined (nd). 64

LIST OF ABBREVIATIONS

CL	cutaneous leishmaniasis
VL	visceral leishmaniasis
HAT	human African trypanosomiasis
kDNA	kinetoplast DNA
spp.	species
PCD	programmed cell death
RCD	regulated cell death
ACD	autophagic cell death
ATG	autophagy related genes
ROS	reactive oxygen species
GSH	glutathione
GPX4	glutathione peroxidase 4
NAD ⁺	nicotinamide adenine dinucleotide
ATP	adenosine tri-phosphate
$\Delta\Psi_m$	mitochondrial membrane potential
MDC	monodansylcadaverine
PI	propidium iodide
BHI	brain-heart infusion
FBS	fetal bovine serum
PLL	poly-l-lysine
RT	room temperature
PBS	phosphate-buffered saline

H₂O₂ hydrogen peroxide

DMSO dimethyl sulfoxide

DNA deoxyribonucleic acid

gDNA genomic DNA

bp base pairs

PC phase contrast

MTP mitochondrial transition pore

Ca²⁺ calcium ions

Mg²⁺ magnesium ions

TMBIM transmembrane Bax inhibitor-1 motif

nd not determined

ETC electron transport chain

1 INTRODUCTION

1.1 Trypanosomatids

1.1.1 *Trypanosomatids, a global burden*

The Family Trypanosomatidae is comprised of exclusively parasitic species that frequently infect insects (1). Although the majority of the species are monoxenous and infect only a single host species during their life-cycles, some trypanosomatids are dixenous and have secondary hosts including mammals and plants (2). Arguably the most relevant dixenous trypanosomatid species for human health are pathogens belonging to the genera *Leishmania* and *Trypanosoma*.

Leishmania spp. are responsible for leishmaniasis and are widespread among tropical and subtropical regions. They are found in nearly 100 countries in Africa, Asia, Europe, North America, and South America (3). Leishmaniasis is considered by the World Health Organization (WHO) to be one of seven most important tropical diseases, affecting more than 12 million people, and placing more than 350 million at risk. These parasites are transmitted via bites of phlebotomine sand flies and cause various clinical forms of the disease in humans (4,5). Depending on the species of infection, leishmaniasis can range from mild dermatologic discomfort to fatality (6). For example, *L. major* and *L. mexicana* cause cutaneous leishmaniasis (CL) while *L. donovani* and *L. infantum* species can cause visceral leishmaniasis (VL) (7). Cutaneous leishmaniasis is the most common form of the disease and affects 600,000 to 1 million people a year (8). Although CL does not lead to death, it is characterized by localized ulcers that oftentimes result in scarring and social stigma (9). Visceral leishmaniasis is the most severe clinical manifestation, resulting in more than 40,000 deaths annually (10). It is

characterized by hepatomegaly, splenomegaly, lymphadenopathy, anemia, leukopenia, thrombocytopenia, fever, and other systemic symptoms (11). Management of the disease depends on species and clinical presentation. Treatment of CL can include topical, oral, systemic, therapy, photo, and laser therapy. There, is however, no established regimen, and evidence of the effectiveness of these therapies are limited and patient-specific (12,13). Treatment of VL involves antiparasitic and antifungal drugs. Drug toxicities, cost, and drug resistance are notable limitations (14-16).

Trypanosoma cruzi, the etiological agent for American trypanosomiasis (Chagas' disease), is endemic to about 20 Latin American countries (17). Transmission of the parasite is most commonly via bite of the vector "kissing bugs". It is also spread by blood transfusion and ingestion of contaminated foods (18). Collectively, the disease affects 6 to 8 million people worldwide, puts up to 100 million at risk, and is responsible for approximately 50,000 deaths annually (19,20). Trypanosomiasis is characterized by two successive phases: the high parasitemia-associated acute phase that clinically presents asymptotically or with anorexia and fever, and the chronic phase that manifests with progressive digestive, cardiac, and neurologic complaints (21). Acute phase disease can be cured in 50-80% of patients with effective early action (22). Unlike leishmaniasis, trypanosomiasis that progresses to the chronic phase is asymptomatic for the majority of cases (23). Of these cases, up to 40% develop digestive, cardiac, or neurologic issues after 10 to 30 years (24). Severe cases of chronic phase disease can involve advanced chronic heart disease and cardiomyopathy in which the only treatment course is heart transplantation (25). Treatment of trypanosomiasis involves antiparasitic drug therapy for acute phase disease and symptomatic care for chronic phase

disease (26). Available antiparasitic drugs pose serious side effects and frequently are discontinued during the treatment course (21,27).

Trypanosoma brucei, the etiological agent for human African trypanosomiasis (HAT, or sleeping sickness), is endemic to about 35 sub-Saharan African countries and is transmitted via the bite of tsetse flies (28). Approximately 11,000 people are infected with *T. brucei* with an additional 70 million individuals at risk and, as of 2016, about 2,000 new cases annually (29-31). Similar to Chagas' disease, HAT evolves through two clinically distinct phases. The first stage begins after a bite that is often accompanied by localized dermatologic symptoms and is followed by intermittent fevers and a combination of lymphatic, endocrine, hepatic, splenic, and cardiac symptoms as parasitemia develops (32,33). The second stage ensues after a few weeks post-infection, when the parasite crosses the blood-brain barrier and invades the central nervous system. This stage is characterized by encephalopathy, headaches, altered mental status and eventually results in a somnolent mental state (33,34). If untreated or mismanaged, the infection is eventually fatal (35). The first stage of HAT is managed well with pharmacologic therapy, albeit with mild toxicity and side effects (32,36). The only treatment of the second stage of infection is an intravenous drug that is considered painful and highly toxic with risk of serious complications and 5-9% post-treatment fatalities (32,36).

Leishmaniasis, trypanosomiasis, and African sleeping sickness are all classified as neglected tropical diseases given the paucity of financial support despite the overwhelming public health burden and poor health outcomes faced by underserved, low-income, and rural regions (11). Despite extensive research efforts globally to better understand trypanosome biology, the arsenal of tools for diagnostics and treatment remains unfortunately limited. Critical research advances including improved *in vitro* cultivation, whole-genome sequencing, and tools

for genetic modification within the last few decades are being leveraged to better study parasite and vector biology. Additional efforts towards expanding translational and pre-clinical applications continue to be warranted (37-40).

1.1.2 Trypanosomatid biology

Trypanosomatids are organisms with unique organelles and physiology. They use a single anterior flagellum to propel themselves in corkscrew-like motions. They possess a single, large mitochondrion that has different morphologies based on life stages (41). For example, *T. brucei* can have mitochondrion that feature abundant cristae and interconnecting networks of branches that undergo fission and fusion processes. On the other hand, the mitochondrion can be much simpler with unbranched tubules and few cristae (42). The complexity of the organelle is directly related to cellular function. The insect forms of trypanosomatids possess enlarged cristae and elaborate mitochondrial networks, reflecting the necessity for high aerobic respiration rates (43). In contrast, blood stream *T. brucei* derive energy from glucose in the host blood and produce ATP by substrate level phosphorylation. As such, the mitochondrion is simpler (44,45).

Belonging to the Class Kinetoplastida, trypanosomatids are all characterized by kinetoplasts, a disk shaped “mitochondrial nucleoid” located in the mitochondrion at the base of flagellum that is essentially a network of genetic material termed kinetoplast-DNA (kDNA). The kDNA network is comprised of a few dozen maxicircles and thousands of minicircles, both of which are interlocking circles of DNA of about 20 kb and 1 kb, respectively (46,47). These encode important mitochondrial genes, including ribosomal RNA and respiratory complex subunits (46). Furthermore, replication of the kDNA is an essential part of the cell cycle and is initiated in G1, prior to nuclear replication (48).

During each phase of their life cycle, these parasites differentiate to various morphological forms, adapting to their environment. For example, while in the human host, *T. brucei* exhibit slender forms with special coats that evade the host immune response. They then differentiate to stumpy forms that promote transmission to their insect hosts upon bloodmeal of the mammalian host. Once the parasites have entered the insect gut, they again change into another form with another distinctive cellular coating that allows for adherence. Finally, they migrate to the salivary glands and proliferate and develop the original special coating in preparation for transmission into the human host (49,50). Each life cycle stage is also characterized by the position of the kinetoplast, which shifts to a specific region in the cell depending on the stage. Although the specific reason for the positioning of the kinetoplast is unknown, it is understood that it is required for the progression of cell division, as it is synchronous with nuclear replication (50).

1.1.3 Crithidia fasciculata as a model organism

Crithidia are monoxenous trypanosomatids that infect a broad range of insects and are non-pathogenic to humans. *Crithidia fasciculata* infect mosquitoes and be found on flowers and fruit, or in water after being voided with feces by infected insects (51). The parasite has two life stages: the amastigote and choanomastigote (52). Amastigotes are non-motile, round cells with a short flagellum and infect mosquitoes when the insects feed on nectar (52). *C. fasciculata* adheres to the mosquito gut and differentiates into choanimastigotes. Choanimastigotes are stumpy, free-swimming cells with long flagellum. After colonizing the mosquito gut, choanimastigotes differentiate to amastigotes.

Choanimastigotes are further divided into two developmental forms, the non-motile haptomonad and the swimming nectomonad. Haptomonads are rounder and have shortened

flagellum used to adhere to the mosquito hindgut and rectal papillae (53). These adherent cells undergo cell division and form large clusters called “rosettes”. Eventually, cells break free from the rosette and develop into nectomonads (54). Brooker (1971) discovered that both nectomonad and haptomonad forms of *C. fasciculata* can be cultivated *in vitro* and that haptomonads attach to artificial surfaces such as cellulose esters and polystyrene (55).

Crithidia fasciculata has been investigated as a model organism for human pathogenic kinetoplastids because the species is not a threat to human health, is easily cultivated in scalable quantities, and is genetically tractable (56). Though the release of the *C. fasciculata* genome has been published (Stephen Beverly, Washington University School of Medicine), the key molecular players in various biological functions remain largely unexplored (57). Genetically, *L. major*, *T. brucei*, *T. cruzi*, and *C. fasciculata* share 6,000 orthologous genes (38).

Physiologically, these parasites share many traits including the flagellar attachment and rosette formation of haptomonads, kinetoplast biology and mechanisms, and mitochondrial architecture, biogenesis, and biology (54,58,59).

1.2 Regulated Cell death

Programmed or regulated cell death (PCD, RCD, cell suicide) are cellular pathways defined by a series of molecular events that lead to organized cell demise. The scientific discovery of apoptosis, the first defined pathway, marked the beginning of the era dedicated to investigation of RCD. Schweichel *et al.* (60) classified RCD into three distinct categories based on morphological profiles. The first was apoptosis, which was characterized by shrinkage of the cell, formation of apoptotic bodies, membrane blebbing, chromatin digestion, and DNA fragmentation. The second was autophagy-related cell death, characterized by autophagic vacuolization of cytosol and organelles. The third was necrosis, characterized by membrane

rupture, swelling of the cell, and swelling of organelles. Since then, there has been a plethora of scientific work performed to better understand these cell death pathways as well as the discovery of multiple other unique pathways. This section provides a brief overview of various PCD pathways, associated morphological characteristics, and molecular machinery of these.

1.2.1 Autophagy

Autophagy is a regulated cell process that provides nutrients to maintain vital functions in response to stressful conditions such as nutrient deprivation and hypoxia (61). Although autophagy has homeostatic functionality, it is also recognized as a regulated cell death pathway. Initially, autophagic cell death (ACD) described cells that showed evidence of autophagy during cell death however recently ACD implicates the mechanistic decision-making that leads to cell death (62,63). Autophagy's association with PCD is however constantly questioned, particularly its role as a true causative factor, whether it is an effect on PCD, or if it solely just a survival mechanism during PCD (64). It is also complicated by evidence that autophagy can activate other cell death pathways such as apoptosis and necroptosis.

Autophagic cell death, death that is dependent of autophagic machinery and without involvement of other cell death processes, is characterized as sequestration of the cytoplasm and its contents by structures termed autophagosomes that become fused with and degraded by lysosomes (65,66). Morphologically, ACD is characterized uniquely by accumulation of autophagosomes and autophagic vacuolization (67). It can also share morphological characteristics with other RCD such as plasma membrane rupture, minor changes to the nucleus and chromatin, and enlargement of other organelles such as the mitochondria (67).

Autophagy begins with formation of autophagosomes and proceeds ultimately to fusion of autophagosomes with lysosomal compartments. This is a complex process and involves over

30, autophagy-related genes (ATG) (68). The TORC1 complex (TORC1-Atg13) inhibits autophagic induction and is inactivated by starvation (and other stressors). The Atg1/ULK complex (Atg1-Atg11-Atg13-Atg17-Atg29-Atg31) regulates induction of autophagosome formation. The Atg9 system (Atg-2-Atg9-Atg18) assists in membrane delivery of the expanding autophagosome. The PtdIns3K complex (Vps15-Vps34-Vps30-Atg14) is involved in vesicle nucleation. The Atg12 (Atg-7-Atg10-Atg12-Atg16) and Atg8 (Atg3-Atg3-Atg7-Atg8) systems are involved in autophagosome expansion. Following completion of the autophagosome, the vesicle will dock and fuse with autolysosomes and become degraded (69-72).

1.2.2 Necroptosis

Necroptosis is defined as a regulated process of necrosis and was initially described as a process that shares both apoptotic and necrotic features alongside inhibition of classical apoptotic pathways (73). Morphologically, cells undergoing necroptosis largely mimic necrosis, characterized by cellular swelling, chromatin condensation followed by nuclear decondensation, rupturing of the plasma membrane, and release of intracellular contents (74-77).

Necroptosis is initiated by signaling from ligation of death molecules to death receptors (FAS/FASL, TNF1/TNF2, TRAILR1/TRALR2). Complex I (TRADD-TRAF2/TRAF5-RIP1-cIAPs-NEMO-CLYD) is a signaling complex and cellular checkpoint that is formed thereafter and can either result in nuclear factor- κ B (NF- κ B) pathway activation and cell survival, or in formation of the death-inducing signaling complex (DISC, or complex II) that promotes cell death (78,79). When caspase 8 is uninhibited, the cell executes apoptotic cell death (80). When caspase 8 is inhibited, however, cIAP1 ubiquitinates RIPK1, causing RIPK1 and RIPK3 to form complex II (*i.e.* necrosome) (81). Complex II leads to the phosphorylation of MLKL, a key step in the execution of necroptosis (82,83). The execution of necroptosis is reported to occur in

multiple ways including events like production of ROS, overactivation of the DNA repair and transcription regulatory PARP1, release of the apoptosis-inducing factor (AIF) from the mitochondria to the nucleus to initiate DNA fragmentation, promotion of pore formation, and PGAM5-induced mitochondrial fragmentation (84-88).

1.2.3 Apoptosis

Apoptosis is considered the most understood PCD pathway and is evolutionarily conserved in metazoans. Apoptosis relies on activation of caspases and proteins that degrade organelles in preparation for controlled cell death (89). Morphological hallmarks of apoptosis are membrane blebbing, cell shrinkage, DNA condensation, DNA fragmentation, and formation of non-lytic apoptotic bodies. This death process is notably non-inflammatory and thus does not damage or stress surrounding cells (90). Intrinsic and extrinsic stimuli can induce apoptosis, and the distinct pathways responsible for these are thus termed the intrinsic pathway and the extrinsic pathway (91,92). Though these pathways differ in induction, they share the same execution phase.

The intrinsic pathway is mediated by the family of Bcl proteins including the pro-apoptotic Bax proteins and the anti-apoptotic Bcl-2 proteins (93). The pro-apoptotic pore-forming proteins BAX and BAK are mitochondrial membrane proteins in the outer membrane and cause outer membrane permeabilization (MOMP) when activated by pro-apoptotic BH3-only proteins (BID, PUMA, BAD, BIK, BIM, BMF, Hrk, and Noxa) (94,95). MOMP releases apoptosis-inducing proteins from the inner mitochondrial membrane (91). These proteins, such as cytochrome c, activate caspases and inhibit caspase-inhibitor proteins. Of particular importance is activation of caspase 9 and the executionary caspases 3, 6, and 7 (96,97). Because apoptosis results in death of cells, there are multiple anti-apoptotic proteins that keep the

pathway tightly regulated. Some of these proteins include BCL-2 proteins (BCL-2, BCL-X_L, BCL-W, BFL1, and MCL1) which inhibit the release of cytochrome c (94). These proteins bind to BIM and BID, preventing BAX and BAK activation.

The extrinsic pathway involves death receptors that interact with specific adaptor proteins. These death receptors are characterized by a conserved domain termed the “death domain” and includes members of the tumor necrosis factor (TNF) family in addition to other ligands and receptors such as Apo3L/DR3, Apo2L/DR4, FasL/FasR, and TNF α /TNFR1 (98). In general, recruitment of FADD, TRADD, and RIP allows for association with procaspase-8, forming a complex called the DISC (98,99). At this point, apoptosis is executed with caspase-8 and caspase-8 cleaving the executionary caspase-3 (100). Some inhibitors for this pathway also exist, including c-FLIP and Toso (101,102).

1.2.4 Ferroptosis

First proposed in 2012, ferroptosis is a non-apoptotic form of PCD directly associated with iron-dependence and abundance of lipid ROS (103). Notably, ferroptosis does not share morphological hallmarks of necrosis (cellular swelling and rupture of the plasma membrane) or apoptosis (cellular shrinkage, chromatin condensation, or apoptotic body formation) (103,104). Instead, cells undergoing ferroptosis exhibit mitochondrial shrinkage, reduction or dissolution of mitochondrial cristae, and increased membrane density (103,105). In mammalian cells, ferroptosis occurs when glutathione (GSH) is depleted, resulting in decreased glutathione peroxidase 4 (GPX4) activity and accumulation of lipid peroxides (105). As a consequence, iron-dependent oxidation of lipids occurs and excessive ROS is produced (105). Multiple molecular systems of ferroptosis have been implicated (106). For example, the Xc⁻ system (SLC7A11-SLC3A2), an amino acid anti-transporter localized to plasma membrane, has antioxidative roles

(107). Cysteine, an amino acid regulated by this system, plays a role in GSH synthesis.

Therefore, when system Xc- is inhibited, GSH cannot reduce ROS via glutathione peroxidases, leading to accumulation of lipid ROS. Additionally, any suppression of GPX4, such as with the inducer of ferroptosis RSL3, results in accumulation of lipid ROS. Excessive ferrous iron can also lead to initiation of ferroptosis due to lipid-peroxidation and production of ROS (108).

There have been connections with other cellular processes as well such as autophagy, the mevalonate pathway, and sulphur-transfer pathways (107-109).

1.2.5 Paraptosis

Paraptosis, first described in 2000, is another non-apoptotic pathway (112). Paraptosis lacks caspase involvement, mitochondrial and endoplasmic reticulum (ER) swelling, and significant cytoplasmic vacuolization (110). Unlike apoptosis, paraptotic cells do not exhibit nuclear fragmentation or membrane blebbing (111). The molecular mechanism of paraptosis is unknown. Inhibition of gene expression with actinomycin D and cycloheximide prevent paraptosis (110).

1.2.6 Oxeiptosis

Oxeiptosis is an RCD program triggered exclusively by elevated ROS. Accumulation of ROS can cause oxidative damage to the intracellular ROS sensor KEAP1, leading to conformational change of the protein and impairing its ability to bind to the transcription factor NRF2. NRF2 then translocates to the nucleus to express cytoprotective genes to protect the cell anti-oxidatively (112,113). Apparently, when ROS levels are excessive, oxeiptosis is triggered and KEAP1 is displaced from the mitochondria, disassociating from the protein PGAM5. PGAM5 internalizes into the mitochondrion from the outer membrane and dephosphorylates AIFM1 to trigger caspase-independent cell death (114,115). Morphological details of cells

undergoing oxeiptosis are largely unexplored. It was identified as a unique cell death process given it is caspase-independent, non-inflammatory, RIPK3-independent, ROS-induced, and KEAP1-PGAM5-AIFM1 dependent (115).

1.2.7 Pyroptosis

Pyroptosis is a lytic inflammatory pathway (the inflammasome pathway) that occurs in immune cells in the innate immune system and is triggered upon infection by intracellular pathogens. It has been associated with regulated lysis of cells infected by viruses, bacteria, fungus, and protozoans (118). Although initially thought to be a form of apoptosis given its shared caspase involvement, DNA fragmentation, and nuclear condensation, pyroptosis is now recognized as having a unique morphologic profile centered on its pro-inflammatory outcome following cellular swelling and plasma membrane rupture (116-119). The process is induced by caspase-1, caspase-4, caspase-5, and caspase-11 (120). Assembly of the inflammasome complex occurs in response to pathogen-associated molecular patterns (PAMPs) and exogenous pathogens and endogenous damage-associated molecular patterns (DAMPs) and endogenous damage (121,122). Sensors for assembly induction include NLRP1, NLRp3, NLRC4, AIM2, and pyrin. Once the sensors are activated by PAMPs and DAMPs, the inflammasome complex (CARD-procaspase-1-NLRP3-PYD) forms, caspase-1 become active and cleaves the executioner gasdermin D (GSDMD), ultimately leading to cell membrane perforation (120,123,124).

1.2.8 Parthanatos

Parthanatos, a pathway identified only a decade ago, is based on genomic stress and the protein poly(ADP-ribose) polymerase-1 (PARP-1), a nuclear enzyme that repairs DNA and is involved in transcription (125). Parthanatos shares similar morphological features with apoptosis and necrosis (nuclear disruption, chromatin condensation, cell lysis, and DNA fragmentation)

(126). PARP-1 associates with poly(ADP-ribose) (PAR), a molecule that binds to target proteins to regulate processes such as DNA repair and transcription (126). When there is DNA damage, PARP-1 becomes active, leading to ADP-ribosylation of transcription factors, single-strand break repair factors, and base-excision repair factors (127). When excess genotoxic stress is apparent in the cell, PARP-1 becomes overexpressed and produces excessive PAR (125). The execution of cell death is thought to be caused by depletion of NAD^+ and ATP, as overactivation of PARP-1 has resulted in fatal energy loss (128). The overactivation of PARP-1 has also been linked to release of AIF from the mitochondria and its associated effects on nuclear apoptosis, as mentioned previously in necroptotic pathways (87).

1.3 Cell Death in Trypanosomatids

Programmed cell death in trypanosomatids was first observed in 1995 in *T. cruzi* during *in vitro* differentiation and was characterized by cytoplasmic changes, nuclear changes, and DNA fragmentation (129). Since then, various features of PCD have been observed in numerous trypanosomatid species. Recently, Menna-Barreto reviewed the current evidence of cell death pathways in pathogenic trypanosomatids, collectively reiterating that trypanosomatids exhibit apoptotic-like phenotypes, undergo autophagy, and exhibit necrosis and emphasizing the following questions: (1) what is the biological relevance of PCD in unicellular protozoans? and (2) what molecular machinery is involved in PCD pathways (130)? There has been evidence that *Trypanosoma* spp. and *Leishmania* spp. exhibit numerous hallmarks of apoptosis and oncosis. These characteristics include DNA fragmentation (129), phosphatidylserine externalization (131), loss of mitochondrial potential ($\Delta\Psi_m$) (132), cytochrome c release (133), chromatin condensation (134), and plasma membrane disruption (135). Additionally, evidence supports the biochemical presence of autophagy as characterized by Atg participation, formation of

phagophores and autophagosomes, and the activity of lysosomes (136). Furthermore, many stress conditions well understood in other models have also prompted cell death responses. These include drug treatment, thermal stress, oxidative stress, starvation, and hypoxia (129,131,137-141). Trypanosomatids also exhibit apoptosis-like features during parasite differentiation (129).

Little is known about the responsible molecular mechanisms responsible for PCD in trypanosomatids as deep genome analysis has not produced homologs of important apoptosis-involved molecules. Various potential players have been investigated. In 1998, Welburn and Murphy identified the trypanosome homologs for prohibitin, a transcriptional modulator, and activated protein kinase C (RACK), a regulator of cell cycle progression (142). They emphasized the upregulation of these genes in *T. brucei* undergoing concanavalin A-induced cell death. It has been proposed that this correlation between RACK, prohibitin, and the apoptotic phenotype is evidence for the convergence between mammalian and parasite pathways (142). Zangger *et al.* demonstrated that *Leishmania* parasites exhibit DNA fragmentation, a late-stage event of apoptosis, and correlated this with presence of internucleosomal nuclease activity by two specific, unidentified nucleases (143). They additionally reported that DNA fragmentation was independent of typical cofactors of mammalian nucleases (Ca^{2+} or Mg^{2+}) and caspase activity. It is known that trypanosomatids lack caspase-activity. Metacaspases, cysteine proteases that are analogous to caspases, induce PCD in plants and fungi (144). Although trypanosomatids metacaspases share the same folding pattern to mammalian caspases, there is no evidence to date that these proteins are involved in PCD (132). In accordance with this, there are multiple studies demonstrating that the parasites die in a metacaspase-independent manner with association with other proteins such as endonuclease G (145), inosine 5' monophosphate dehydrogenase (146), and cysteine proteases CPA and CPB (143).

Similar to mammalian models, it is apparent the trypanosomatids mitochondrion plays an important role in cell death (147). Conditions such as H₂O₂, starvation, heat stress, ER stress, and antiparasitic drugs have been shown to induce cell death across various trypanosomatids and additionally results in loss in $\Delta\Psi_m$ (132,134,148,149). This is further supported by evidence of induction of apoptosis-like death with Ca²⁺ imbalance and chemical inducers of ROS production (148). Smirlis *et al.* reviewed two present suggested pathways that describe the interplay of Ca²⁺, ROS, and $\Delta\Psi_m$ (150). The first pathway involves cytosolic Ca²⁺ elevation, which enters the mitochondria and disrupts the $\Delta\Psi_m$ and ROS production. Excessive mitochondrial Ca²⁺ accumulation and cell death ensue in *T. cruzi* following treatment of parasites to fresh human serum. The second pathway involves induction of ROS production which triggers lipid peroxidation. The peroxidation of lipids thereafter results in membrane fluidity and functionality of Ca²⁺ channels, leading to excess accumulation of Ca²⁺ and loss of $\Delta\Psi_m$ (151). This pathway was seen in *L. donovani* parasites following treatment with complex II inhibitor thenyltrifluoroacetone and H₂O₂ (151). Downstream effects that follow $\Delta\Psi_m$ disruption of either pathway result in the execution of apoptosis include protease and nuclease activation.

Menna-Barreto concluded their review by reiterating the fact that there are currently no biochemical or molecular tools catered to protozoa for investigating programmed cell death. There are no streamlined or commercially-available tools exist to track these apoptotic-like or autophagic events. The magnitude of the mystery that is PCD in trypanosomatids continues to warrant investigation given the established clinical burden of these parasites.

2 RATIONALE

2.1 Hypothesis

Given the evolutionary and phylogenetic relationship of *Crithidia fasciculata* with human pathogens of *Trypanosoma* and *Leishmania*, I hypothesize that *C. fasciculata* will exhibit apoptosis-like and oncosis-like morphological characteristics in response to thermal stress, oxidative stress, rotenone, and nutrient deprivation. I also hypothesize that these parasites will largely lack homologs for key molecules involved in established cell death pathways as seen in mammalian systems.

2.2 Specific Aims

2.2.1 *Identify trypanosomatid homologs of potential proteins involved in cell death*

As apoptosis and autophagy are well characterized systems, the search for key molecules involved in these pathways has previously been conducted in trypanosomatids. Limited data have been published on protein partners involved in more novel cell death pathways. This project aims to perform a comprehensive analysis of trypanosomatids genomes for all major molecules involved in eight different regulated cell death pathways. To achieve this, I:

- Performed BLASTp analysis of trypanosomatid genomes for homologs of key molecules involved in various PCD pathways
- Reviewed the literature to understanding roles of homologs in trypanosomatids, and
- Connected existing key molecules and physiological profiles to determine possible existing PCD's in *C. fasciculata*

2.2.2 Determine methods to induce and measure cell death in *C. fasciculata*

Thus far, there have been little data published on methods to induce cell death in *C. fasciculata*. Although certain stressors and their effects have been explored in pathogenic trypanosomatids, differences in treatment conditions have been observed between these species. For example, apoptosis-like death in *T. cruzi* in response to H₂O₂ occurs in the micromolar range however in *L. donovani*, optimal treatment is in the millimolar range (132,152). Given there seem to be specific pathways in higher eukaryotes to combat specific triggers of cell death, it is critical to investigate how cells react to individual stressors. To investigate patterns of cell death, I aim to:

- Optimize the staining conditions of Hoechst 33342, propidium iodide, annexin-V, and monodansylcadaverine
- Determine conditions to induce cell death (but not necrosis)
- Determine the ranges of temperatures at which *C. fasciculata* undergo necrosis
- Determine concentrations at which H₂O₂ and rotenone are cytotoxic
- Determine the conditions at which *C. fasciculata* form autophagic vacuoles

2.2.3 Characterize cellular morphology during cell death

Each cell death pathway is characterized by cellular morphological profiles. Although some features may be shared between RCD pathways, analyzing a morphological profile during cell death can be useful in identifying the pathway at hand. Rather than functionally investigate molecular partners responsible for certain cell death pathways, this study aims to determine the various morphological characteristics that *C. fasciculata* display when undergoing cell death.

Characterization of morphological profiles involved:

- Capturing and identifying morphological patterns when cells were stressed
- Describing a morphological “sequence” of cell death
- Identifying instances of mammalian hallmarks such as cell shrinkage and swelling
- Comparing witnessed morphological profiles to those of existing regulated cell death pathways

2.2.4 Characterize nuclear changes during cell death

Many PCD pathways involve damage to DNA and understanding processes that occur in the nucleus can help in characterizing differences in cell death pathways. It has previously been shown that some trypanosomatids display different nuclear changes from mammals, despite attempts at mimicking specific stressors applied in mammalian systems (148). Furthermore, little is known about the role of the kinetoplast during cell death processes. Thus far, no studies address nuclear morphology of *C. fasciculata* in response to stress. In order to characterize nuclear changes, the following steps were taken:

- Determine the optimal method of staining and analyzing DNA bodies
- Identify patterns of nuclear changes during cellular stress
- Identify instances of mammalian hallmarks such as DNA fragmentation and chromatin condensation
- Compare nuclear morphological profiles to those of existing regulated cell death pathways

3 METHODS

3.1 Reagents

Brain heart infusion (BHI) media was obtained from Becton Dickinson. Fetal bovine serum (FBS) was obtained from Atlanta Biologicals. Penicillin-streptomycin was obtained from CellGro. Hemin was obtained from Alfa Aesar. GeneJet Genomic DNA Purification Kit, SYBR Safe DNA Stain, and 1Kb Plus DNA ladder were obtained from Thermo Scientific. Agarose and phenol/chloroform/isoamyl alcohol, chloroform, and absolute ethanol was obtained from Fisher Bioreagents. Poly-l-lysine, propidium iodide, monodansylcadaverine, and rotenone were obtained from Sigma Aldrich. Hoechst 33342 was obtained from Invitrogen. The Annexin V Fluorescence Microscopy kit was obtained from BD Biosciences. Three percent (3%) hydrogen peroxide was obtained from Walmart. Sixteen percent (16%) paraformaldehyde was obtained from Electron Microscopy Sciences. Isoamyl alcohol was obtained from Mallinckrodt.

3.2 Parasite culture

Wild type *Crithidia fasciculata* (Cf-CI strain generously provided by Dan Ray, UCLA) were typically grown at room temperature and shielded from light in non-treated tissue culture flasks. Cells were maintained in BHI media supplemented with FBS, hemin ($2.5 \mu\text{g mL}^{-1}$), and penicillin-streptomycin ($100 \text{ IU} / 100 \mu\text{g mL}^{-1}$). Regular cell maintenance typically involved passage of $500 \mu\text{L}$ of cells into 5 mL complete media every 5-7 days. When preparing for morphology experiments, cells were passaged to a new cell culture flask and incubated at room temperature (RT) on an orbital tabletop shaker under a sheet of aluminum foil (58). Experiments were conducted on cells in mid-log phase, approximately $10^8 \text{ cells mL}^{-1}$. For cultures grown in static conditions, this was typically achieved in 24-48 hours. For rotating cultures, this was typically achieved in 24 hours. Cell density was determined by counting on a hemocytometer.

3.3 Bioinformatics analysis

Literature review was conducted to identify relevant molecules involved in apoptosis, necroptosis, ferroptosis, oxeiptosis, paraptosis, pyroptosis, autophagy, and parthanatos. Accension numbers of each protein and the respective amino acid sequences were obtained from the UniProt database (153). For autophagy, protein from *Saccharomyces cerevisiae* were used as query sequences for BLASTp with the exception of ATG25 from *Pichia angusta*. For all other pathways, *Homo sapiens* proteins were used. FASTA-formatted, amino acid sequences were used for BLASTP against TriTrypDB (v.56) (144) with target organisms *Crithidia fasciculata* strain Cf-Cl, *Leishmania major* strain Friedlin, *Trypanosoma cruzi* strain CL Brener Esmeraldo-like, and *Trypanosoma brucei* strain TREU927 (154,155). The maximal e-value was set to 10, and the maximum descriptions/alignments was set to 50. The low complexity filter was enabled. Homologs were determined by assessing significance of e-values (less than e^{-4}) and score (greater than 40). When it was apparent that multiple homologs may exist, the trypanosomatid sequences were reverse-searched by submission to NCBI's BLASTp function against *H. sapiens* (or the respective yeast for autophagy). In order to qualify as a homolog, the query protein needed to be the top hit.

3.4 Stress treatments

Prior to stress treatments, cells were passaged at least twice to ensure a healthy, active culture. Twenty four hours (rotating cultures) or 48 hours (static cultures) after passage, cells density was determined to ensure mid-log phase. Inside the biosafety cabinet, cells were generally washed once with room temperature, sterile PBS and resuspended in complete BHI media at the original volume prior to treatment. All washing steps involved centrifugation at 8,000 RCF for 5 minutes at room temperature.

3.4.1 Thermal stress

Depending on the volume of the sample of cells, heat stress was applied via three different methods: (1) tabletop heat block, (2) thermal cycler, (3) or water bath. Cells were suspended in complete BHI media at the appropriate volume and exposed to constant heat at specified temperatures. Following treatment, cells were washed once with PBS before staining.

For heat shock treatments, similar steps were taken with the exception of shortening the exposure time to 15 minutes and allowing cells to rest at RT, without shaking, and shielded from light for 4 hours.

3.4.2 Starvation

Starvation involved washing cells with sterile PBS three times to remove residual media. Cells were then resuspended in either BHI media depleted of FBS or sterile PBS. Flasks were then left at RT, without shaking, and shielded from light for the set period of time.

3.4.3 Oxidative stress

Cells were centrifuged and resuspended in complete BHI with hydrogen peroxide at 25, 50, 100, 250, and 500 mM. Because stock hydrogen peroxide was 0.88 M (3% in water), a large volume of peroxide had to be added to attain higher doses. Thus, of the total sample volume in some cases, 56% of the total volume was water added with the peroxide. To account for possible cell volume stress, the percent of water for each sample was controlled by adding water to the same final concentration in the control and all treatments. Following treatment, cells were washed twice with PBS to remove residual H₂O₂. This prevented continued exposure to drug when moving to staining and slide preparation.

3.4.4 Rotenone

Rotenone was made by dissolving in 100% ethanol to a 2.5 mM (1 mg mL⁻¹) solution. Cells in fresh complete BHI media were treated with the appropriate concentrations of rotenone (2 μM and 10 μM). As ethanol can be toxic towards the parasites, rotenone treatments involved adding low volumes of solubilized drug (0.08% to 0.4% of total volume). Treatments were performed at RT, static, shielded from light, for 24 hours. Following treatments, cells were washed twice with PBS to remove residual drug.

3.5 Staining and Microscopy

3.5.1 Slide preparation

Coverslips were coated with poly-l-lysine (diluted 1:10 from stock in PBS) for 5 minutes followed by 15 minutes of air drying. Following treatment and the appropriate wash steps, cells were stained with fluorescent dyes, washed with PBS, and aliquoted onto a glass microscope slide. PLL coverslips were then placed onto the cells and allowed to adhere for 10 minutes. The perimeter of coverslips was then sealed with clear nail polish.

3.5.2 Staining parameters

Prior to labeling with annexin-V, cells were washed once with PBS containing calcium followed by an additional wash with a 1:1 ratio of annexin-V binding buffer. Cells were then resuspended in annexin-V binding buffer containing annexin-V (diluted 1:10 from manufacturer) and propidium iodide at 1.5 μM (1 μg mL⁻¹) and incubated 15 minutes in the dark.

Cells were stained with propidium iodide at a final concentration of 1.5 μM. Stock PI was prepared by dissolving in PBS at either 748 μM (0.5 mg mL⁻¹) or 1.5 mM (1 mg mL⁻¹).

Monodansylcadaverine (MDC) was dissolved in DMSO, and aliquots were stored at -20 °C. MDC staining was at 50 μM. Due to cytotoxic properties of DMSO, MDC was dissolved at

2.98 mM (1 mg mL⁻¹) to minimize the amount of DMSO added per sample. Cells were stained for 30 minutes in the dark.

Hoechst 33342 (stock of 22 mM, 10 mg mL⁻¹) staining was conducted at 4.42 mM (2 µg mL⁻¹) for 30 minutes in the dark. Generally, stained cells were not washed prior to analysis.

3.5.3 Data collection

Phase contrast and fluorescence images were captured under non-saturating conditions using Axio Imager.A1 fluorescence microscope (Zeiss) with an AI-6MPCMPS digital camera driven by AI View software (Aiken Instruments). Filter sets for the microscope included: HQ545/30 + HQ610/75M (Red, Chroma), HQ480/40X + HQ535/50 (Green, Chroma), and G365 + BP445/50 (Blue, Zeiss). Slides were first visualized on phase contrast and frames containing cells were haphazardly selected for data collection. In general, if a frame had cells that were in the same focal plane and not overlapping with other cells, the field of view was selected for analysis. Following capture of phase contrast images, fluorescence images were taken. In cases where Hoechst 33342 was used, the Hoechst 33342 images were taken first due to the dye's tendency to bleach. Care was taken to image fields not previously exposed to excitation light to minimize bleaching. For each slide, at least 300 cells were captured and analyzed. Clusters or clumps of cells, cells near the perimeter of the cover slip, or cells in air pockets were excluded from analysis. Post-capture modifications (*e.g.*, sharpness, contrast, and brightness) to improve visibility were applied equally to all photos via PowerPoint (Microsoft). All experiments were performed in triplicate.

3.6 Assessing morphology

To assess the effects of stress on morphology of the nectomonad, swimming cells, flasks were cultured on a shaker as described above. They were then stressed at necrosis-inducing (46-

50 °C) and non-necrosis-inducing (38-44 °C) temperatures for 1 hour in a heat block. Cells were then fixed with 4% paraformaldehyde for 15 minutes, stained with propidium iodide, and analyzed. Slides were first viewed under phase contrast and scanned for reoccurring cell phenotypes (*e.g.*, rounding, swelling, shrinkage) across all treatment groups followed by capturing of fluorescence images. Post-capture, phase contrast images were first grouped categorically via cell phenotype followed by assessment of patterns in propidium iodide staining.

To assess changes in nuclear morphology, cells were either stressed with rotenone (2 µM) or heat stressed (44 °C) as described above. Cells were then double-stained with Hoechst 33342 and propidium iodide. Given the difficulty to discern differences in shapes of the nucleus via Hoechst staining, changes in nuclear morphology were gauged by chromatin condensation. To this end, it was important to begin experiments with control groups and maintain the same exposure and gain for all filter sets of the following treatment groups. To differentiate between the nucleus and kinetoplast, which are always present when staining DNA, the nucleus was identified as the larger, dimmer organelle, and the kinetoplast was identified as the relatively smaller, brighter organelle.

3.7 DNA fragmentation assay

To obtain genomic DNA for fragmentation analysis, each sample of parasites was grown in a 75 cm², non-treated cell culture flasks with a total culture volume of 15 mL. Once the appropriate density and mid-log phase was reached, cells were then stressed with the treatment of interest. Following stress, cells were pelleted down at 1550 g at RT for 10 minutes, and the supernatant was removed. Pellets were stored at -80 °C until ready for nucleic acid extraction.

Genomic DNA extraction begun with thawing frozen cell pellets to RT and washing once with RT PBS. Cells were resuspended in 1000 μ L GeneJET Genomic DNA purification lysis solution with 1/10 volume proteinase K solution and incubated at 56 °C for 4 hours. The solution was intermittently vortexed to promote lysis. Cell debris was pelleted down at 18,000 \times g for 15 minutes at 4 °C. After addition of 1/20 volume of RNase A solution, lysates (supernatants) were incubated at 37 °C for an additional hour. One volume of phenol:chloroform:isoamyl alcohol (25:24:1) was added to the sample and vortexed at max setting for 30 seconds. Samples were then centrifuged at 16,000 \times g for 5 minutes at RT. The upper aqueous layer containing DNA was transferred and mixed with an equal volume of RT chloroform:isoamyl alcohol (24:1) by vortex for 30 seconds. The centrifugation step was repeated and again the upper aqueous layer was transferred to a new tube. DNA was precipitated by adding 1/10 volume of 3M NH_4OAc and 2.5 volumes of ice cold 100% ethanol. Samples were incubated at -20 °C overnight. Samples were then centrifuged for 15 minutes at maximum speed at 4 °C, and the pellet was washed once with ice cold 80% absolute ethanol. The pellet was air dried for 5 minutes, resuspended in elution buffer, and quantified via spectrophotometer (NanoDrop).

A 1% agarose gel was created by boiling 0.4 g of agarose in 40 mL TAE buffer. Before casting the gel, 4 μ L of SYBR safe DNA stain (0.01%) was added and well mixed. After the gel solidified, 10 μ g of DNA diluted with 1X loading dye (made in house) was loaded in the gel and electrophoresed at 135 volts and 125 milliamps. DNA was visualized with a Safe Imager Blue Light Transilluminator (Invitrogen), and photos were captured with a mobile phone camera. Post-modification of gel images (invert, desaturate, contrasts) was applied non-favorably to all gels via Microsoft PowerPoint. The experiment, including all treatment groups and separate gDNA extractions, were repeated once.

3.8 Statistical analysis

Statistics were performed via Prism 9.2 (GraphPad). Data was analyzed by one-way analysis of variance (ANOVA), and differences between control and experimental groups were analyzed by t-test. *p* values less than 0.05 were considered statistically significant.

4 RESULTS

4.1 Identification of homologs associated with cell death processes

To determine if relevant genes involved in various cell death processes existed in trypanosomatids genomes, amino acid sequences of proteins from reference species were submitted to BLASTp analysis against reference strains of *C. fasciculata*, *L. major*, *T. brucei*, and *T. cruzi* (Tables 1-8). Homology was determined by TriTrypDB scoring and e-value and further supported, when applicable, by identification of conserved superfamily or family domains. Homology required single, confident results that matched the query. In instances where multiple hits to homologous hypothetical proteins, amino acid sequences in question were submitted to reverse-BLASTp search against the reference species to confirm match. In order to better understand the potential presence of each PCD pathway in trypanosome biology, each protein was generally categorized by function, members, or pathways depending on current understanding of each regulated cell death pathway (Figure 1).

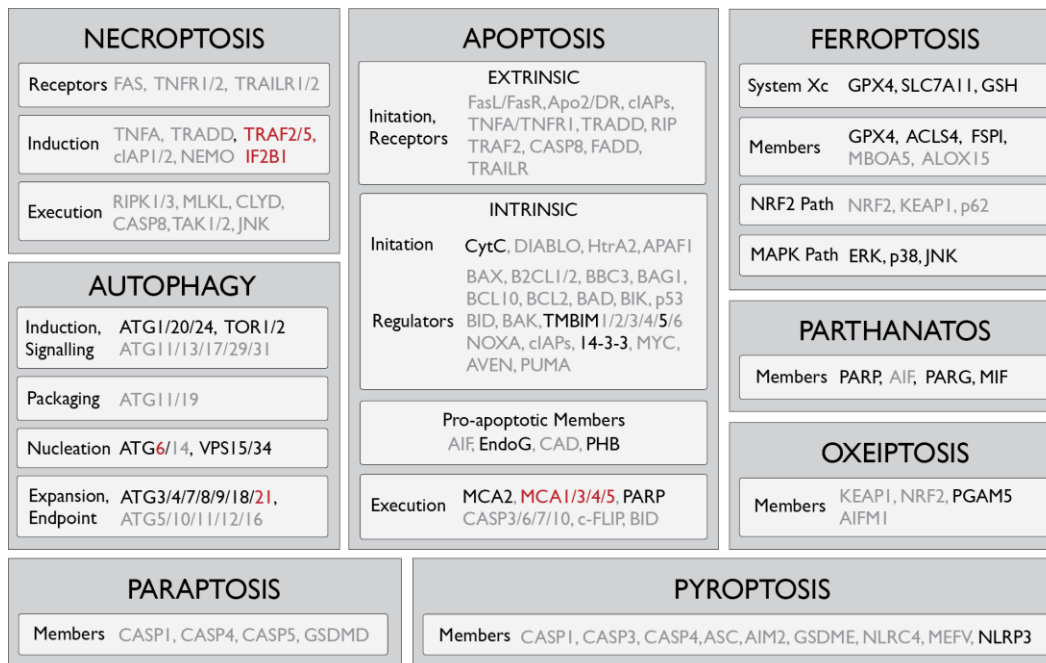


Figure 1 Trypanosomatids lack key molecules involved in necroptosis, apoptosis, paraptosis, pyroptosis, and oxeiptosis. They however have conserved genes involved in ferroptosis, autophagy, and parthanatos. Molecules involved in PCD pathways were categorized by function, members, or pathways. Presence of homologs identified by BLASTp of *C. fasciculata*, *L. major*, *T. brucei*, and *T. cruzi* genomes is indicated by highlighting. **Red text** indicates homology in 1-3 parasites. **Black text** indicates homology in all 4 species. **Grey text** indicates homology was not identified in trypanosomatid genome..

Aside from ATG21, all 4 species share significant orthology for proteins involved in autophagic induction and signaling (ATG1, ATG20, ATG24, TOR1, TOR2), nucleation (VPS15, VPS34), and expansion and endpoint (ATG3, ATG4, ATG7, ATG8, ATG9, ATG18). However, nearly half of the ATG's identified in the representative species *S. cerevisiae* are absent (Table 1). A potential ATG21 homolog is evident in the *Trypanosoma* spp. genome but is absent from both *C. fasciculata* and *L. major*. Proteins involved in autophagic packaging were not identified any of the trypanosomatid genomes.

Trypanosomatids appear to lack all key molecules involved in necroptosis, including proteins involved in death signaling and receptors, complex I and complex II formation, and

execution (Table 2). Additionally, *ZFP36*, the gene encoding for mRNA decay activator protein, a stabilizer of RIP1 and ripoptosome assembly, is conserved in all species except *T. cruzi*. Of note, a single hit for TRAF2 was identified for *C. fasciculata* (CFAC1_220030700) due to identification of the TRAF superfamily domain. Similarly, a hit for TRAF5 was identified each in *L. major* (LmjF.07.0370) and *T. brucei* (Tb927.11.4660).

As apoptosis is the most well defined cell death pathway, extensive BLASTp involved search of numerous proteins in the trypanosome genome (Table 3). In agreement with present data, trypanosomatids lack almost all proteins involved in extrinsic and intrinsic apoptosis aside from cytochrome c, 14-3-3 proteins, endonuclease G, prohibitin, and TMBIM5 (130). TMBIM5 is involved in organization of the mitochondrial architecture and release of cytochrome c, an important molecule in initiating apoptosis (156). Prohibitin is known to play a role in mitochondrial-associated apoptosis (142). Endonuclease G is responsible for fragmenting DNA during apoptosis (143). Trypanosomatids lack procaspases but have conserved genes for metacaspases-1, -2, -3, -4, and -5, none of which have been functionally linked to regulated cell death in protozoans (130).

Although only a few key molecules in parthanatos have been identified, three of these (PARP1, PARG, and MIF) are selectively conserved in trypanosomatids (Table 4). *Leishmania major* lacks homology for PARP1 and PARG. *Trypanosoma* spp. do not possess proteins homologous for MIF. AIF was not identified for any of the species.

Trypanosomatids possess putative homologs for multiple key molecules involved in ferroptosis including GPX4, FSP1, DHODH, ACSL4, SLC7A11, GSH, and GBLB (Table 5).

As aforementioned, the molecular machinery involved in paraptosis is largely unexplored though it is noted that trypanosomatids do not possess homologs for caspases-1, -4, or -5 or GDSMD (Table 6).

As trypanosomatids do not possess immune systems, it could have been expected that they do not have conserved genes involved in pyroptosis aside from NLRP3, one of the known receptors responsible for initiating inflammasome assembly (Table 7).

Although trypanosomatids possess orthologs for PGAM5, they lack orthologs for KEAP1, both of which encode for the two key molecules involved in oxeiptosis (Table 8).

Table 1. Genes involved in autophagy and identified trypanosomatid homologs

Gene Identification numbers of relevant *Saccharomyces cerevisiae* molecules were identified by UniProt and homologs in trypanosomatids were determined via BLASTp search. *ATG25* was represented by *Pichia angusta* as this gene is not present in *S. cerevisiae*. Orthologs between the four trypanosomatid species were identified by TriTrypDB version 54.

GeneID	Organism	UniProt ID	Organism	TriTrypDB ID	Score	E-value
<i>VPS34</i>	<i>S. cerevisiae</i>	p22543	<i>C. fasciculata</i>	CFAC1_250050500	223	3.00E ⁻⁶⁰
			<i>L. major</i>	LmjF.24.2010	221	1.00E ⁻⁵⁹
			<i>T. brucei</i>	Tb427.08.6210	271	7.00E ⁻⁷⁶
			<i>T. cruzi</i>	TcCLB.511065.50	239	3.00E ⁻⁷⁰
<i>ATG1</i>	<i>S. cerevisiae</i>	p53104	<i>C. fasciculata</i>	CFAC1_200027900	122	8.00E ⁻²⁸
			<i>L. major</i>	LmjF.29.2020	120	4.00E ⁻²⁷
			<i>T. brucei</i>	Tb927.3.4560	116	6.00E ⁻²⁶
			<i>T. cruzi</i>	TcCLB.504089.54	117	5.00E ⁻²⁶
<i>ATG13</i>	<i>S. cerevisiae</i>	Q06628	None identified			
<i>ATG6</i>	<i>S. cerevisiae</i>	Q02948	None identified			
<i>ATG5</i>	<i>S. cerevisiae</i>	Q12380	None identified			
<i>ATG20</i>	<i>S. cerevisiae</i>	Q07528	<i>C. fasciculata</i>	CFAC1_300073200	47.4	3.00E ⁻⁰⁵
			<i>L. major</i>	LmjF.35.2420	50.4	3.00E ⁻⁰⁶
			<i>T. brucei</i>	Tb927.9.13380	50.8	2.00E ⁻⁰⁶
			<i>T. cruzi</i>	TcCLB.510749.30	58.9	6.00E ⁻⁰⁹
<i>ATG17</i>	<i>S. cerevisiae</i>	Q06410	None identified			
<i>VPS53</i>	<i>S. cerevisiae</i>	P47061	<i>C. fasciculata</i>	CFAC1_170016900	214	1.00E ⁻⁵⁸
			<i>L. major</i>	LmjF.19.0810	216	1.00E ⁻⁵⁸
			<i>T. brucei</i>	Tb927.10.15540	184	3.00E ⁻⁴⁸
			<i>T. cruzi</i>			
<i>ATG24</i>	<i>S. cerevisiae</i>	P47057	<i>C. fasciculata</i>	CFAC1_300073200	47.4	5.00E ⁻⁰⁵
			<i>L. major</i>	LmjF.35.2420	49.3	1.00E ⁻⁰⁵
			<i>T. brucei</i>	Tb927.9.13380	77.8	9.00E ⁻¹⁵
			<i>T. cruzi</i>	TcCLB.510749.30	74.7	1.00E ⁻¹³
<i>ATG11</i>	<i>S. cerevisiae</i>	Q12527	None identified			

<i>ATG19</i>	<i>S. cerevisiae</i>	P35193	None identified			
<i>ATG 3</i>	<i>S. cerevisiae</i>	P40344	<i>C. fasciculata</i>	CFAC1_280011000	99.8	2.00E ⁻²³
			<i>L. major</i>	LmjF.33.0295	108	1.00E ⁻²⁶
			<i>T. brucei</i>	Tb927.2.1890	67	7.00E ⁻¹²
			<i>T. cruzi</i>	TcCLB.510257.90	103	2.00E ⁻²⁴
<i>ATG14</i>	<i>S. cerevisiae</i>	P38270	None identified			
<i>ATG4</i>	<i>S. cerevisiae</i>	P53867	<i>C. fasciculata</i>	CFAC1_300048700	90.9	2.00E ⁻¹⁹
			<i>L. major</i>	LmjF.32.3890	96.7	2.00E ⁻²¹
			<i>T. brucei</i>	Tb927.11.16290	98.2	3.00E ⁻²²
			<i>T. cruzi</i>	TcCLB.511527.50	118	3.00E ⁻²⁹
<i>ATG5</i>	<i>S. cerevisiae</i>	Q12380	None identified			
<i>ATG7</i>	<i>S. cerevisiae</i>	P38862	<i>C. fasciculata</i>	CFAC1_080005700	310	2.00E ⁻⁹⁴
			<i>L. major</i>	LmjF.07.0010	297	8.00E ⁻⁹⁰
			<i>T. brucei</i>	Tb927.10.11180	328	4.00E ⁻¹⁰¹
			<i>T. cruzi</i>	TcCLB.507711.150	343	7.00E ⁻¹⁰⁷
<i>ATG8</i>	<i>S. cerevisiae</i>	P38182	<i>C. fasciculata</i>	CFAC1_210026000	129	1.00E ⁻³⁸
			<i>L. major</i>	LmjF.19.1630	130	4.00E ⁻³⁹
			<i>T. brucei</i>	Tb927.7.5900	132	1.00E ⁻³⁹
			<i>T. cruzi</i>	TcCLB.510533.180	92	5.00E ⁻²³
<i>ATG10</i>	<i>S. cerevisiae</i>	Q07879	None identified			
<i>ATG12</i>	<i>S. cerevisiae</i>	P38316	None identified			
<i>ATG16</i>	<i>S. cerevisiae</i>	Q03818	None identified			
<i>ATG21</i>	<i>S. cerevisiae</i>	Q02887	<i>C. fasciculata</i>			
			<i>L. major</i>			
			<i>T. brucei</i>	Tb927.3.4150	55.52	5.00E ⁻⁰⁹
			<i>T. cruzi</i>	TcCLB.509669.100	53	2.00E ⁻⁰⁷
<i>ATG27</i>	<i>S. cerevisiae</i>	P46989	None identified			
<i>ATG2</i>	<i>S. cerevisiae</i>	P53855	None identified			
<i>ATG23</i>	<i>S. cerevisiae</i>	Q06671	None identified			

ATG22	<i>S. cerevisiae</i>	P25568	None identified			
ATG25	<i>P. angusta</i>	Q6JUT9	None identified			
ATG26	<i>S. cerevisiae</i>	Q06321	<i>C. fasciculata</i>	CFAC1_110012800	46	2.00E ⁻⁰⁴
			<i>L. major</i>			
			<i>T. brucei</i>			
			<i>T. cruzi</i>	TcCLB.508089.20	45.1	4.00E ⁻⁰⁴
ATG9	<i>S. cerevisiae</i>	Q12142	<i>C. fasciculata</i>	CFAC1_230049000	49.3	2.00E ⁻⁰⁵
			<i>L. major</i>	LmjF.27.0390	57.8	5.00E ⁻⁰⁸
			<i>T. brucei</i>	Tb927.11.990	44.7	1.00E ⁻⁰⁴
			<i>T. cruzi</i>	TcCLB.506925.450	50.1	9.00E ⁻⁰⁶
ATG18	<i>S. cerevisiae</i>	P43601	<i>C. fasciculata</i>	CFAC1_200022900	53.5	3.00E ⁻⁰⁷
			<i>L. major</i>	LmjF.29.1575	59.7	4.00E ⁻⁰⁹
			<i>T. brucei</i>	Tb927.3.4150	97.8	1.00E ⁻²¹
			<i>T. cruzi</i>	TcCLB.509669.100	90.5	4.00E ⁻¹⁹
ATG15	<i>S. cerevisiae</i>	P25641	None identified			
ATG29	<i>S. cerevisiae</i>	Q12092	None identified			
ATG31	<i>S. cerevisiae</i>	Q12421	None identified			
VPS15	<i>S. cerevisiae</i>	P22219	<i>C. fasciculata</i>	CFAC1_300029500	120	6.00E ⁻²⁷
			<i>L. major</i>	LmjF.28.1760	102	3.00E ⁻²¹
			<i>T. brucei</i>	Tb927.11.9190	129	1.00E ⁻²⁹
			<i>T. cruzi</i>	TcCLB.503715.40	59.7	2.00E ⁻⁰⁸
VPS38	<i>S. cerevisiae</i>	Q05919	None identified			
VPS30	<i>S. cerevisiae</i>	Q02948	<i>C. fasciculata</i>			
			<i>L. major</i>			
			<i>T. brucei</i>			
			<i>T. cruzi</i>	TcCLB.507809.119	53.5	4.00E ⁻⁰⁷
ATG32	<i>S. cerevisiae</i>	P40458	None identified			
TOR1	<i>S. cerevisiae</i>	P35169	<i>C. fasciculata</i>	CFAC1_280071400	627	0
			<i>C. fasciculata</i>	CFAC1_290074900	617	0

<i>TOR2</i>	<i>S. cerevisiae</i>	P32600	<i>L. major</i>	LmjF.36.6320	774	0
			<i>L. major</i>	LmjF.34.4530	729	0
			<i>T. brucei</i>	Tb927.10.8420	812	0
			<i>T. brucei</i>	Tb927.4.420	644	0
			<i>T. cruzi</i>	TcCLB.508231.30	844	0
			<i>T. cruzi</i>	TcCLB.510689.40	723	0

Table 2 Genes involved in necroptosis and their trypanosomatid homologs
Gene Identification numbers of relevant *H. sapiens* molecules were identified by UniProt and homologs in trypanosomatids were determined via BLASTp search. Orthologs among the four trypanosomatid species were identified by TriTrypDB version 54.

GeneID	Organism	UniProt ID	Organism	TriTrypDB ID	Score	E-value
<i>RIPK3</i>	<i>H. sapiens</i>	Q9Y572	None identified			
<i>RIPK1</i>	<i>H. sapiens</i>	Q13546	None identified			
<i>MLKL</i>	<i>H. sapiens</i>	Q8NB16	None identified			
<i>BIRC2</i>	<i>H. sapiens</i>	Q13490	None identified			
<i>BIRC3</i>	<i>H. sapiens</i>	Q13489	None identified			
<i>CYLD</i>	<i>H. sapiens</i>	Q9NQC7	None identified			
<i>TNFA</i>	<i>H. sapiens</i>	P01375	None identified			
<i>CASP8</i>	<i>H. sapiens</i>	Q14790	None identified			
<i>NR2C2</i>	<i>H. sapiens</i>	P49116	None identified			
<i>TRAF2</i>	<i>H. sapiens</i>	Q12933	<i>C. fasciculata</i>	CFAC1_220030700	48.9	9.00E ⁻⁰⁶
			<i>L. major</i>			
			<i>T. brucei</i>			
			<i>T. cruzi</i>			
<i>TRAF5</i>	<i>H. sapiens</i>	O00463	<i>C. fasciculata</i>			
			<i>L. major</i>	LmjF.07.0370	52.8	8.00E ⁻⁰⁷
			<i>T. brucei</i>	Tb927.11.4660	46.2	8.00E ⁻⁰⁵
			<i>T. cruzi</i>			
<i>Fas</i>	<i>H. sapiens</i>	P25445	None identified			

<i>TRAILR2</i>	<i>H. sapiens</i>	O14763	None identified			
<i>TNFR1</i>	<i>H. sapiens</i>	P19438	None identified			
<i>TRAILR1</i>	<i>H. sapiens</i>	O00220	None identified			
<i>TRADD</i>	<i>H. sapiens</i>	Q15628	None identified			
<i>FADD</i>	<i>H. sapiens</i>	O15519	None identified			
<i>NEMO</i>	<i>H. sapiens</i>	Q9Y6K9	None identified			
<i>IF2B1</i>	<i>H. sapiens</i>	Q9NZI8	<i>C. fasciculata</i>	CFAC1_200020600	172	1.00E ⁻⁴⁸
			<i>L. major</i>	LmjF.29.1370	48.1	2.00E ⁻⁰⁵
			<i>T. brucei</i>			
			<i>T. cruzi</i>			
			None identified			
<i>OPTN</i>	<i>H. sapiens</i>	Q96CV9	None identified			
<i>JNK</i>	<i>H. sapiens</i>	P45984	<i>C. fasciculata</i>	CFAC1_170008200	172	1.00E ⁻⁴⁸
			<i>L. major</i>	LmjF.19.0180	173	3.00E ⁻⁴⁹
			<i>T. brucei</i>	Tb927.10.14800	144	6.00E ⁻³⁹
			<i>T. cruzi</i>	TcCLB.506211.180	177	1.00E ⁻⁵⁰
			None identified			
<i>ERK2</i>	<i>H. sapiens</i>	P27361	<i>C. fasciculata</i>	CFAC1_280073900	223	4.00E ⁻⁶⁹
			<i>L. major</i>	LmjF.36.6470	225	2.00E ⁻⁶⁹
			<i>T. brucei</i>	TcCLB.504167.30	233	1.00E ⁻⁷²
			<i>T. cruzi</i>	Tb927.10.7780	225	1.00E ⁻⁶⁹
			None identified			
<i>ERK1</i>	<i>H. sapiens</i>	P28482	<i>C. fasciculata</i>	CFAC1_280024800	221	9.00E ⁻⁶⁸
			<i>L. major</i>	LmjF.10.0490	267	2.00E ⁻⁸⁶
			<i>T. brucei</i>	Tb927.8.3550	254	1.00E ⁻⁸¹
			<i>T. cruzi</i>	TcCLB.509475.10	142	4.00E ⁻⁴⁰
			None identified			
<i>p38</i>	<i>H. sapiens</i>	Q15759	<i>C. fasciculata</i>	CFAC1_280024800	251	2.00E ⁻⁸⁰
			<i>L. major</i>	LmjF.33.1380	256	6.00E ⁻⁸²
			<i>T. brucei</i>	Tb927.10.12040	261	4.00E ⁻⁸⁴
			<i>T. cruzi</i>	TcCLB.510123.20	248	5.00E ⁻⁷⁹
			None identified			
<i>TLR4</i>	<i>H. sapiens</i>	O00206	None identified			
<i>ZFP36</i>	<i>H. sapiens</i>	P26651	<i>C. fasciculata</i>	CFAC1_020008000	44.3	9.00E ⁻⁰⁵

			<i>L. major</i>	LmjF.35.1040	44.7	7.00E ⁻⁰⁵
			<i>T. brucei</i>	Tb927.5.1580	49.7	2.00E ⁻⁰⁶
			<i>T. cruzi</i>			
<i>DAPK1</i>	<i>H. sapiens</i>	P53355	None identified			
<i>RAC1</i>	<i>H. sapiens</i>	P63000	None identified			
<i>TCAM1</i>	<i>H. sapiens</i>	Q8IUC6	None identified			
<i>ZBP1</i>	<i>H. sapiens</i>	Q9H171	None identified			
<i>PLAT4</i>	<i>H. sapiens</i>	Q9UL19	None identified			

Table 3 Genes involved in apoptosis and their trypanosomatid homologs
Gene Identification numbers of relevant *H. sapiens* molecules were identified by UniProt and homologs in trypanosomatids were determined via BLASTp search. *MCA1-5* were represented by *Trypanosoma brucei*. Orthologs among the four trypanosomatid species were identified by TriTrypDB version 54.

GeneID	Organism	UniProt ID	Organism	TriTrypDB ID	Score	E-value
<i>NFKB1</i>	<i>H. sapiens</i>	P19838	None identified			
<i>NFKB2</i>	<i>H. sapiens</i>	Q00653	None identified			
<i>RelA</i>	<i>H. sapiens</i>	Q04206	None identified			
<i>RelB</i>	<i>H. sapiens</i>	Q01201	None identified			
<i>Rel</i>	<i>H. sapiens</i>	Q04864	None identified			
<i>TLR3</i>	<i>H. sapiens</i>	O15455	None identified			
<i>TNFL6</i>	<i>H. sapiens</i>	P48023	None identified			
<i>TNF12</i>	<i>H. sapiens</i>	O43508	None identified			
<i>TNR25</i>	<i>H. sapiens</i>	Q93038	None identified			
<i>TNF10</i>	<i>H. sapiens</i>	P50591	None identified			
<i>DEDD2</i>	<i>H. sapiens</i>	Q8WXF8	None identified			
<i>CFLAR</i>	<i>H. sapiens</i>	O15519	None identified			
<i>DIABLO</i>	<i>H. sapiens</i>	Q9NR28	None identified			
<i>HTRA2</i>	<i>H. sapiens</i>	O43464	None identified			
<i>APAF</i>	<i>H. sapiens</i>	O14727	None identified			
<i>DFFB</i>	<i>H. sapiens</i>	O76075	None identified			

<i>B2CL1</i>	<i>H. sapiens</i>	Q07817	None identified			
<i>BCL2</i>	<i>H. sapiens</i>	P10415	None identified			
<i>B2CL2</i>	<i>H. sapiens</i>	Q92843	None identified			
<i>BAG1</i>	<i>H. sapiens</i>	Q99933	None identified			
<i>BCL10</i>	<i>H. sapiens</i>	O95999	None identified			
<i>BAX</i>	<i>H. sapiens</i>	Q07812	None identified			
<i>BAK</i>	<i>H. sapiens</i>	Q16611	None identified			
<i>BID</i>	<i>H. sapiens</i>	P55957	None identified			
<i>BAD</i>	<i>H. sapiens</i>	Q92934	None identified			
<i>BIK</i>	<i>H. sapiens</i>	Q13323	None identified			
<i>BBC3</i>	<i>H. sapiens</i>	Q9BXH1	None identified			
<i>APR</i>	<i>H. sapiens</i>	Q13794	None identified			
<i>AVEN</i>	<i>H. sapiens</i>	Q9NQS1	None identified			
<i>MYC</i>	<i>H. sapiens</i>	P01106	None identified			
<i>14-3-3E</i>	<i>H. sapiens</i>	P62258	<i>C. fasciculata</i>	CFAC1_130009500	263	9.00E ⁻⁸⁷
			<i>L. major</i>	LmjF.11.0350	265	7.00E ⁻⁸⁸
			<i>T. brucei</i>	Tb927.11.6870	243	8.00E ⁻⁸¹
			<i>T. cruzi</i>	TcCLB.506775.80	262	2.00E ⁻⁸⁶
<i>MCA1</i>	<i>S. cerevisiae</i>	Q08601	<i>C. fasciculata</i>	CFAC1_010008300	344	2.00E ⁻¹¹⁷
			<i>L. major</i>	LmjF.35.1580	280	3.00E ⁻⁹¹
			<i>T. brucei</i>	None identified		
			<i>T. cruzi</i>	None identified		
<i>MCA2</i>	<i>T. brucei</i>	Q585F3	<i>C. fasciculata</i>	CFAC1_300060100	273	2.00E ⁻⁸⁸
			<i>L. major</i>	LmjF.35.1580	295	2.00E ⁻⁹⁷
			<i>T. brucei</i>	Tb927.6.940	0	0
			<i>T. cruzi</i>	TcCLB.507537.40	384	2.00E ⁻¹³³
<i>MCA3</i>	<i>T. brucei</i>	Q8T8E6	<i>C. fasciculata</i>	None identified		
			<i>L. major</i>	None identified		
			<i>T. brucei</i>	Tb927.6.930	0	0

			<i>T. cruzi</i>	TcCLB.506531.50	405	3.00E ⁻¹⁴¹
<i>MCA4</i>	<i>T. brucei</i>	Q8T8E5	<i>C. fasciculata</i>	None identified		
			<i>L. major</i>	None identified		
			<i>T. brucei</i>	Tb927.10.2440	705	0
			<i>T. cruzi</i>	None identified		
<i>MCA5</i>	<i>T. brucei</i>	Q8IEW1	<i>C. fasciculata</i>	None identified		
			<i>L. major</i>			
			<i>T. brucei</i>	Tb927.9.14220	781	0
			<i>T. cruzi</i>	TcCLB.510759.160	481	7.00E ⁻¹⁶⁸
<i>EndoG</i>	<i>H. sapiens</i>	Q14249	<i>C. fasciculata</i>	CFAC1_040014100	112	1.00E ⁻²⁷
			<i>L. major</i>	LmjF.10.0610	105	3.00E ⁻²⁵
			<i>T. brucei</i>	Tb927.8.4040	100	1.00E ⁻²³
			<i>T. cruzi</i>	TcCLB.506867.10	103	1.00E ⁻²⁴
<i>PHB</i>	<i>H. sapiens</i>	P325232	<i>C. fasciculata</i>	CFAC1_120028100	204	3.00E ⁻⁶⁵
			<i>L. major</i>	LmjF.16.1610	204	9.00E ⁻⁹⁵
			<i>T. brucei</i>	Tb927.8.4810	218	3.00E ⁻⁷⁰
			<i>T. cruzi</i>	TcCLB.508837.120	214	1.00E ⁻⁶⁸
<i>TMBIM1</i>	<i>H. sapiens</i>	Q969X1	None identified			
<i>TMBIM2</i>	<i>H. sapiens</i>	Q9BWQ8	None identified			
<i>TMBIM3</i>	<i>H. sapiens</i>	Q7Z429	None identified			
<i>TMBIM4</i>	<i>H. sapiens</i>	Q9HC24	None identified			
<i>TMBIM5</i>	<i>H. sapiens</i>	Q9H3K2	<i>C. fasciculata</i>	CFAC1_210021700	61.6	2.00E ⁻¹⁰
			<i>L. major</i>	LmjF.24.1190	59.7	7.00E ⁻¹⁰
			<i>T. brucei</i>	Tb927.11.5820	64	2.00E ⁻¹¹
			<i>T. cruzi</i>	TcCLB.503487.70	63.2	8.00E ⁻¹¹
<i>TMBIM6</i>	<i>H. sapiens</i>	P55061	None identified			
<i>EF1A1</i>	<i>H. sapiens</i>	P68104	<i>C. fasciculata</i>	CFAC1_090006400	694	0
			<i>L. major</i>	LmjF.17.0080	720	0
			<i>T. brucei</i>	Tb927.10.2090	739	0

			<i>T. cruzi</i>	TcCLB.511369.20	720	0
<i>CASP7</i>	<i>H. sapiens</i>	P55210	None identified			
<i>CASP3</i>	<i>H. sapiens</i>	P70677	None identified			
<i>CASP6</i>	<i>H. sapiens</i>	O08738	None identified			
<i>CASP10</i>	<i>H. sapiens</i>	Q92851	None identified			
<i>DFFA</i>	<i>H. sapiens</i>	O00273	None identified			
<i>DFFB</i>	<i>H. sapiens</i>	O76075	None identified			
<i>NUMA1</i>	<i>H. sapiens</i>	Q14980	None identified			
<i>SPTN1</i>	<i>H. sapiens</i>	Q13813	None identified			

Table 4 Genes involved in parthanatos and their trypanosomatid homologs
Gene Identification numbers of relevant *H. sapiens* molecules were identified by UniProt and homologs in trypanosomatids were determined via BLASTp search. Orthologs in the four trypanosomatid species were identified by TriTrypDB version 54.

GeneID	Organism	UniProt ID	Organism	TriTrypDB ID	Score	E-value
<i>PARP1</i>	<i>H. sapiens</i>	P09874	<i>C. fasciculata</i>	CFAC1_020022700	368	6.00E ⁻¹¹⁴
			<i>L. major</i>	None identified		
			<i>T. brucei</i>	Tb927.5.3050	410	4.00E ⁻¹³⁰
			<i>T. cruzi</i>	CFAC1_020022700	362	1.00E ⁻¹¹¹
<i>AIF</i>	<i>H. sapiens</i>	O95831	None identified			
<i>PARG</i>	<i>H. sapiens</i>	Q86W56	<i>C. fasciculata</i>	CFAC1_300079100	183	3.00E ⁻⁴⁸
			<i>L. major</i>	None identified		
			<i>T. brucei</i>	Tb927.9.12810	191	2.00E ⁻⁵¹
			<i>T. cruzi</i>	TcCLB.507013.24	189	1.00E ⁻⁵⁰
<i>MIF</i>	<i>H. sapiens</i>	P14174	<i>C. fasciculata</i>	CFAC1_230019300	42.7	4.00E ⁻⁶⁰
			<i>L. major</i>	LmjF.33.1740	40.8	2.00E ⁻⁰⁵
			<i>T. brucei</i>	None identified		
			<i>T. cruzi</i>	None identified		

Table 5 Genes involved in ferroptosis and their trypanosomatid homologs
Gene Identification numbers of relevant *H. sapiens* proteins were identified by UniProt and homologs in trypanosomatids were determined via BLASTp search.

GeneID	Organism	UniProt ID	Organism	TriTrypDB ID	Score	E-value
<i>GPX4</i>	<i>H. sapiens</i>	P36969	<i>C. fasciculata</i>	CFAC1_290014000	80.1	1.00E ⁻¹⁷
			<i>L. major</i>	LmjF.26.0820	78.6	1.00E ⁻¹⁷
			<i>T. brucei</i>	Tb927.7.1120	87.8	5.00E ⁻²¹
			<i>T. cruzi</i>	TcCLB.503899.110	84.3	7.00E ⁻²⁰
<i>FSP1</i>	<i>H. sapiens</i>	Q9BRQ8	<i>C. fasciculata</i>	CFAC1_110012400	45.8	5.00E ⁻⁰⁵
			<i>L. major</i>	LmjF.14.0440	55.1	5.00E ⁻⁰⁸
			<i>T. brucei</i>	Tb927.7.4310	54.3	8.00E ⁻⁰⁸
			<i>T. cruzi</i>	TcCLB.508089.50	60.8	8.00E ⁻¹⁰
<i>ACSL4</i>	<i>H. sapiens</i>	O60488	<i>C. fasciculata</i>	CFAC1_050011200	318	1.00E ⁻⁹⁶
			<i>L. major</i>	LmjF.01.0520	316	6.00E ⁻⁹⁶
			<i>T. brucei</i>	Tb927.9.4230	332	4.00E ⁻¹⁰²
			<i>T. cruzi</i>	TcCLB.503575.50	315	9.00E ⁻⁹⁶
<i>DHODH</i>	<i>H. sapiens</i>	Q02127	<i>C. fasciculata</i>	CFAC1_120013000	75.9	5.00E ⁻¹⁵
			<i>L. major</i>	LmjF.16.0530	71.2	2.00E ⁻¹³
			<i>T. brucei</i>	Tb927.5.3830	78.2	3.00E ⁻¹⁴
			<i>T. cruzi</i>	TcCLB.508375.50	73.6	5.00E ⁻¹⁵
<i>MBOA5</i>	<i>H. sapiens</i>	Q6P1A2	None identified			
<i>ALOX15</i>	<i>H. sapiens</i>	P16050	None identified			
<i>SLC7A11</i>	<i>H. sapiens</i>	Q9UPY5	<i>C. fasciculata</i>	CFAC1_260058200	61.1	3.00E ⁻⁰⁹
			<i>L. major</i>	LmjF.14.0320	50.4	3.00E ⁻⁰⁶
			<i>T. brucei</i>	TcCLB.504213.110	57.4	2.00E ⁻⁰⁸
			<i>T. cruzi</i>	Tb927.6.4660	51.1	4.00E ⁻⁰⁶
<i>GSH</i>	<i>H. sapiens</i>	P48637	<i>C. fasciculata</i>	CFAC1_110019200	106	3.00E ⁻²⁴
			<i>L. major</i>	LmjF.14.0910	138	4.00E ⁻³⁵
			<i>T. brucei</i>	Tb927.7.4000	168	3.00E ⁻⁴⁵
			<i>T. cruzi</i>	TcCLB.506659.30	139	1.00E ⁻³⁵

<i>GBLB</i>	<i>H. sapiens</i>	Q8NCG7	<i>C. fasciculata</i>	CFAC1_140007500	156	7.00E ⁻³⁸
			<i>L. major</i>	LmjF.18.0160	156	7.00E ⁻⁴⁰
			<i>T. brucei</i>	Tb927.10.13680	147	1.00E ⁻⁴⁶
			<i>T. cruzi</i>	TcCLB.507993.180	139	5.00E ⁻³⁹
<i>P62</i>	<i>H. sapiens</i>	Q13501	None identified			
<i>NF2L2</i>	<i>H. sapiens</i>	Q16236	None identified			
<i>TFR1</i>	<i>H. sapiens</i>	P02786	None identified			

Table 6 Genes involved in paraptosis and their trypanosomatid homologs

Gene Identification numbers of relevant *H. sapiens* molecules were identified by UniProt and homologs in trypanosomatids were determined via BLASTp search. Orthologs between the 4 trypanosomatid species were identified by TriTrypDB version 54. Score and e values were determined via TriTrypDB BLASTp parameters.

GeneID	Organism	UniProt ID	Organism	TriTrypDB ID	Score	E-value
<i>CASP1</i>	<i>H. sapiens</i>	P29466	None identified			
<i>CASP4</i>	<i>H. sapiens</i>	P49662	None identified			
<i>CASP5</i>	<i>H. sapiens</i>	P51878	None identified			
<i>GSDMD</i>	<i>H. sapiens</i>	P57764	None identified			

Table 7 Genes involved in pyroptosis and their trypanosomatid homologs

Gene Identification numbers of relevant *H. sapiens* molecules were identified by UniProt and homologs in trypanosomatids were determined via BLASTp search. Orthologs among the four trypanosomatid species were identified by TriTrypDB version 54. Score and E-values were determined via TriTrypDB BLASTp parameters.

GeneID	Organism	UniProt ID	Organism	TriTrypDB ID	Score	E-value
<i>CASP1</i>	<i>H. sapiens</i>	P29466	None identified			
<i>CASP3</i>	<i>H. sapiens</i>	P70677	None identified			
<i>CASP4</i>	<i>H. sapiens</i>	P49662	None identified			
<i>CASP5</i>	<i>H. sapiens</i>	P51878	None identified			
<i>ASC</i>	<i>H. sapiens</i>	Q9ULZ3	None identified			
<i>AIM2</i>	<i>H. sapiens</i>	O14862	None identified			
<i>GSDME</i>	<i>H. sapiens</i>	O60443	None identified			

<i>NLRC4</i>	<i>H. sapiens</i>	Q9NPP4	None identified		
<i>MEFV</i>	<i>H. sapiens</i>	O15553	None identified		
<i>NLRP3</i>	<i>H. sapiens</i>	Q96P20	<i>C. fasciculata</i>	CFAC1_290010800	76.3
			<i>L. major</i>	LmjF.26.0500	63.9
			<i>T. brucei</i>	Tb927.7.1430	49.5
			<i>T. cruzi</i>	TcCLB.503579.20	44.7

Table 8 Genes involved in oxepitosis and their trypanosomatid homologs
Gene Identification numbers of relevant *H. sapiens* molecules were identified by UniProt and homologs in trypanosome were determined via BLASTp search. Orthologs among the four trypanosomatid species were identified by TriTrypDB version 54. Score and E-values were determined via TriTrypDB BLASTp parameters.

GeneID	Organism	UniProt ID	Organism	TriTrypDB ID	Score	E-value
<i>KEAP1</i>	<i>H. sapiens</i>	Q14145	None identified			
<i>PGAM5</i>	<i>H. sapiens</i>		<i>C. fasciculata</i>	CFAC1_280045600	97.8	4.00E ⁻²³
			<i>L. major</i>	LmjF.36.4070	100	8.00E ⁻²⁴
			<i>T. brucei</i>	Tb927.11.10340	136	4.00E ⁻³⁷
			<i>T. cruzi</i>	TcCLB.510283.40	125	8.00E ⁻³³

4.2 Heat stress induces cell death

Parasites were subjected to thermal stress at various temperatures (38–50 °C) for 1 hour prior to staining with annexin-V and PI (Figure 3). Intuitively, there is a correlation between temperature and cell death (Figure 2). As temperature rises, more cells begin to die. Cells begin to die (~35% PI positive) around 40 °C to 42 °C, and PI positive cells occur 2.5 to 3-fold more frequently (~35% of population) compared to cells treated at 38 °C. At temperatures of 45 °C, cell death increases to 70%. These data suggest that, once temperatures become too high, cells undergo unavoidable trauma and necrosis. Morphologically, cells begin to assume a teardrop-shape phenotype when stressed at 38 °C. Higher temperatures lead to a shift to more rounded cells with increased frequency of membrane rupture, cellular swelling, and changes in cellular translucency.

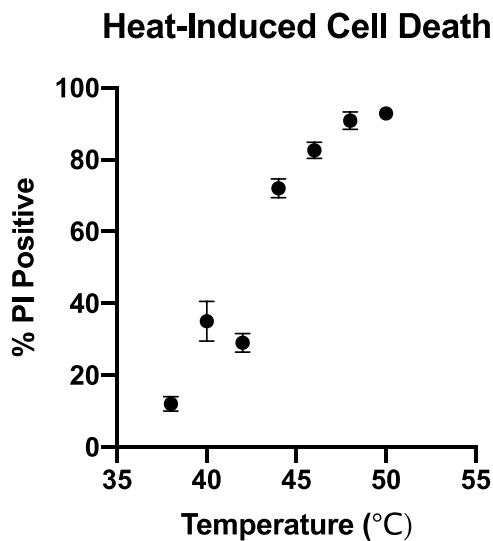


Figure 2 Quantification of cells thermally stressed identify standard temperatures to induce necrosis. Cells were treated at a range of temperatures for 1 hour and stained with PI. Percentage of PI positive cells in a sample was determined. Data is presented as arithmetic mean \pm S.E.M. $p \leq 0.05$ ($n=3$, one-way ANOVA $p < 0.05$, unpaired *T*-test significance $p \leq 0.05$)

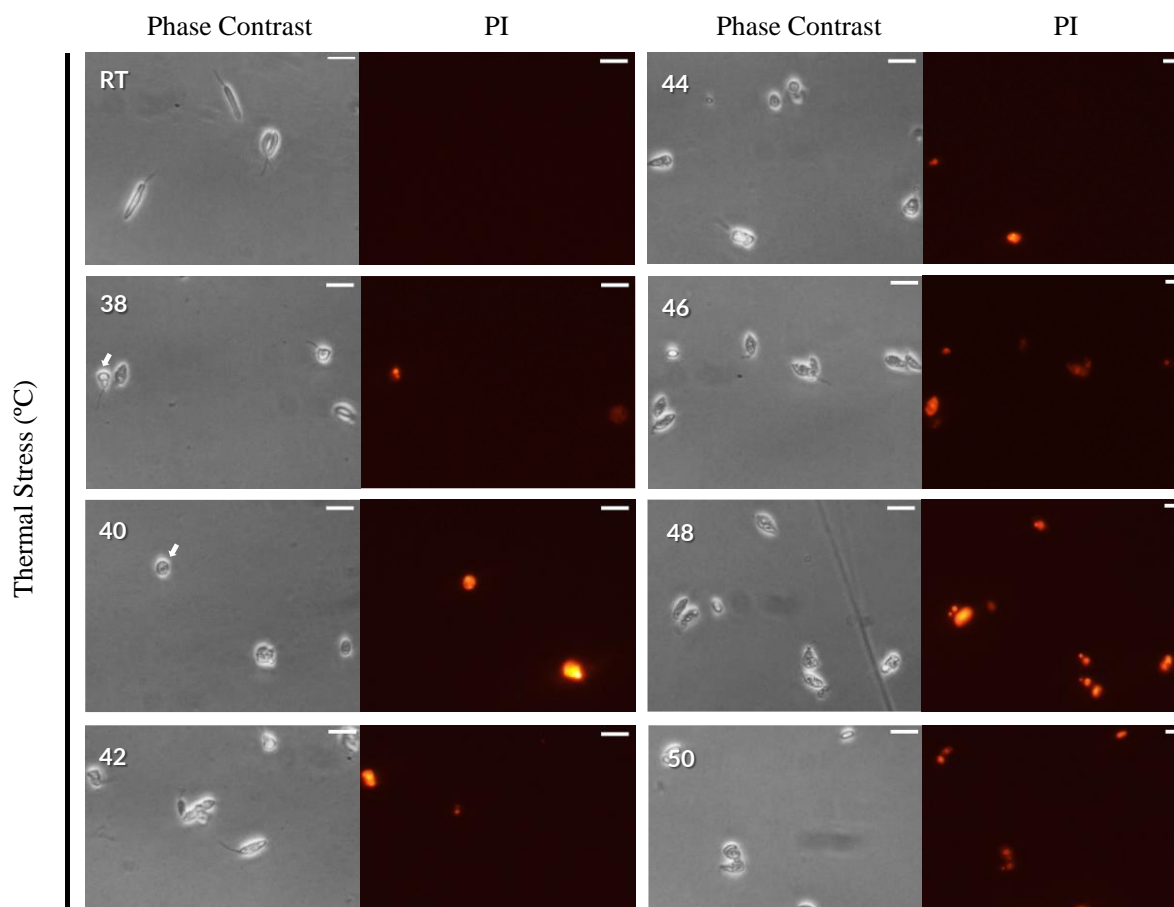


Figure 3 Thermal stress causes morphological changes and induces cell death. Representative slides from samples quantified in Figure 2 illustrating cellular response to thermal stress as characterized by uptake of propidium iodide. Scale bars represent 10 μm .

4.3 Hydrogen peroxide induces cell death

Parasites were exposed to increasing concentrations of H₂O₂ for 1 day prior to staining for cell death via PI (Figure 4). Dead cells from all treatment groups were characterized by bright, diffuse PI staining. The proportion of PI positive cells increased in a dose-dependent manner (Figure 5). At 25 mM H₂O₂, cells begin to exhibit the teardrop phenotype that was seen with cells exposed to temperature over 38 °C. At 50 mM H₂O₂, cells began to exhibit rounding, and this morphology becomes increasingly prominent at higher concentrations. Parasites seem to be able to tolerate H₂O₂ concentrations at or below 100 mM ($\leq 20\%$ PI⁺). However, once the dosage reaches higher concentrations (250 and 500 mM), there is a 2 to 4-fold increase. Membrane rupture is observed at 50 mM and above.

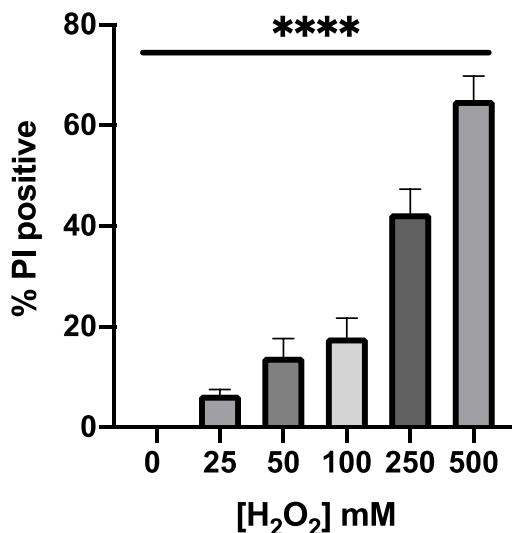


Figure 4 Quantification of cells oxidatively stressed present a dose-dependent response.

Cells were treated at a range of hydrogen peroxide for 1 day and stained with PI and percentage of PI positive cells in a sample was determined. Data are presented as arithmetic mean \pm S.E.M. ($n=3$, one-way ANOVA significance $p < 0.05$, unpaired T-test significance $p \leq 0.05$)

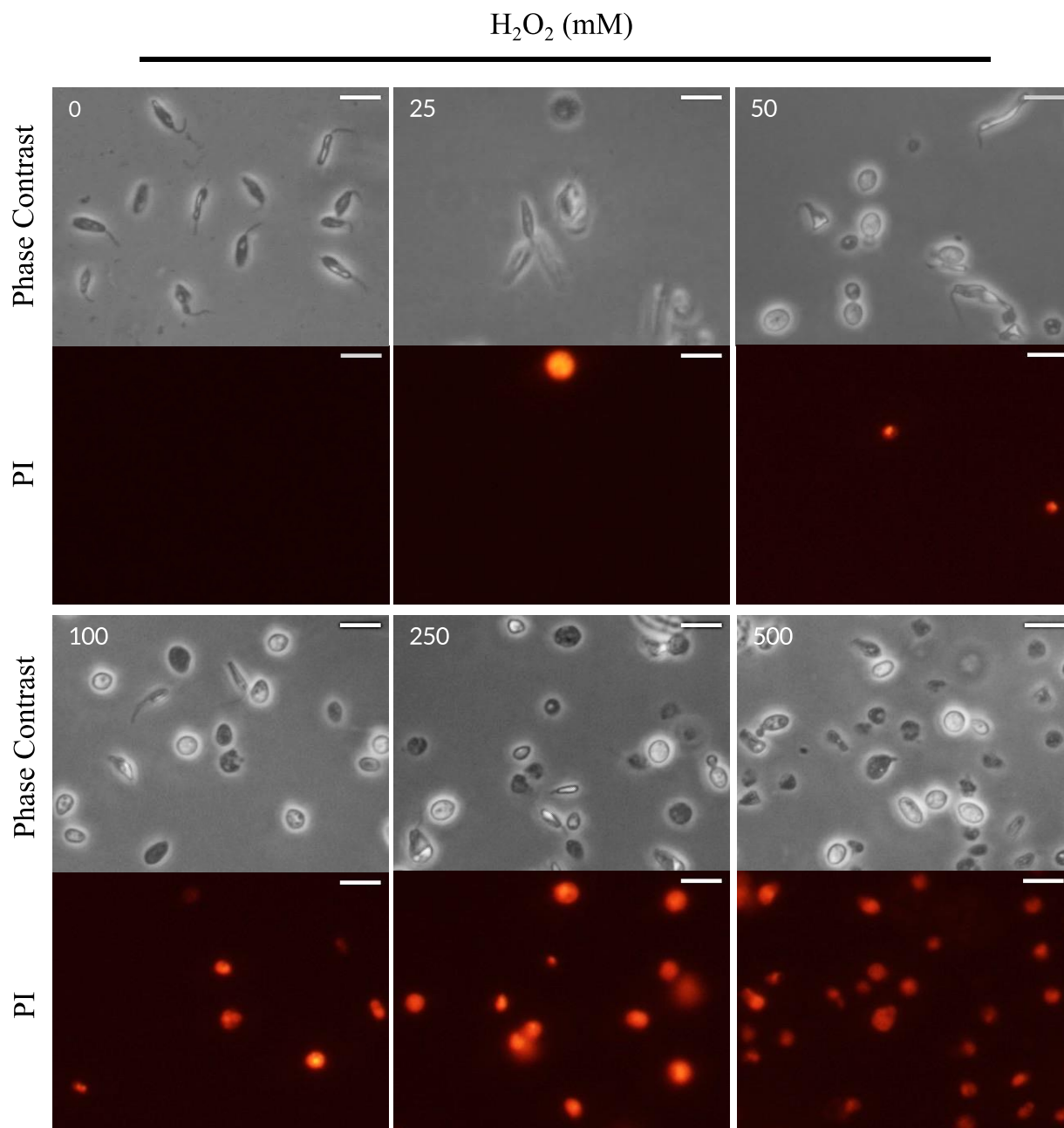


Figure 5 Hydrogen peroxide causes morphological changes and induces cell death. Representative slides from samples quantified in figure 4 illustrating cellular response to oxidative stress as characterized by uptake of propidium iodide. Scale bars represent 10 μm .

4.4 Rotenone induces cell death

Parasites were treated with either 2 μM or 10 μM rotenone for 1 day prior to staining dead cells with PI (Figure 5). There was a dose-dependent response observed, with a near 2-fold increase in percentage of cells staining positive for PI (Figure 6). In contrast to cells treated with hydrogen peroxide, rotenone treatment did not result in major changes in cell shape though PI positive cells continued to be rounded. There was no evidence of membrane rupture. Of note, PI staining in cells treated with 2 μM of rotenone was relatively dimmer and staining largely retained the shape of the kinetoplast and nucleus. However, in the 10 μM of rotenone sample, PI staining was much brighter and diffuse to the cell, with few instances of localized nuclear staining.

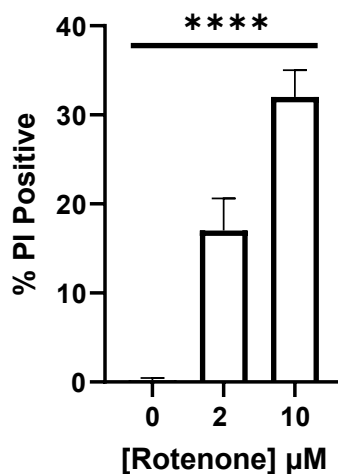


Figure 6 Quantification of cells treated with rotenone present a dose-dependent response. Cells were treated at 2 different doses of rotenone for 1 day and stained with PI and percentage of PI positive cells in a sample was determined. Data is presented as arithmetic mean \pm S.E.M. ($n=3$, one-way ANOVA significance $p < 0.05$, unpaired T-test significance $p \leq 0.05$)

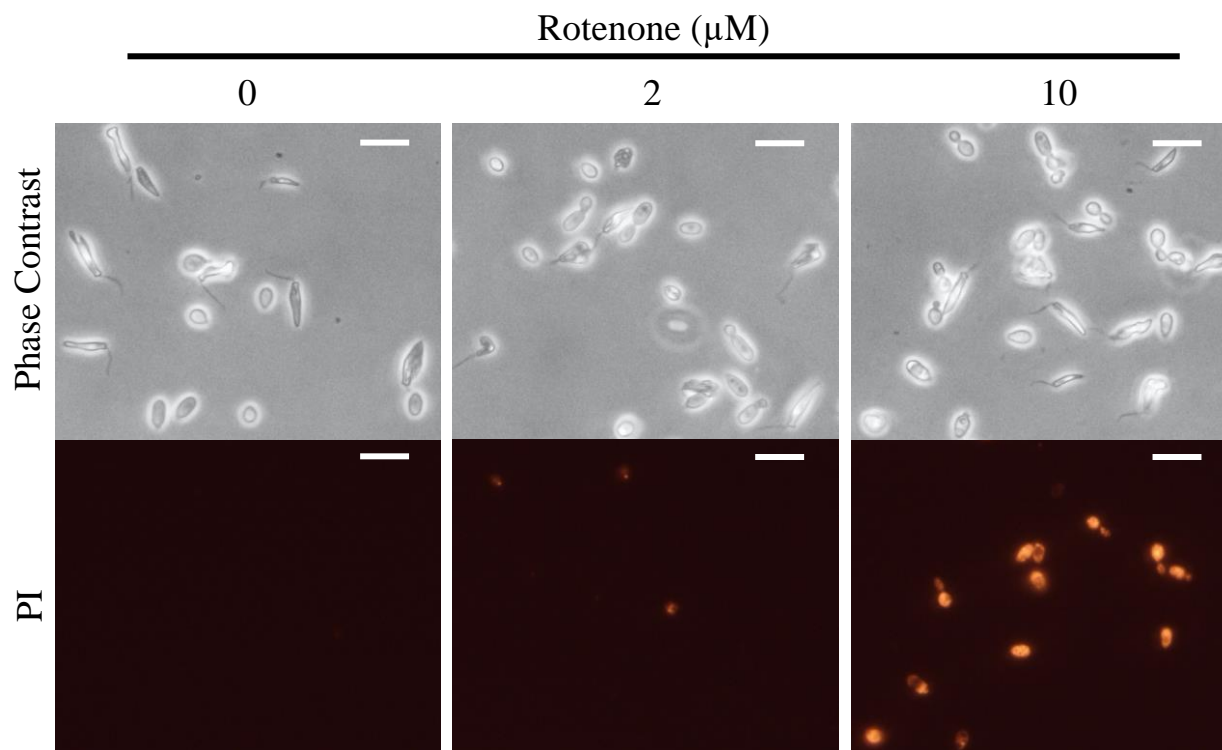


Figure 7 Rotenone causes morphological changes and induces cell death. Representative slides from samples quantified in Figure 6 illustrating cellular response to rotenone treatment as characterized by uptake of propidium iodide. Scale bars represent 10 μm .

4.5 Starvation induces autophagic processes

Parasites were washed multiple times with sterile PBS to remove residual media and either (1) nutrient starved in PBS or (2) serum starved in media not complemented with FBS. After starvation, autophagic vacuoles were stained with MDC (Figure 7). Three days after initiation of starvation, diffuse visualization of autophagic vacuoles were visible (data not shown). By day 7, cells starved in PBS exhibit formation of multiple, brightly fluorescent, autophagic vacuoles. In mammalian cells, a typical way to induce starvation is to deplete media of serum. To mimic this, cells were depleted of FBS for 1 day. Indeed, these cells began to form autophagic vacuoles (data not shown). To test a more time efficient method of autophagic induction, cells were serum starved for 1 hour. After 1 hour, autophagic vacuoles were also seen in the cells.

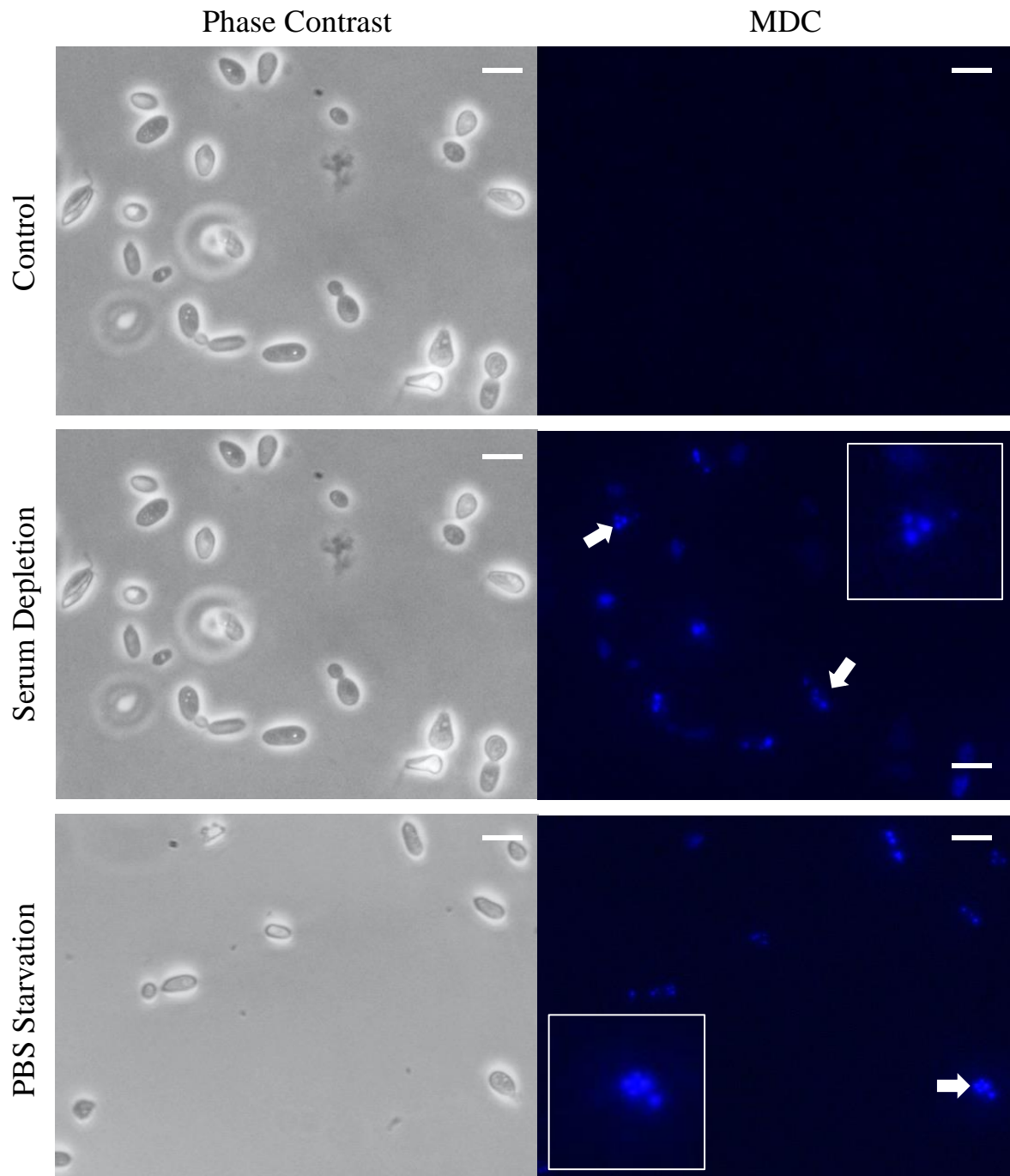


Figure 8 Serum depletion and nutrient starvation induces autophagic vacuole formation. Cells were either grown in regular media without FBS for 1 hour or in PBS for 7 days and stained with MDC. Arrows highlight clusters of autophagic vacuoles observed in single cells (enlarged in insets).

4.6 Cell death processes involve intranuclear DNA fragmentation

To test for changes in genomic DNA patterns, parasites were stressed and gDNA was separated by electrophoresis (Figure 8). To mimic known inducers of necrosis in mammalian cells, cells were treated with Triton X-100 (157). A sample was also heat shocked at 55 °C for 4 hours to also induce necrosis. Otherwise, treatments replicated previously established conditions including 44 °C for 1 day, 100 mM H₂O₂ for 1 day, serum starvation for 3 days, and 10 µM rotenone. The distinctive laddering pattern seen in mammalian models is not apparent in *C. fasciculata* under any stressors. Though bands are visible between 2000 and 3000 base pairs (bp) for cells treated with rotenone, Triton X-100, heat shock, thermal stress, and hydrogen peroxide. In addition to these, there are bands between 1500 and 2000 bp as well as above 3000 bp in the serum starvation sample. Although necrosis is typically characterized by smearing of gDNA on agarose gel, the supposed positive controls for necrosis resulted in presence of fragmented bands. It is important to note that cell samples were not homogenous prior to gDNA extraction. That is, only a small percentage of the pellet were dead cells.

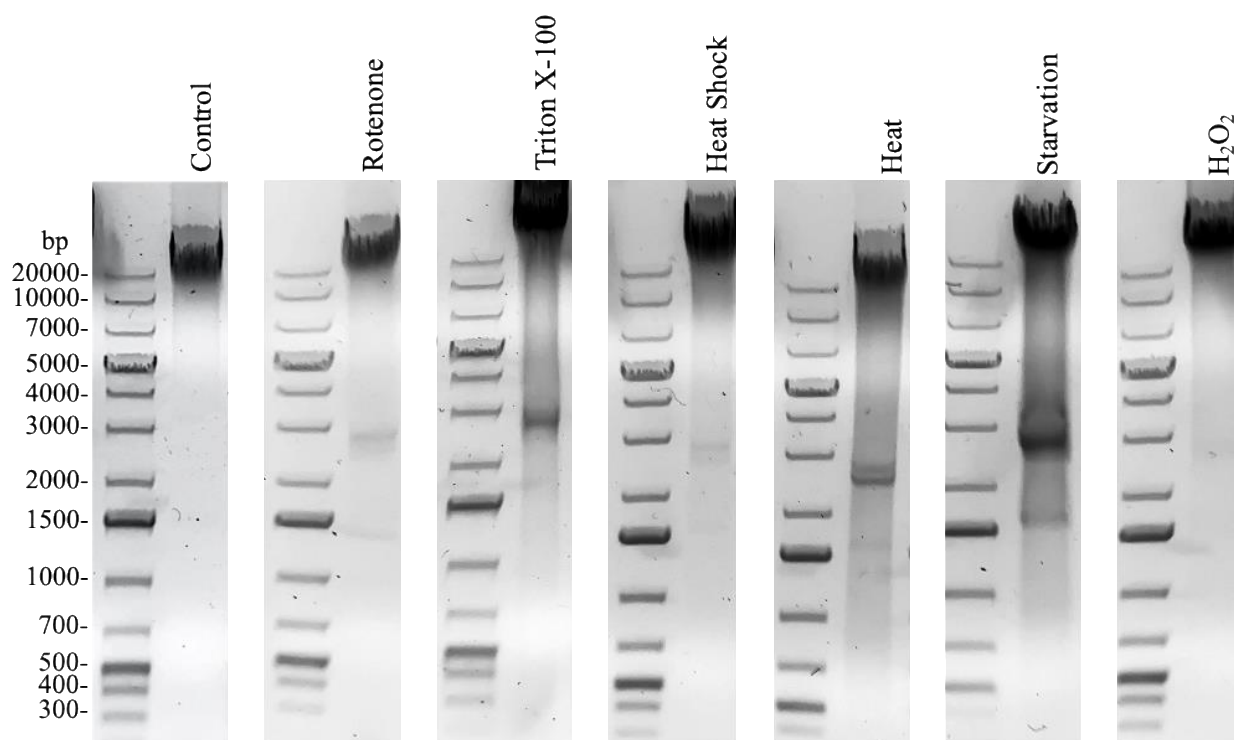


Figure 9 Variable changes in genomic pattern occur in response to cellular stress. Cells were stressed with 10 μ M rotenone (1 day), 44°C (1 day), serum starvation (3 days), or 100 mM hydrogen peroxide in accordance to established conditions. In an effort to mimic necrotic patterns as seen in mammalian systems, cells were also treated with 0.01% Triton X-100 (4 hours) and heat shock at 55°C (15 minutes). Ten micrograms of gDNA were separated on a 1% agarose gel.

4.7 Cellular stress induces nuclear morphology changes

To assess chromatin condensation arising from stress, parasites were either treated with 2 μ M rotenone or 44 °C thermal stress for 1 day prior to staining with Hoechst 33342 and PI (Figure 9) (158,159). Cells treated with low-dose rotenone exhibited similar representation of cell death as previously presented. Interestingly, these cells also had mild evidence of chromatin condensation as determined by Hoechst staining, as characterized by dim fluorescence. Overall, however, rotenone treated samples had notably less bright Hoechst staining than thermally-stressed cells. PI positive cells also had brightly fluorescent Hoechst 33342.

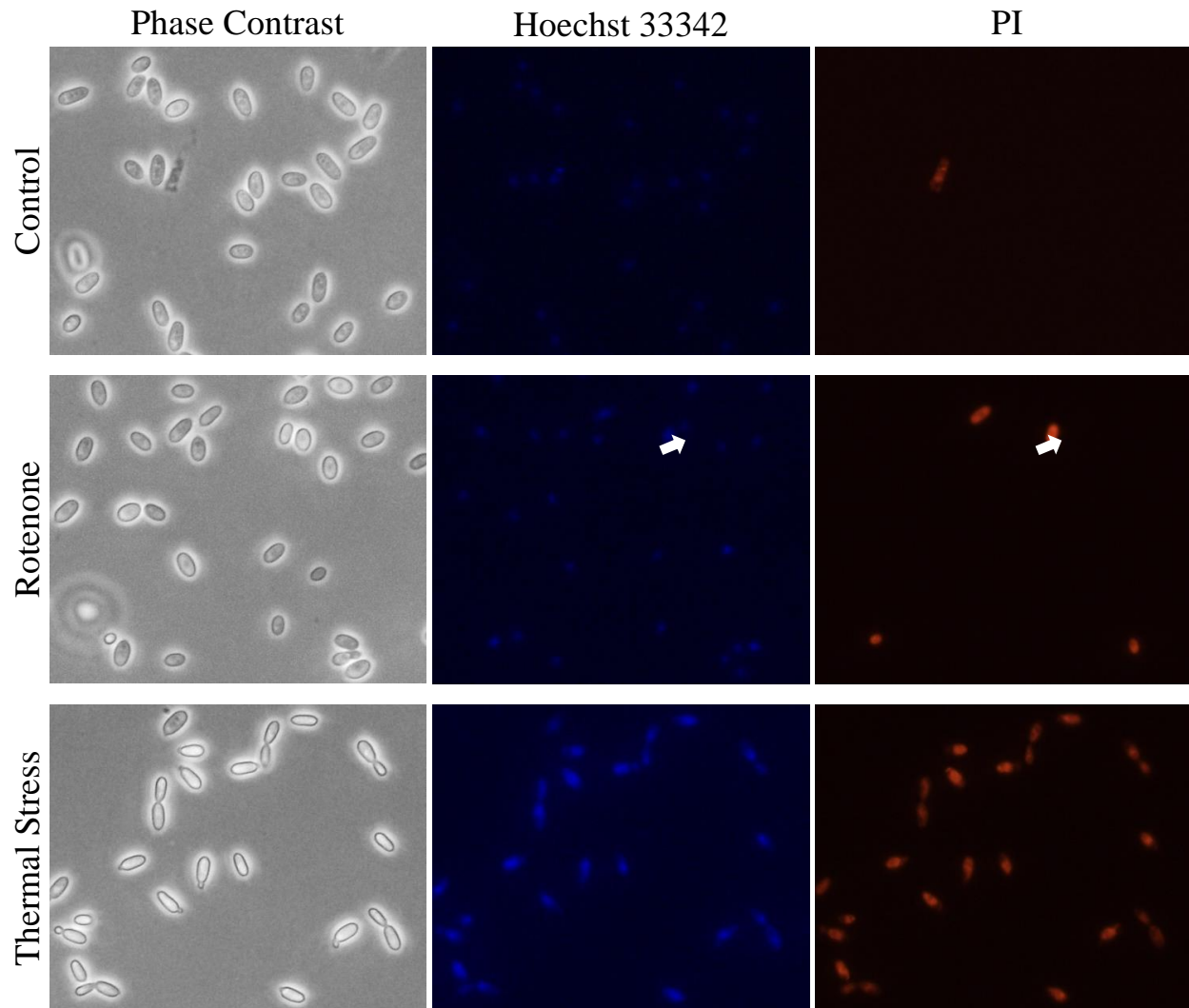


Figure 10 Cell death can be characterized by chromatin condensation. Cells were either treated with 2 μ M rotenone or at 44°C for 1 day and stained with Hoechst33342 to visualize changes in DNA and PI to confirm cell demise. While Hoechst 33342 is permeant to the nuclear and cell membrane, it only dimly stains cells at baseline (control group) but increases in brightness in cells undergoing cell death. Arrows highlight an example of a PI-positive and Hoechst 33342-positive cell in the rotenone treated group.

4.8 Characterizing cell death by morphological changes

Since thermal stress is the simplest and most efficient method to induce cell death in *C. fasciculata*, heat treatments were used to assess cell morphology more closely. Cells were exposed to non-necrosis-inducing (38 °C to 44 °C) and necrosis-inducing temperatures (46 °C to 50 °C) for 1 hour prior to staining with annexin-V and PI (Figure 10). Notable patterns of cell shape included the teardrop phenotype and cellular swelling and ballooning (Figure 10.D). The teardrop phenotype develops possibly as a result of sublethal stress. These cells stain neither for annexin-V nor PI. Cellular ballooning and swelling are described as enlarged, circular shape that is different from that of rounded dying cells, immotile attached cells, and shrunken cells and presumably present prior to membrane rupture. These cells either lacked staining of annexin-V and PI or had very faint annexin-V staining and staining of the nuclear bodies. Rupture of the plasma membrane was captured in multiple instances and is described as obvious displacement of the perimeter of the cell (Figure 10.H). These instances are all characterized as diffuse annexin-V staining and PI staining of the nuclear bodies. In a few instances in cells that appear to be undergoing membrane rupture, there can be observed release of intracellular contents as determined by both diffuse, dim “halo” staining of PI surrounding the cell as well as brightly stained small, punctate specks (Figure 10.F).

Observation of the nucleus and kinetoplast with PI reveal instances of karyorrhexis (fragmentation of the nucleus), nuclear dissolution, and nuclear condensation. Various cells exhibited signs of nuclear fragmentation, described by more than two brightly stained bodies (Figure 10.C) against a diffusely stained cell. This event may precede or follow nuclear condensation, as described by larger and relatively brighter stained nuclear bodies (Figure 10.D).

Finally, nuclear dissolution is evident and described as fluorescence of the entire cell body without discernable nuclear bodies.

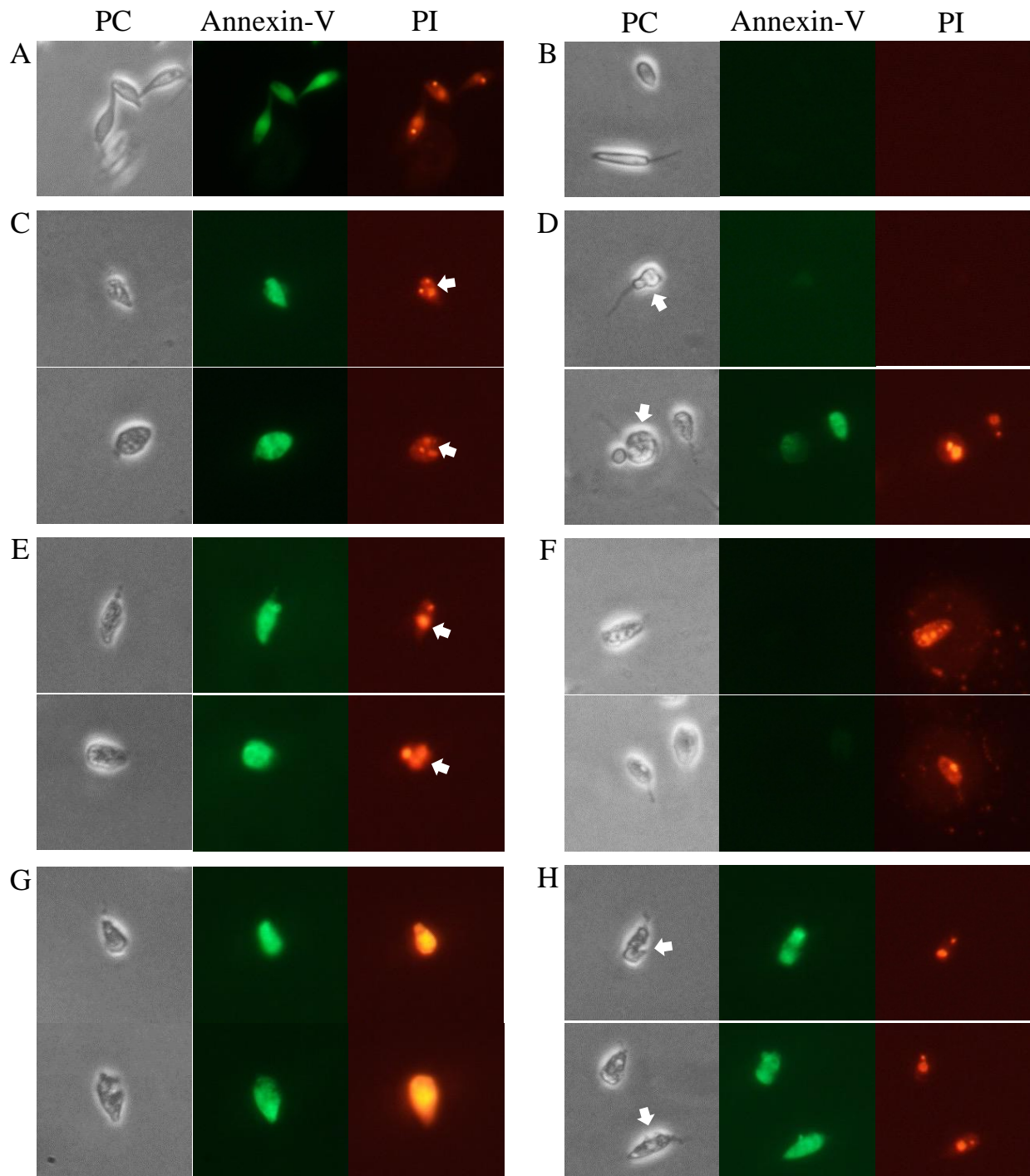


Figure 11 Distinct patterns of nuclear morphology and cell shape are observed in dying cells. Parasites were thermally stressed for 1 hour prior to staining with annexin-V and PI. Patterns of morphological changes were captured and categorized by (B) baseline, non-stressed, (C) nuclear fragmentation, (D) “teardropping” and ballooning, (E) DNA condensation, (F) release of intracellular contents, (G) dissolution of the nuclear bodies, and (H) membrane rupture.

5 DISCUSSION

The concept of manipulating apoptosis and other regulated cell death pathways to combat human pathologies and disease has yielded multiple advancements in modern medicine (160). Since the observation of the apoptotic-like phenotype and autophagic process in trypanosomatids (129,133,161), many questions have been raised regarding the potential applications of these mysterious pathways. For example, trypanosomatids lack key molecules involved in RCD that are present in their human hosts, suggesting that unique, undiscovered pathways could be druggable targets (162). Furthermore, investigation of various organelle roles in cell death is another area of interest. This can involve development of antiparasitic drugs or therapies that prompt dysfunction of certain organelles such as the mitochondrion or endoplasmic reticulum and thereby execute cell death (163). The biological relevance of the existence of these pathways in unicellular organisms also remains a question. Thus far, various hypotheses have been raised including altruism, maximizing biological fitness, population density control, and evasion of the host immune system (131,133,164,165). Despite the scientific interest in PCD in trypanosomes, there remains no comprehensive understanding of the molecular mechanisms underlying these processes in these parasites. Furthermore, basic questions remain regarding morphological characteristics of parasites undergoing programmed death and clarification of these features beyond the ambiguity conveyed by the term “apoptotic-like phenotype”.

This study aimed to establish the means of utilizing *C. fasciculata* as a model organism to study cell death processes in trypanosomatids. The comprehensive goal was to align the morphological and genomic profile of *C. fasciculata* against known regulated cell death pathways in other systems (Figure 12). Firstly, targeted investigation of *C. fasciculata*, *T. brucei*, *T. cruzi*, and *L. major* genomes illustrates that key molecules involved in necroptosis, apoptosis,

paraptosis, pyroptosis, and oxeiptosis do not exist in trypanosomatid genomes. In contrast, trypanosomatids possess multiple key partners involved in ferroptosis and parthanatos. Additionally, multiple ATG proteins responsible for important steps in autophagy in other systems are present in trypanosomatids, consistent with prior studies that these parasites are capable of engaging in autophagy (166-171). Furthermore, it is presented here that *Crithidia* produce autophagic vacuoles in starvation conditions. These findings suggest that trypanosomatids may have a divergent or unique mechanism of cell death and/or engage in parthanatos or ferroptosis. In 2020, Teulière *et al.* investigated the characteristic genes associated with various forms of RCD across mitochondriate protists including *Trypanosoma* and *Leishmania* spp. (172). They concluded that presence of aerobic mitochondria was coupled with the conservation of apoptosis-associated genes, supporting the endosymbiotic origin pathway. They also suggest that selection for RCD pathways such as apoptosis are developmentally linked to multicellularity. Kaczanowski *et al.* also used bioinformatics to suggest that apoptotic mechanisms in protozoan parasites have diverged during evolution and existing homologs are shared while other key proteins are “replaced” by uncharacterized molecules with similar biochemical function (173). This supports the observations, both in published studies and this project, that protozoal parasites can undergo apoptosis-like cell death but lack the molecules normally thought to mediate these processes(129,174).

Secondly, exposure of *C. fasciculata* to various stressors result in induction of cell death, but variations in the patterns suggest that multiple pathways for cell death exist. This may resemble RCD in multicellular organisms in which the response to stress in cells depends on the nature and duration of the exogenous factors of stressors (175). For example, cells respond differentially towards DNA damage and oxidative stress. In this study, when parasites are

thermally stressed below the temperatures of 46 °C, they display features of swelling, lysis, chromatin condensation, DNA fragmentation, nuclear dissolution, and membrane rupture, consistent with necroptosis. It has been suggested that thermal stress-induced death in mammalian systems is necroptotic (176,177). Key molecules like necroptosome forming RIPK1-RIPK3 and cell permeabilizing protein MLKL are absent in trypanosome genomes. In addition to necroptosis, heat stress is also linked to various cell death pathways including apoptosis in mammalian cells via irreversible damage to DNA, RNA, and proteins, cessation of the cell cycle, and the relationship with increased ROS (178). Thermotolerance in these models is mediated by heat shock proteins (HSP), a family of proteins that can protect cells from multiple stressors including ROS and UV (179). HSPs play roles in various cell death pathways including intrinsic and extrinsic apoptosis and necroptosis. HSPs can regulate stress kinases JNK and ERK, control the release of cytochrome c, and block execution of apoptosis via caspase-3, Apaf-1, and cytochrome c (180,181). HSPs are well conserved in trypanosomatids and have been implicated in thermotolerance and survival in the host that occur as parasites adjust to temperature changes that occur within the environment and during life cycles (182,183). Interestingly, trypanosomatids also possess homologs for the MAPK stress pathway (ERK, JNK, and p38), and studies have identified these proteins are critical for proliferation *in vivo* (184,185). It is evident here that parasites may possess molecular mechanisms divergent from mammalian caspase-centralized apoptosis and necroptosis. These pathways could involve HSPs and possibly the MAPK pathway, which can mediate cellular responses to thermal stress and lead to a cascade of events that is “oncosis-like”, as characterized by cell swelling and membrane rupture.

Similar to mammalian systems, the mitochondria play a central role in RCD in trypanosomatids (147,151,186), and investigation of mitochondrial activity and morphology can

be informative in defining cell death pathways. For example, defects and dysregulation of complex I of the electron transport chain is linked to cell death in mammalian cell models. In these models, rotenone inhibits oxidative phosphorylation activity of complex I, causing incomplete electron transfer to oxygen (187). It therefore induces apoptosis via excess production of mitochondrial ROS, opening of the mitochondrial permeability transition pore (MTP), cytochrome c release, and caspase-3 execution (188,189). Rotenone inhibits complex I activity in *T. brucei* (190). *Crithidia fasciculata* is also evidently sensitive to rotenone (Figure 7). The drug induces cell death in *C. fasciculata* and is associated with what appears to be nuclear fragmentation and chromatin condensation. However, these events are not accompanied with an oncosis-like phenotype. Given trypanosomatids lack homologs for caspase-3, it is unlikely that they share the same mitochondrial mechanism that is seen in the mammalian cell death pathway. Interestingly, a transmembrane Bax inhibitor-1 motif 5 homolog (TMBIM5) is present in trypanosomatids, suggesting a possible mechanism for executing cell death by other means. The mammalian, TMBIM family consists of six proteins with different subcellular localizations who are collectively involved in cellular Ca^{2+} signaling, cell survival, and stress resistance (191). In mammals, TMBIM5 localizes to the mitochondrion and regulates cytochrome c release in the context of activating intrinsic apoptosis (156). TMBIM5 is the sole representative of this protein family in trypanosomatid genomes. Another interesting mitochondrial protein encoded in the trypanosomatid genomes is endonuclease G, a protein that in mammals is involved in caspase-independent apoptosis by degrading DNA via translocation to the nucleus as a consequence of oxidative stress (192). Evaluation of the endoG homolog in *T. brucei* and *Leishmania* has proven its functional capacity for intrinsic nuclease activity under oxidative or differentiation-related

stress (193). It is possible a mitochondrial, “apoptotic-like” mechanism exists in trypanosomatids and involves TMBIM5, endonuclease G, and cytochrome c.

Another mitochondrial-associated source of cell death is oxidative stress, which is triggered by excess ROS production including H_2O_2 , a byproduct of mitochondrial respiration and superoxide dismutase activity. Excess levels of ROS, occurring when the cell’s antioxidant and scavenging system are overwhelmed, causes irreversible damage to DNA and organelles, and leads to regulated cell death. Cytochrome c is known to play a role in regulating H_2O_2 activity so that mitochondrial ROS levels are below the apoptosis-triggering threshold. Cytochrome c has a ROS-scavenger role as in non-apoptotic conditions. Cytochrome c released from the mitochondria caused by ROS production can actually have antioxidant properties (194). In this study, *Crithidia* treated with external H_2O_2 displayed signs of induced-cell death in an oncosis-like manner as characterized by nuclear dissolution, cellular swelling, membrane rupture, and release of intracellular contents (Figure 5). Ferroptosis is a PCD pathway that is triggered by failure of antioxidant systems and the subsequent accumulation of lipid peroxidation following ROS/free radical-associated fatty acid radical production, as catalyzed by free iron. Various antioxidant and ROS-scavenging properties have been identified in *Leishmania* and *Trypanosoma* spp. including catalase, glutathione reductase, and glutathione peroxidase (195-197). Trypanosomatids also possess genes encoding key proteins associated with ferroptosis (GPX4, FSP1, DHODH, ACLS4, and SLC7A11). There has been limited investigation of ferroptosis in trypanosomatids. In 2018 Bocacz observed ferroptosis-like cell death in *T. brucei* and determined that tryparedoxin peroxidases, molecular relative of glutathione peroxidase 4, play key role in the antioxidantizing of lipid-derived hydroperoxides (198). Bogacz additionally reported that the species is likely sensitive to iron-induced lipid peroxidation originating at the

mitochondrial level, as obvious morphological and biochemical changes were noted in the mitochondria (198). In mammalian cells, it was recently established that the protein dihydroorotate dehydrogenase (DHODH) plays a key role in mitigating lipid peroxidation and limits mitochondrially-mediated ferroptosis similar to that of the FSP1 and GPX4 (199). Functional investigation of *Trypanosoma* DHODH has been performed, establishing that is a key component of the pyrimidine biosynthetic pathway. However, the role of DHODH has not been investigated with respect to ferroptosis. This protein and other molecules involved in the ferroptosis system could possibly contribute to an oxidative stress-induced cell death pathway.

Trypanosomatids additionally possess homologs for PARP and PARG, key players in the mitochondrial-associated, caspase-independent cell death pathway called parthanatos. This cell death process is triggered by oxidative stress and genotoxic damage in mammalian systems, resulting in DNA fragmentation and chromatin condensation (125). Investigation of PARP and PARG in *T. brucei* highlighted changes in resistance to H₂O₂ and genotoxic stimuli, resulting in cell death (200). Parthanatos is dependent on the apoptosis-inducing factor protein (AIF) in mammalian models. This protein was not identified in the trypanosomatid genomes in the current study. It is suspected that these proteins could have a mechanism different than mammalian models, independent of AIF, in trypanosomatids alluding towards a unique regulated cell death pathway.

	<i>C. fasciculata</i>	Apoptosis	Necroptosis	Ferroptosis	Paraptosis	Oxeiptosis	Pyroptosis	Parthanatos
Cell lysis	+	-	+	-	-	-	+	+
Cell swelling	+	-	+	+	-	?	+	-
Membrane blebbing	nd	+	-	-	-	?	+	-
Mitochondrial swelling	nd		-	-	+	?	?	-
DNA fragmentation	+	+	+	-	-	?	-	+
Nucleus intact	-/+	-	-	+	+	?	+	-
Chromatin condensation	+	+	+	-	-	?	+	+
Inflammation	nd	-	+	+	-	-	+	+

Figure 12 *Crithidia fasciculata*'s morphological profile of cell death is evidently unique from currently described patterns. Literature review was conducted to determine known characteristics of the PCD pathways of interest. Negative (-), red boxes indicate lack of that particular feature. Positive (+), green boxes indicate presence of that particular feature. Question marks (?) indicate that current understandings of this pathway have not reviewed these features. In this study, multiple features were not investigated and therefore not determined (nd).

In conclusion, it is evident that trypanosomatids are capable of engaging in a regulated cell death pathway, characterized by differential changes in the cell in response to various stressors. When comparing the observed nuclear and morphological changes as well as the homology profile of *C. fasciculata* with that already known in other species, it is evident that trypanosomatids possess unique pathways of regulated cell death inaccurately referred to as "apoptosis-like". It is clear that the parasites can engage in at least two distinct pathways, one characterized by swelling, membrane rupture, and release of intracellular contents, and one without these characteristics. This study highlights multiple avenues of mystery that require further investigation to better understand PCD in these influential parasites.

REFERENCES

1. Podlipaev, S. (2001) The more insect trypanosomatids under study-the more diverse Trypanosomatidae appears. *Int J Parasitol* **31**, 648-652
2. Simpson, A. G., Stevens, J. R., and Lukes, J. (2006) The evolution and diversity of kinetoplastid flagellates. *Trends Parasitol* **22**, 168-174
3. Alvar, J., Velez, I. D., Bern, C., Herrero, M., Desjeux, P., Cano, J., Jannin, J., den Boer, M., and Team, W. H. O. L. C. (2012) Leishmaniasis worldwide and global estimates of its incidence. *PLoS One* **7**, e35671
4. Bates, P. A. (2007) Transmission of *Leishmania* metacyclic promastigotes by phlebotomine sand flies. *Int J Parasitol* **37**, 1097-1106
5. Maroli, M., Feliciangeli, M. D., Bichaud, L., Charrel, R. N., and Gradoni, L. (2013) Phlebotomine sandflies and the spreading of leishmaniasis and other diseases of public health concern. *Med Vet Entomol* **27**, 123-147
6. Andrade-Narvaez, F. J., Vargas-Gonzalez, A., Canto-Lara, S. B., and Damian-Centeno, A. G. (2001) Clinical picture of cutaneous leishmaniasis due to *Leishmania* (*Leishmania*) *mexicana* in the Yucatan peninsula, Mexico. *Mem Inst Oswaldo Cruz* **96**, 163-167
7. Sunter, J., and Gull, K. (2017) Shape, form, function and *Leishmania* pathogenicity: from textbook descriptions to biological understanding. *Open Biol* **7**
8. (2017) Global leishmaniasis update, 2006-2015: a turning point in leishmaniasis surveillance. *Wkly Epidemiol Rec* **92**, 557-565
9. Bennis, I., De Brouwere, V., Belrhiti, Z., Sahibi, H., and Boelaert, M. (2018) Psychosocial burden of localised cutaneous Leishmaniasis: a scoping review. *BMC Public Health* **18**, 358
10. Organization, W. H. (2010) Control of the leishmaniasis: report of a meeting of the WHO Expert Committee on the Control of Leishmaniasis, Geneva. *WHO Technical Report Series*
11. Torres-Guerrero, E., Quintanilla-Cedillo, M. R., Ruiz-Esmenjaud, J., and Arenas, R. (2017) Leishmaniasis: a review. *F1000Res* **6**, 750
12. Barrett, M. P., and Croft, S. L. (2012) Management of trypanosomiasis and leishmaniasis. *Br Med Bull* **104**, 175-196
13. Aronson, N., Herwaldt, B. L., Libman, M., Pearson, R., Lopez-Velez, R., Weina, P., Carvalho, E., Ephros, M., Jeronimo, S., and Magill, A. (2017) Diagnosis and Treatment of Leishmaniasis: Clinical Practice Guidelines by the Infectious Diseases Society of America (IDSA) and the American Society of Tropical Medicine and Hygiene (ASTMH). *Am J Trop Med Hyg* **96**, 24-45
14. Mann, S., Frasca, K., Scherrer, S., Henao-Martinez, A. F., Newman, S., Ramanan, P., and Suarez, J. A. (2021) A Review of Leishmaniasis: Current Knowledge and Future Directions. *Curr Trop Med Rep*, 1-12
15. Sundar, S., and Chakravarty, J. (2013) Leishmaniasis: an update of current pharmacotherapy. *Expert Opin Pharmacother* **14**, 53-63
16. Sundar, S., Thakur, B. B., Tandon, A. K., Agrawal, N. R., Mishra, C. P., Mahapatra, T. M., and Singh, V. P. (1994) Clinicoepidemiological study of drug resistance in Indian kala-azar. *BMJ* **308**, 307
17. Perez-Molina, J. A., and Molina, I. (2018) Chagas disease. *Lancet* **391**, 82-94
18. (2019) Chagas disease (American trypanosomiasis). *World Health Organization*

20. Schofield, C. J., Jannin, J., and Salvatella, R. (2006) The future of Chagas disease control. *Trends Parasitol* **22**, 583-588
21. Lidani, K. C. F., Andrade, F. A., Bavia, L., Damasceno, F. S., Beltrame, M. H., Messias-Reason, I. J., and Sandri, T. L. (2019) Chagas Disease: From Discovery to a Worldwide Health Problem. *Front Public Health* **7**, 166
22. Guarner, J. (2019) Chagas disease as example of a reemerging parasite. *Semin Diagn Pathol* **36**, 164-169
23. Rassi, A., Jr., Rassi, A., and Marin-Neto, J. A. (2010) Chagas disease. *Lancet* **375**, 1388-1402
24. Vago, A. R., Andrade, L. O., Leite, A. A., d'Avila Reis, D., Macedo, A. M., Adad, S. J., Tostes, S., Jr., Moreira, M. C., Filho, G. B., and Pena, S. D. (2000) Genetic characterization of *Trypanosoma cruzi* directly from tissues of patients with chronic Chagas disease: differential distribution of genetic types into diverse organs. *Am J Pathol* **156**, 1805-1809
25. Fiorelli, A. I., Santos, R. H., Oliveira, J. L., Jr., Lourenco-Filho, D. D., Dias, R. R., Oliveira, A. S., da Silva, M. F., Ayoub, F. L., Bacal, F., Souza, G. E., Bocchi, E. A., and Stolf, N. A. (2011) Heart transplantation in 107 cases of Chagas' disease. *Transplant Proc* **43**, 220-224
26. Ribeiro, V., Dias, N., Paiva, T., Hagstrom-Bex, L., Nitz, N., Pratesi, R., and Hecht, M. (2020) Current trends in the pharmacological management of Chagas disease. *Int J Parasitol Drugs Drug Resist* **12**, 7-17
27. Nunes, M. C., Dones, W., Morillo, C. A., Encina, J. J., Ribeiro, A. L., and Council on Chagas Disease of the Interamerican Society of, C. (2013) Chagas disease: an overview of clinical and epidemiological aspects. *J Am Coll Cardiol* **62**, 767-776
28. Stich, A., Abel, P. M., and Krishna, S. (2002) Human African trypanosomiasis. *BMJ* **325**, 203-206
29. Global Burden of Disease Cancer, C., Fitzmaurice, C., Abate, D., Abbasi, N., Abbastabar, H., Abd-Allah, F., Abdel-Rahman, O., Abdelalim, A., Abdoli, A., Abdollahpour, I., Abdulle, A. S. M., Abebe, N. D., Abraha, H. N., Abu-Raddad, L. J., Abualhasan, A., Adedeji, I. A., Advani, S. M., Afarideh, M., Afshari, M., Aghaali, M., Agius, D., Agrawal, S., Ahmadi, A., Ahmadian, E., Ahmadpour, E., Ahmed, M. B., Akbari, M. E., Akinyemiju, T., Al-Aly, Z., AlAbdulKader, A. M., Alahdab, F., Alam, T., Alamene, G. M., Alemnew, B. T. T., Alene, K. A., Alinia, C., Alipour, V., Aljunid, S. M., Bakeshei, F. A., Almadi, M. A. H., Almasi-Hashiani, A., Alsharif, U., Alsowaidi, S., Alvis-Guzman, N., Amini, E., Amini, S., Amoako, Y. A., Anbari, Z., Anber, N. H., Andrei, C. L., Anjomshoa, M., Ansari, F., Ansariadi, A., Appiah, S. C. Y., Arab-Zozani, M., Arabloo, J., Arefi, Z., Aremu, O., Areri, H. A., Artaman, A., Asayesh, H., Asfaw, E. T., Ashagre, A. F., Assadi, R., Ataenia, B., Atalay, H. T., Ataro, Z., Atique, S., Ausloos, M., Avila-Burgos, L., Avokpaho, E., Awasthi, A., Awoke, N., Ayala Quintanilla, B. P., Ayanore, M. A., Ayele, H. T., Babaee, E., Bacha, U., Badawi, A., Bagherzadeh, M., Bagli, E., Balakrishnan, S., Balouchi, A., Barnighausen, T. W., Battista, R. J., Behzadifar, M., Behzadifar, M., Bekele, B. B., Belay, Y. B., Belayneh, Y. M., Berfield, K. K. S., Berhane, A., Bernabe, E., Beuran, M., Bhakta, N., Bhattacharyya, K., Biadgo, B., Bijani, A., Bin Sayeed, M. S., Birungi, C., Bisignano, C., Bitew, H., Bjorge, T., Bleyer, A., Bogale, K. A., Bojia, H. A., Borzi, A. M., Bosetti, C., Bou-Orm, I. R., Brenner, H., Brewer, J. D., Briko, A. N., Briko, N. I., Bustamante-Teixeira, M. T., Butt, Z. A.,

Carreras, G., Carrero, J. J., Carvalho, F., Castro, C., Castro, F., Catala-Lopez, F., Cerin, E., Chaiah, Y., Chanie, W. F., Chattu, V. K., Chaturvedi, P., Chauhan, N. S., Chehrazi, M., Chiang, P. P., Chichiabellu, T. Y., Chido-Amajuoyi, O. G., Chimed-Ochir, O., Choi, J. J., Christopher, D. J., Chu, D. T., Constantin, M. M., Costa, V. M., Crocetti, E., Crowe, C. S., Curado, M. P., Dahlawi, S. M. A., Damiani, G., Darwish, A. H., Daryani, A., das Neves, J., Demeke, F. M., Demis, A. B., Demissie, B. W., Demoz, G. T., Denova-Gutierrez, E., Derakhshani, A., Deribe, K. S., Desai, R., Desalegn, B. B., Desta, M., Dey, S., Dharmaratne, S. D., Dhimal, M., Diaz, D., Dinberu, M. T. T., Djalalinia, S., Doku, D. T., Drake, T. M., Dubey, M., Dubljanin, E., Duken, E. E., Ebrahimi, H., Effiong, A., Eftekhari, A., El Sayed, I., Zaki, M. E. S., El-Jaafary, S. I., El-Khatib, Z., Elemineh, D. A., Elkout, H., Ellenbogen, R. G., Elsharkawy, A., Emamian, M. H., Endalew, D. A., Endries, A. Y., Eshrati, B., Fadhil, I., Fallah Omrani, V., Faramarzi, M., Farhangi, M. A., Farioli, A., Farzadfar, F., Fentahun, N., Fernandes, E., Feyissa, G. T., Filip, I., Fischer, F., Fisher, J. L., Force, L. M., Foroutan, M., Freitas, M., Fukumoto, T., Futran, N. D., Gallus, S., Gankpe, F. G., Gayesa, R. T., Gebrehiwot, T. T., Gebremeskel, G. G., Gedefaw, G. A., Gelaw, B. K., Geta, B., Getachew, S., Gezae, K. E., Ghafourifard, M., Ghajar, A., Ghashghaee, A., Gholamian, A., Gill, P. S., Ginindza, T. T. G., Girmay, A., Gizaw, M., Gomez, R. S., Gopalani, S. V., Gorini, G., Goulart, B. N. G., Grada, A., Ribeiro Guerra, M., Guimaraes, A. L. S., Gupta, P. C., Gupta, R., Hadkhale, K., Haj-Mirzaian, A., Haj-Mirzaian, A., Hamadeh, R. R., Hamidi, S., Hanfore, L. K., Haro, J. M., Hasankhani, M., Hasanzadeh, A., Hassen, H. Y., Hay, R. J., Hay, S. I., Henok, A., Henry, N. J., Herteliu, C., Hidru, H. D., Hoang, C. L., Hole, M. K., Hoogar, P., Horita, N., Hosgood, H. D., Hosseini, M., Hosseinzadeh, M., Hostiuc, M., Hostiuc, S., Househ, M., Hussen, M. M., Ileanu, B., Ilic, M. D., Innos, K., Irvani, S. S. N., Iseh, K. R., Islam, S. M. S., Islami, F., Jafari Balalami, N., Jafarinia, M., Jahangiry, L., Jahani, M. A., Jahanmehr, N., Jakovljevic, M., James, S. L., Javanbakht, M., Jayaraman, S., Jee, S. H., Jenabi, E., Jha, R. P., Jonas, J. B., Jonnagaddala, J., Joo, T., Jungari, S. B., Jurisson, M., Kabir, A., Kamangar, F., Karch, A., Karimi, N., Karimian, A., Kasaeian, A., Kasahun, G. G., Kassa, B., Kassa, T. D., Kassaw, M. W., Kaul, A., Keiyoro, P. N., Kelbore, A. G., Kerbo, A. A., Khader, Y. S., Khalilarjmandi, M., Khan, E. A., Khan, G., Khang, Y. H., Khatab, K., Khater, A., Khayamzadeh, M., Khazaei-Pool, M., Khazaei, S., Khoja, A. T., Khosravi, M. H., Khubchandani, J., Kianipour, N., Kim, D., Kim, Y. J., Kisa, A., Kisa, S., Kissimova-Skarbek, K., Komaki, H., Koyanagi, A., Krohn, K. J., Bicer, B. K., Kugbey, N., Kumar, V., Kuupiel, D., La Vecchia, C., Lad, D. P., Lake, E. A., Lakew, A. M., Lal, D. K., Lami, F. H., Lan, Q., Lasrado, S., Lauriola, P., Lazarus, J. V., Leigh, J., Leshargie, C. T., Liao, Y., Limenih, M. A., Listl, S., Lopez, A. D., Lopukhov, P. D., Lunevicius, R., Madadin, M., Magdeldin, S., El Razek, H. M. A., Majeed, A., Maleki, A., Malekzadeh, R., Manafi, A., Manafi, N., Manamo, W. A., Mansourian, M., Mansournia, M. A., Mantovani, L. G., Maroufizadeh, S., Martini, S. M. S., Mashamba-Thompson, T. P., Massenburg, B. B., Maswabi, M. T., Mathur, M. R., McAlinden, C., McKee, M., Meheretu, H. A. A., Mehrotra, R., Mehta, V., Meier, T., Melaku, Y. A., Meles, G. G., Meles, H. G., Melese, A., Melku, M., Memiah, P. T. N., Mendoza, W., Menezes, R. G., Merat, S., Meretoja, T. J., Mestrovic, T., Miazgowski, B., Miazgowski, T., Mihretie, K. M. M., Miller, T. R., Mills, E. J., Mir, S. M., Mirzaei, H., Mirzaei, H. R., Mishra, R., Moazen, B., Mohammad, D. K., Mohammad, K. A., Mohammad, Y., Darwesh, A. M., Mohammadbeigi, A., Mohammadi, H., Mohammadi, M., Mohammadian, M.,

Mohammadian-Hafshejani, A., Mohammadoo-Khorasani, M., Mohammadpourhodki, R., Mohammed, A. S., Mohammed, J. A., Mohammed, S., Mohebi, F., Mokdad, A. H., Monasta, L., Moodley, Y., Moosazadeh, M., Moossavi, M., Moradi, G., Moradi-Joo, M., Moradi-Lakeh, M., Moradpour, F., Morawska, L., Morgado-da-Costa, J., Morisaki, N., Morrison, S. D., Mosapour, A., Mousavi, S. M., Muche, A. A., Muhammed, O. S. S., Musa, J., Nabhan, A. F., Naderi, M., Nagarajan, A. J., Nagel, G., Nahvijou, A., Naik, G., Najafi, F., Naldi, L., Nam, H. S., Nasiri, N., Nazari, J., Negroi, I., Neupane, S., Newcomb, P. A., Nggada, H. A., Ngunjiri, J. W., Nguyen, C. T., Nikniaz, L., Ningrum, D. N. A., Nirayo, Y. L., Nixon, M. R., Nnaji, C. A., Nojomi, M., Nosratnejad, S., Shiadeh, M. N., Obsa, M. S., Ofori-Asenso, R., Ogbo, F. A., Oh, I. H., Olagunju, A. T., Olagunju, T. O., Oluwasanu, M. M., Omonisi, A. E., Onwujekwe, O. E., Oommen, A. M., Oren, E., Ortega-Altamirano, D. D. V., Ota, E., Otstavnov, S. S., Owolabi, M. O., P, A. M., Padubidri, J. R., Pakhale, S., Pakpour, A. H., Pana, A., Park, E. K., Parsian, H., Pashaei, T., Patel, S., Patil, S. T., Pennini, A., Pereira, D. M., Piccinelli, C., Pillay, J. D., Pirestani, M., Pishgar, F., Postma, M. J., Pourjafar, H., Pourmalek, F., Pourshams, A., Prakash, S., Prasad, N., Qorbani, M., Rabiee, M., Rabiee, N., Radfar, A., Rafiei, A., Rahim, F., Rahimi, M., Rahman, M. A., Rajati, F., Rana, S. M., Raoofi, S., Rath, G. K., Rawaf, D. L., Rawaf, S., Reiner, R. C., Renzaho, A. M. N., Rezaei, N., Rezapour, A., Ribeiro, A. I., Ribeiro, D., Ronfani, L., Roro, E. M., Roshandel, G., Rostami, A., Saad, R. S., Sabbagh, P., Sabour, S., Saddik, B., Safiri, S., Sahebkar, A., Salahshoor, M. R., Salehi, F., Salem, H., Salem, M. R., Salimzadeh, H., Salomon, J. A., Samy, A. M., Sanabria, J., Santric Milicevic, M. M., Sartorius, B., Sarveazad, A., Sathian, B., Satpathy, M., Savic, M., Sawhney, M., Sayyah, M., Schneider, I. J. C., Schottker, B., Sekerija, M., Sepanlou, S. G., Sepehrimanesh, M., Seyedmousavi, S., Shaahmadi, F., Shabaninejad, H., Shahbaz, M., Shaikh, M. A., Shamshirian, A., Shamsizadeh, M., Sharafi, H., Sharafi, Z., Sharif, M., Sharifi, A., Sharifi, H., Sharma, R., Sheikh, A., Shirkoohi, R., Shukla, S. R., Si, S., Siabani, S., Silva, D. A. S., Silveira, D. G. A., Singh, A., Singh, J. A., Sisay, S., Sitas, F., Sobngwi, E., Soofi, M., Soriano, J. B., Stathopoulou, V., Sufiyan, M. B., Tabares-Seisdedos, R., Tabuchi, T., Takahashi, K., Tamtaji, O. R., Tarawneh, M. R., Tassew, S. G., Taymoori, P., Tehrani-Banhashemi, A., Temsah, M. H., Temsah, O., Tesfay, B. E., Tesfay, F. H., Teshale, M. Y., Tessema, G. A., Thapa, S., Tlaye, K. G., Topor-Madry, R., Tovani-Palone, M. R., Traini, E., Tran, B. X., Tran, K. B., Tsadik, A. G., Ullah, I., Uthman, O. A., Vacante, M., Vaezi, M., Varona Perez, P., Veisani, Y., Vidale, S., Violante, F. S., Vlassov, V., Vollset, S. E., Vos, T., Vosoughi, K., Vu, G. T., Vujcic, I. S., Wabinga, H., Wachamo, T. M., Wagnew, F. S., Waheed, Y., Weldegebreel, F., Weldesamuel, G. T., Wijeratne, T., Wondafrash, D. Z., Wonde, T. E., Wondmieneh, A. B., Workie, H. M., Yadav, R., Yadegar, A., Yadollahpour, A., Yaseri, M., Yazdi-Feyzabadi, V., Yeshaneh, A., Yimam, M. A., Yimer, E. M., Yisma, E., Yonemoto, N., Younis, M. Z., Yousefi, B., Yousefifard, M., Yu, C., Zabeh, E., Zadnik, V., Moghadam, T. Z., Zaidi, Z., Zamani, M., Zandian, H., Zangeneh, A., Zaki, L., Zendehtdel, K., Zenebe, Z. M., Zewale, T. A., Ziapour, A., Zodpey, S., and Murray, C. J. L. (2019) Global, Regional, and National Cancer Incidence, Mortality, Years of Life Lost, Years Lived With Disability, and Disability-Adjusted Life-Years for 29 Cancer Groups, 1990 to 2017: A Systematic Analysis for the Global Burden of Disease Study. *JAMA Oncol* 5, 1749-1768

30. Simarro, P. P., Cecchi, G., Franco, J. R., Paone, M., Diarra, A., Ruiz-Postigo, J. A., Fevre, E. M., Mattioli, R. C., and Jannin, J. G. (2012) Estimating and mapping the population at risk of sleeping sickness. *PLoS Negl Trop Dis* **6**, e1859
31. WHO. (2018) Neglected Diseases Data Interactive Map. World Health Organization
32. Kennedy, P. G. (2013) Clinical features, diagnosis, and treatment of human African trypanosomiasis (sleeping sickness). *Lancet Neurol* **12**, 186-194
33. Kennedy, P. G. E., and Rodgers, J. (2019) Clinical and Neuropathogenetic Aspects of Human African Trypanosomiasis. *Front Immunol* **10**, 39
34. Kennedy, P. G. (2008) The continuing problem of human African trypanosomiasis (sleeping sickness). *Ann Neurol* **64**, 116-126
35. Greenwood, B. M., and Whittle, H. C. (1980) The pathogenesis of sleeping sickness. *Trans R Soc Trop Med Hyg* **74**, 716-725
36. Buscher, P., Cecchi, G., Jamonneau, V., and Priotto, G. (2017) Human African trypanosomiasis. *Lancet* **390**, 2397-2409
37. Cavalli, A., and Bolognesi, M. L. (2009) Neglected tropical diseases: multi-target-directed ligands in the search for novel lead candidates against *Trypanosoma* and *Leishmania*. *J Med Chem* **52**, 7339-7359
38. Stuart, K., Brun, R., Croft, S., Fairlamb, A., Gurtler, R. E., McKerrow, J., Reed, S., and Tarleton, R. (2008) Kinetoplastids: related protozoan pathogens, different diseases. *J Clin Invest* **118**, 1301-1310
39. Beneke, T., and Gluenz, E. (2019) LeishGEdit: A Method for Rapid Gene Knockout and Tagging Using CRISPR-Cas9. *Methods Mol Biol* **1971**, 189-210
40. Beneke, T., Madden, R., Makin, L., Valli, J., Sunter, J., and Gluenz, E. (2017) A CRISPR Cas9 high-throughput genome editing toolkit for kinetoplastids. *R Soc Open Sci* **4**, 170095
41. Vickerman, K. (1985) Developmental cycles and biology of pathogenic trypanosomes. *Br Med Bull* **41**, 105-114
42. Priest, J. W., and Hajduk, S. L. (1994) Developmental regulation of mitochondrial biogenesis in *Trypanosoma brucei*. *J Bioenerg Biomembr* **26**, 179-191
43. Westermann, B. (2012) Bioenergetic role of mitochondrial fusion and fission. *Biochim Biophys Acta* **1817**, 1833-1838
44. Povelones, M. L., Tiengwe, C., Gluenz, E., Gull, K., Englund, P. T., and Jensen, R. E. (2013) Mitochondrial shape and function in trypanosomes requires the outer membrane protein, TbLOK1. *Mol Microbiol* **87**, 713-729
45. Clarkson, A. B., Jr., Bienen, E. J., Pollakis, G., and Grady, R. W. (1989) Respiration of bloodstream forms of the parasite *Trypanosoma brucei brucei* is dependent on a plant-like alternative oxidase. *J Biol Chem* **264**, 17770-17776
46. Liu, B., Liu, Y., Motyka, S. A., Agbo, E. E., and Englund, P. T. (2005) Fellowship of the rings: the replication of kinetoplast DNA. *Trends Parasitol* **21**, 363-369
47. Shapiro, T. A. (1993) Kinetoplast DNA maxicircles: networks within networks. *Proc Natl Acad Sci U S A* **90**, 7809-7813
48. Woodward, R., and Gull, K. (1990) Timing of nuclear and kinetoplast DNA replication and early morphological events in the cell cycle of *Trypanosoma brucei*. *J Cell Sci* **95** (Pt 1), 49-57
49. Pays, E., Vanhamme, L., and Perez-Morga, D. (2004) Antigenic variation in *Trypanosoma brucei*: facts, challenges and mysteries. *Curr Opin Microbiol* **7**, 369-374

50. Matthews, K. R. (2005) The developmental cell biology of *Trypanosoma brucei*. *J Cell Sci* **118**, 283-290
51. Wallace, F. G. (1902) Flagellate Parasites of Mosquitoes with Special Reference to *Crithidia fasciculata*. *The Journal of Paraistology* **29**, 196-205
52. Olsen, O. W. (1986) *Animal Parasites: Their Life Cycles and Ecology*,
53. Wallace, F. G. (1966) The trypanosomatid parasites of insects and arachnids. *Exp Parasitol* **18**, 124-193
54. Scolaro, E. J., Ames, R. P., and Brittingham, A. (2005) Growth-phase dependent substrate adhesion in *Crithidia fasciculata*. *J Eukaryot Microbiol* **52**, 17-22
55. Brooker, B. E. (1971) Flagellar attachment and detachment of *Crithidia fasciculata* to Milli-pore filters. *Protoplasma* **72**, 19-25
56. DiMaio, J., Ruthel, G., Cannon, J. J., Malfara, M. F., and Povelones, M. L. (2018) The single mitochondrion of the kinetoplastid parasite *Crithidia fasciculata* is a dynamic network. *PLoS One* **13**, e0202711
57. Alcolea, P. J., Alonso, A., Garcia-Tabares, F., Torano, A., and Larraga, V. (2014) An Insight into the proteome of *Crithidia fasciculata* choanomastigotes as a comparative approach to axenic growth, peanut lectin agglutination and differentiation of *Leishmania* spp. promastigotes. *PLoS One* **9**, e113837
58. Filosa, J. N., Berry, C. T., Ruthel, G., Beverley, S. M., Warren, W. C., Tomlinson, C., Myler, P. J., Dudkin, E. A., Povelones, M. L., and Povelones, M. (2019) Dramatic changes in gene expression in different forms of *Crithidia fasciculata* reveal potential mechanisms for insect-specific adhesion in kinetoplastid parasites. *PLoS Negl Trop Dis* **13**, e0007570
59. Guilbride, D. L., and Englund, P. T. (1998) The replication mechanism of kinetoplast DNA networks in several trypanosomatid species. *J Cell Sci* **111 (Pt 6)**, 675-679
60. Schweichel, J. U., and Merker, H. J. (1973) The morphology of various types of cell death in prenatal tissues. *Teratology* **7**, 253-266
61. Dikic, I., and Elazar, Z. (2018) Mechanism and medical implications of mammalian autophagy. *Nat Rev Mol Cell Biol* **19**, 349-364
62. Tsujimoto, Y., and Shimizu, S. (2005) Another way to die: autophagic programmed cell death. *Cell Death Differ* **12 Suppl 2**, 1528-1534
63. Jung, S., Jeong, H., and Yu, S. W. (2020) Autophagy as a decisive process for cell death. *Exp Mol Med* **52**, 921-930
64. Kroemer, G., and Levine, B. (2008) Autophagic cell death: the story of a misnomer. *Nat Rev Mol Cell Biol* **9**, 1004-1010
65. Khandia, R., Dadar, M., Munjal, A., Dhama, K., Karthik, K., Tiwari, R., Yattoo, M. I., Iqbal, H. M. N., Singh, K. P., Joshi, S. K., and Chaicumpa, W. (2019) A Comprehensive Review of Autophagy and Its Various Roles in Infectious, Non-Infectious, and Lifestyle Diseases: Current Knowledge and Prospects for Disease Prevention, Novel Drug Design, and Therapy. *Cells* **8**
66. Yang, Z., and Klionsky, D. J. (2010) Eaten alive: a history of macroautophagy. *Nat Cell Biol* **12**, 814-822
67. Liu, Y., and Levine, B. (2015) Autosis and autophagic cell death: the dark side of autophagy. *Cell Death Differ* **22**, 367-376

68. Klionsky, D. J., Cregg, J. M., Dunn, W. A., Jr., Emr, S. D., Sakai, Y., Sandoval, I. V., Sibirny, A., Subramani, S., Thumm, M., Veenhuis, M., and Ohsumi, Y. (2003) A unified nomenclature for yeast autophagy-related genes. *Dev Cell* **5**, 539-545
69. Xie, Z., and Klionsky, D. J. (2007) Autophagosome formation: core machinery and adaptations. *Nat Cell Biol* **9**, 1102-1109
70. Suzuki, K., Kubota, Y., Sekito, T., and Ohsumi, Y. (2007) Hierarchy of Atg proteins in pre-autophagosomal structure organization. *Genes Cells* **12**, 209-218
71. Mizushima, N., Yoshimori, T., and Ohsumi, Y. (2011) The role of Atg proteins in autophagosome formation. *Annu Rev Cell Dev Biol* **27**, 107-132
72. Feng, Y., He, D., Yao, Z., and Klionsky, D. J. (2014) The machinery of macroautophagy. *Cell Res* **24**, 24-41
73. Degtarev, A., Huang, Z., Boyce, M., Li, Y., Jagtap, P., Mizushima, N., Cuny, G. D., Mitchison, T. J., Moskowitz, M. A., and Yuan, J. (2005) Chemical inhibitor of nonapoptotic cell death with therapeutic potential for ischemic brain injury. *Nat Chem Biol* **1**, 112-119
74. Belizario, J., Vieira-Cordeiro, L., and Enns, S. (2015) Necroptotic Cell Death Signaling and Execution Pathway: Lessons from Knockout Mice. *Mediators Inflamm* **2015**, 128076
75. Dhuriya, Y. K., and Sharma, D. (2018) Necroptosis: a regulated inflammatory mode of cell death. *J Neuroinflammation* **15**, 199
76. Vanden Berghe, T., Vanlangenakker, N., Parthoens, E., Deckers, W., Devos, M., Festjens, N., Guerin, C. J., Brunk, U. T., Declercq, W., and Vandenabeele, P. (2010) Necroptosis, necrosis and secondary necrosis converge on similar cellular disintegration features. *Cell Death Differ* **17**, 922-930
77. Vandenabeele, P., Galluzzi, L., Vanden Berghe, T., and Kroemer, G. (2010) Molecular mechanisms of necroptosis: an ordered cellular explosion. *Nat Rev Mol Cell Biol* **11**, 700-714
78. Micheau, O., and Tschopp, J. (2003) Induction of TNF receptor I-mediated apoptosis via two sequential signaling complexes. *Cell* **114**, 181-190
79. Oberst, A., Dillon, C. P., Weinlich, R., McCormick, L. L., Fitzgerald, P., Pop, C., Hakem, R., Salvesen, G. S., and Green, D. R. (2011) Catalytic activity of the caspase-8-FLIP(L) complex inhibits RIPK3-dependent necrosis. *Nature* **471**, 363-367
80. O'Donnell, M. A., Perez-Jimenez, E., Oberst, A., Ng, A., Massoumi, R., Xavier, R., Green, D. R., and Ting, A. T. (2011) Caspase 8 inhibits programmed necrosis by processing CYLD. *Nat Cell Biol* **13**, 1437-1442
81. Xie, T., Peng, W., Yan, C., Wu, J., Gong, X., and Shi, Y. (2013) Structural insights into RIP3-mediated necroptotic signaling. *Cell Rep* **5**, 70-78
82. Sun, X., Lee, J., Navas, T., Baldwin, D. T., Stewart, T. A., and Dixit, V. M. (1999) RIP3, a novel apoptosis-inducing kinase. *J Biol Chem* **274**, 16871-16875
83. Cai, Z., Jitkaew, S., Zhao, J., Chiang, H. C., Choksi, S., Liu, J., Ward, Y., Wu, L. G., and Liu, Z. G. (2014) Plasma membrane translocation of trimerized MLKL protein is required for TNF-induced necroptosis. *Nat Cell Biol* **16**, 55-65
84. Kroemer, G., Galluzzi, L., and Brenner, C. (2007) Mitochondrial membrane permeabilization in cell death. *Physiol Rev* **87**, 99-163
85. Wang, Z., Jiang, H., Chen, S., Du, F., and Wang, X. (2012) The mitochondrial phosphatase PGAM5 functions at the convergence point of multiple necrotic death pathways. *Cell* **148**, 228-243

86. Los, M., Mozoluk, M., Ferrari, D., Stepczynska, A., Stroh, C., Renz, A., Herceg, Z., Wang, Z. Q., and Schulze-Osthoff, K. (2002) Activation and caspase-mediated inhibition of PARP: a molecular switch between fibroblast necrosis and apoptosis in death receptor signaling. *Mol Biol Cell* **13**, 978-988
87. Yu, S. W., Wang, H., Poitras, M. F., Coombs, C., Bowers, W. J., Federoff, H. J., Poirier, G. G., Dawson, T. M., and Dawson, V. L. (2002) Mediation of poly(ADP-ribose) polymerase-1-dependent cell death by apoptosis-inducing factor. *Science* **297**, 259-263
88. Kraus, W. L. (2008) Transcriptional control by PARP-1: chromatin modulation, enhancer-binding, coregulation, and insulation. *Curr Opin Cell Biol* **20**, 294-302
89. Ke, F. F. S., Vanyai, H. K., Cowan, A. D., Delbridge, A. R. D., Whitehead, L., Grabow, S., Czabotar, P. E., Voss, A. K., and Strasser, A. (2018) Embryogenesis and Adult Life in the Absence of Intrinsic Apoptosis Effectors BAX, BAK, and BOK. *Cell* **173**, 1217-1230 e1217
90. Los, M., Van de Craen, M., Penning, L. C., Schenk, H., Westendorp, M., Baeuerle, P. A., Droge, W., Krammer, P. H., Fiers, W., and Schulze-Osthoff, K. (1995) Requirement of an ICE/CED-3 protease for Fas/APO-1-mediated apoptosis. *Nature* **375**, 81-83
91. Singh, R., Letai, A., and Sarosiek, K. (2019) Regulation of apoptosis in health and disease: the balancing act of BCL-2 family proteins. *Nat Rev Mol Cell Biol* **20**, 175-193
92. Elmore, S. (2007) Apoptosis: a review of programmed cell death. *Toxicol Pathol* **35**, 495-516
93. Aggarwal, V., Tuli, H. S., Varol, A., Thakral, F., Yerer, M. B., Sak, K., Varol, M., Jain, A., Khan, M. A., and Sethi, G. (2019) Role of Reactive Oxygen Species in Cancer Progression: Molecular Mechanisms and Recent Advancements. *Biomolecules* **9**
94. Shamas-Din, A., Kale, J., Leber, B., and Andrews, D. W. (2013) Mechanisms of action of Bcl-2 family proteins. *Cold Spring Harb Perspect Biol* **5**, a008714
95. Yin, X. M., Oltvai, Z. N., and Korsmeyer, S. J. (1994) BH1 and BH2 domains of Bcl-2 are required for inhibition of apoptosis and heterodimerization with Bax. *Nature* **369**, 321-323
96. Miller, D. K. (1997) The role of the Caspase family of cysteine proteases in apoptosis. *Semin Immunol* **9**, 35-49
97. Li, P., Zhou, L., Zhao, T., Liu, X., Zhang, P., Liu, Y., Zheng, X., and Li, Q. (2017) Caspase-9: structure, mechanisms and clinical application. *Oncotarget* **8**, 23996-24008
98. Papenfuss, K., Cordier, S. M., and Walczak, H. (2008) Death receptors as targets for anti-cancer therapy. *J Cell Mol Med* **12**, 2566-2585
99. Zhou, X., Jiang, W., Liu, Z., Liu, S., and Liang, X. (2017) Virus Infection and Death Receptor-Mediated Apoptosis. *Viruses* **9**
100. Brentnall, M., Rodriguez-Menocal, L., De Guevara, R. L., Cepero, E., and Boise, L. H. (2013) Caspase-9, caspase-3 and caspase-7 have distinct roles during intrinsic apoptosis. *BMC Cell Biol* **14**, 32
101. Scaffidi, C., Schmitz, I., Krammer, P. H., and Peter, M. E. (1999) The role of c-FLIP in modulation of CD95-induced apoptosis. *J Biol Chem* **274**, 1541-1548
102. Hitoshi, Y., Lorens, J., Kitada, S. I., Fisher, J., LaBarge, M., Ring, H. Z., Francke, U., Reed, J. C., Kinoshita, S., and Nolan, G. P. (1998) Toso, a cell surface, specific regulator of Fas-induced apoptosis in T cells. *Immunity* **8**, 461-471
103. Dixon, S. J., Lemberg, K. M., Lamprecht, M. R., Skouta, R., Zaitsev, E. M., Gleason, C. E., Patel, D. N., Bauer, A. J., Cantley, A. M., Yang, W. S., Morrison, B., 3rd, and

- Stockwell, B. R. (2012) Ferroptosis: an iron-dependent form of nonapoptotic cell death. *Cell* **149**, 1060-1072
104. Xie, Y., Hou, W., Song, X., Yu, Y., Huang, J., Sun, X., Kang, R., and Tang, D. (2016) Ferroptosis: process and function. *Cell Death Differ* **23**, 369-379
105. Yang, W. S., and Stockwell, B. R. (2008) Synthetic lethal screening identifies compounds activating iron-dependent, nonapoptotic cell death in oncogenic-RAS-harboring cancer cells. *Chem Biol* **15**, 234-245
106. Li, J., Cao, F., Yin, H. L., Huang, Z. J., Lin, Z. T., Mao, N., Sun, B., and Wang, G. (2020) Ferroptosis: past, present and future. *Cell Death Dis* **11**, 88
107. Yu, H., Guo, P., Xie, X., Wang, Y., and Chen, G. (2017) Ferroptosis, a new form of cell death, and its relationships with tumourous diseases. *J Cell Mol Med* **21**, 648-657
108. Han, C., Liu, Y., Dai, R., Ismail, N., Su, W., and Li, B. (2020) Ferroptosis and Its Potential Role in Human Diseases. *Front Pharmacol* **11**, 239
109. Chen, X., Li, J., Kang, R., Klionsky, D. J., and Tang, D. (2021) Ferroptosis: machinery and regulation. *Autophagy* **17**, 2054-2081
110. Sperandio, S., de Belle, I., and Bredesen, D. E. (2000) An alternative, nonapoptotic form of programmed cell death. *Proc Natl Acad Sci U S A* **97**, 14376-14381
111. Maryam Khalili, J. A. R. (2018) Paraptosis. in *Apoptosis and Beyond: The Many Ways Cells Die*, John Wiley & Sons. pp
112. Suzuki, T., and Yamamoto, M. (2017) Stress-sensing mechanisms and the physiological roles of the Keap1-Nrf2 system during cellular stress. *J Biol Chem* **292**, 16817-16824
113. Kobayashi, A., Kang, M. I., Okawa, H., Ohtsuji, M., Zenke, Y., Chiba, T., Igarashi, K., and Yamamoto, M. (2004) Oxidative stress sensor Keap1 functions as an adaptor for Cul3-based E3 ligase to regulate proteasomal degradation of Nrf2. *Mol Cell Biol* **24**, 7130-7139
114. Scaturro, P., and Pichlmair, A. (2018) Oxeiptosis-a cell death pathway to mitigate damage caused by radicals. *Cell Death Differ* **25**, 1191-1193
115. Holze, C., Michaudel, C., Mackowiak, C., Haas, D. A., Benda, C., Hubel, P., Pennemann, F. L., Schnepf, D., Wettmarshausen, J., Braun, M., Leung, D. W., Amarasinghe, G. K., Perocchi, F., Staeheli, P., Ryffel, B., and Pichlmair, A. (2018) Oxeiptosis, a ROS-induced caspase-independent apoptosis-like cell-death pathway. *Nat Immunol* **19**, 130-140
116. Chen, Y., Smith, M. R., Thirumalai, K., and Zychlinsky, A. (1996) A bacterial invasin induces macrophage apoptosis by binding directly to ICE. *EMBO J* **15**, 3853-3860
117. Chen, X., He, W. T., Hu, L., Li, J., Fang, Y., Wang, X., Xu, X., Wang, Z., Huang, K., and Han, J. (2016) Pyroptosis is driven by non-selective gasdermin-D pore and its morphology is different from MLKL channel-mediated necroptosis. *Cell Res* **26**, 1007-1020
118. D'Souza, C. A., and Heitman, J. (2001) Dismantling the Cryptococcus coat. *Trends Microbiol* **9**, 112-113
119. Kurokawa, M., and Kornbluth, S. (2009) Caspases and kinases in a death grip. *Cell* **138**, 838-854
120. Kovacs, S. B., and Miao, E. A. (2017) Gasdermins: Effectors of Pyroptosis. *Trends Cell Biol* **27**, 673-684
121. Liston, A., and Masters, S. L. (2017) Homeostasis-altering molecular processes as mechanisms of inflammasome activation. *Nat Rev Immunol* **17**, 208-214

122. Strowig, T., Henao-Mejia, J., Elinav, E., and Flavell, R. (2012) Inflammasomes in health and disease. *Nature* **481**, 278-286
123. Bergsbaken, T., Fink, S. L., and Cookson, B. T. (2009) Pyroptosis: host cell death and inflammation. *Nat Rev Microbiol* **7**, 99-109
124. Yu, S. Y., and Li, X. L. (2021) Pyroptosis and inflammasomes in obstetrical and gynecological diseases. *Gynecol Endocrinol* **37**, 385-391
125. David, K. K., Andrabi, S. A., Dawson, T. M., and Dawson, V. L. (2009) Parthanatos, a messenger of death. *Front Biosci (Landmark Ed)* **14**, 1116-1128
126. Yu, S. W., Andrabi, S. A., Wang, H., Kim, N. S., Poirier, G. G., Dawson, T. M., and Dawson, V. L. (2006) Apoptosis-inducing factor mediates poly(ADP-ribose) (PAR) polymer-induced cell death. *Proc Natl Acad Sci U S A* **103**, 18314-18319
127. D'Amours, D., Desnoyers, S., D'Silva, I., and Poirier, G. G. (1999) Poly(ADP-ribosylation) reactions in the regulation of nuclear functions. *Biochem J* **342 (Pt 2)**, 249-268
128. Chiarugi, A. (2005) Intrinsic mechanisms of poly(ADP-ribose) neurotoxicity: three hypotheses. *Neurotoxicology* **26**, 847-855
129. Ameisen, J. C., Idziorek, T., Billaut-Mulot, O., Loyens, M., Tissier, J. P., Potentier, A., and Ouaiissi, A. (1995) Apoptosis in a unicellular eukaryote (*Trypanosoma cruzi*): implications for the evolutionary origin and role of programmed cell death in the control of cell proliferation, differentiation and survival. *Cell Death Differ* **2**, 285-300
130. Menna-Barreto, R. F. S. (2019) Cell death pathways in pathogenic trypanosomatids: lessons of (over)kill. *Cell Death Dis* **10**, 93
131. Debrabant, A., Lee, N., Bertholet, S., Duncan, R., and Nakhasi, H. L. (2003) Programmed cell death in trypanosomatids and other unicellular organisms. *Int J Parasitol* **33**, 257-267
132. Das, M., Mukherjee, S. B., and Shaha, C. (2001) Hydrogen peroxide induces apoptosis-like death in *Leishmania donovani* promastigotes. *J Cell Sci* **114**, 2461-2469
133. Duszenko, M., Figarella, K., Macleod, E. T., and Welburn, S. C. (2006) Death of a trypanosome: a selfish altruism. *Trends Parasitol* **22**, 536-542
134. Lee, N., Bertholet, S., Debrabant, A., Muller, J., Duncan, R., and Nakhasi, H. L. (2002) Programmed cell death in the unicellular protozoan parasite *Leishmania*. *Cell Death Differ* **9**, 53-64
135. Sousa, P. L., Souza, R., Tessarolo, L. D., de Menezes, R., Sampaio, T. L., Canuto, J. A., and Martins, A. M. C. (2017) Betulinic acid induces cell death by necrosis in *Trypanosoma cruzi*. *Acta Trop* **174**, 72-75
136. Herman, M., Gillies, S., Michels, P. A., and Rigden, D. J. (2006) Autophagy and related processes in trypanosomatids: insights from genomic and bioinformatic analyses. *Autophagy* **2**, 107-118
137. Benitez, D., Pezaroglo, H., Martinez, V., Casanova, G., Cabrera, G., Galanti, N., Gonzalez, M., and Cerecetto, H. (2012) Study of *Trypanosoma cruzi* epimastigote cell death by NMR-visible mobile lipid analysis. *Parasitology* **139**, 506-515
138. Dos Anjos, D. O., Sobral Alves, E. S., Goncalves, V. T., Fontes, S. S., Nogueira, M. L., Suarez-Fontes, A. M., Neves da Costa, J. B., Rios-Santos, F., and Vannier-Santos, M. A. (2016) Effects of a novel beta-lapachone derivative on *Trypanosoma cruzi*: Parasite death involving apoptosis, autophagy and necrosis. *Int J Parasitol Drugs Drug Resist* **6**, 207-219

139. Piacenza, L., Peluffo, G., and Radi, R. (2001) L-arginine-dependent suppression of apoptosis in *Trypanosoma cruzi*: contribution of the nitric oxide and polyamine pathways. *Proc Natl Acad Sci U S A* **98**, 7301-7306
140. Ouaisi, A. (2003) Apoptosis-like death in trypanosomatids: search for putative pathways and genes involved. *Kinetoplastid Biol Dis* **2**, 5
141. Jimenez, V., Paredes, R., Sosa, M. A., and Galanti, N. (2008) Natural programmed cell death in *T. cruzi* epimastigotes maintained in axenic cultures. *J Cell Biochem* **105**, 688-698
142. Welburn, S. C., and Murphy, N. B. (1998) Prohibitin and RACK homologues are up-regulated in trypanosomes induced to undergo apoptosis and in naturally occurring terminally differentiated forms. *Cell Death Differ* **5**, 615-622
143. Zangger, H., Mottram, J. C., and Fasel, N. (2002) Cell death in *Leishmania* induced by stress and differentiation: programmed cell death or necrosis? *Cell Death Differ* **9**, 1126-1139
144. Bozhkov, P. V., Suarez, M. F., Filonova, L. H., Daniel, G., Zamyatnin, A. A., Jr., Rodriguez-Nieto, S., Zhivotovsky, B., and Smertenko, A. (2005) Cysteine protease mcII-Pa executes programmed cell death during plant embryogenesis. *Proc Natl Acad Sci U S A* **102**, 14463-14468
145. BoseDasgupta, S., Das, B. B., Sengupta, S., Ganguly, A., Roy, A., Dey, S., Tripathi, G., Dinda, B., and Majumder, H. K. (2008) The caspase-independent algorithm of programmed cell death in *Leishmania* induced by baicalein: the role of LdEndoG, LdFEN-1 and LdTatD as a DNA 'degradesome'. *Cell Death Differ* **15**, 1629-1640
146. Pitaluga, A. N., Moreira, M. E., and Traub-Cseko, Y. M. (2015) A putative role for inosine 5' monophosphate dehydrogenase (IMPDH) in *Leishmania amazonensis* programmed cell death. *Exp Parasitol* **149**, 32-38
147. Piacenza, L., Irigoien, F., Alvarez, M. N., Peluffo, G., Taylor, M. C., Kelly, J. M., Wilkinson, S. R., and Radi, R. (2007) Mitochondrial superoxide radicals mediate programmed cell death in *Trypanosoma cruzi*: cytoprotective action of mitochondrial iron superoxide dismutase overexpression. *Biochem J* **403**, 323-334
148. Figarella, K., Uzcategui, N. L., Beck, A., Schoenfeld, C., Kubata, B. K., Lang, F., and Duszenko, M. (2006) Prostaglandin-induced programmed cell death in *Trypanosoma brucei* involves oxidative stress. *Cell Death Differ* **13**, 1802-1814
149. Goldshmidt, H., Matas, D., Kabi, A., Carmi, S., Hope, R., and Michaeli, S. (2010) Persistent ER stress induces the spliced leader RNA silencing pathway (SLS), leading to programmed cell death in *Trypanosoma brucei*. *PLoS Pathog* **6**, e1000731
150. Irigoien, F., Inada, N. M., Fernandes, M. P., Piacenza, L., Gadelha, F. R., Vercesi, A. E., and Radi, R. (2009) Mitochondrial calcium overload triggers complement-dependent superoxide-mediated programmed cell death in *Trypanosoma cruzi*. *Biochem J* **418**, 595-604
151. Mukherjee, S. B., Das, M., Sudhandiran, G., and Shaha, C. (2002) Increase in cytosolic Ca²⁺ levels through the activation of non-selective cation channels induced by oxidative stress causes mitochondrial depolarization leading to apoptosis-like death in *Leishmania donovani* promastigotes. *J Biol Chem* **277**, 24717-24727
152. Finzi, J. K., Chiavegatto, C. W., Corat, K. F., Lopez, J. A., Cabrera, O. G., Mielniczki-Pereira, A. A., Colli, W., Alves, M. J., and Gadelha, F. R. (2004) *Trypanosoma cruzi*

- response to the oxidative stress generated by hydrogen peroxide. *Mol Biochem Parasitol* **133**, 37-43
153. Apweiler, R., Bairoch, A., Wu, C. H., Barker, W. C., Boeckmann, B., Ferro, S., Gasteiger, E., Huang, H., Lopez, R., Magrane, M., Martin, M. J., Natale, D. A., O'Donovan, C., Redaschi, N., and Yeh, L. S. (2004) UniProt: the Universal Protein knowledgebase. *Nucleic Acids Res* **32**, D115-119
 154. Altschul, S. F., Madden, T. L., Schaffer, A. A., Zhang, J., Zhang, Z., Miller, W., and Lipman, D. J. (1997) Gapped BLAST and PSI-BLAST: a new generation of protein database search programs. *Nucleic Acids Res* **25**, 3389-3402
 155. Aslett, M., Aurrecoechea, C., Berriman, M., Brestelli, J., Brunk, B. P., Carrington, M., Depledge, D. P., Fischer, S., Gajria, B., Gao, X., Gardner, M. J., Gingle, A., Grant, G., Harb, O. S., Heiges, M., Hertz-Fowler, C., Houston, R., Innamorato, F., Iodice, J., Kissinger, J. C., Kraemer, E., Li, W., Logan, F. J., Miller, J. A., Mitra, S., Myler, P. J., Nayak, V., Pennington, C., Phan, I., Pinney, D. F., Ramasamy, G., Rogers, M. B., Roos, D. S., Ross, C., Sivam, D., Smith, D. F., Srinivasamoorthy, G., Stoeckert, C. J., Jr., Subramanian, S., Thibodeau, R., Tivey, A., Treatman, C., Velarde, G., and Wang, H. (2010) TriTrypDB: a functional genomic resource for the *Trypanosomatidae*. *Nucleic Acids Res* **38**, D457-462
 156. Rojas-Rivera, D., and Hetz, C. (2015) TMBIM protein family: ancestral regulators of cell death. *Oncogene* **34**, 269-280
 157. Lecoeur, H., Prevost, M. C., and Gougeon, M. L. (2001) Oncosis is associated with exposure of phosphatidylserine residues on the outside layer of the plasma membrane: a reconsideration of the specificity of the annexin V/propidium iodide assay. *Cytometry* **44**, 65-72
 158. Kim, Y. (2010) The effects of nutrient depleted microenvironments and delta-like 1 homologue (DLK1) on apoptosis in neuroblastoma. *Nutr Res Pract* **4**, 455-461
 159. Lema, C., Varela-Ramirez, A., and Aguilera, R. J. (2011) Differential nuclear staining assay for high-throughput screening to identify cytotoxic compounds. *Curr Cell Biochem* **1**, 1-14
 160. Fischer, U., and Schulze-Osthoff, K. (2005) Apoptosis-based therapies and drug targets. *Cell Death Differ* **12 Suppl 1**, 942-961
 161. Vickerman, K., and Tetley, L. (1977) Recent ultrastructural studies on trypanosomes. *Ann Soc Belg Med Trop* **57**, 441-457
 162. Barrett, M. P., Mottram, J. C., and Coombs, G. H. (1999) Recent advances in identifying and validating drug targets in trypanosomes and leishmanias. *Trends Microbiol* **7**, 82-88
 163. Smirlis, D., Duszenko, M., Ruiz, A. J., Scoulica, E., Bastien, P., Fasel, N., and Soteriadou, K. (2010) Targeting essential pathways in trypanosomatids gives insights into protozoan mechanisms of cell death. *Parasit Vectors* **3**, 107
 164. Nguewa, P. A., Fuertes, M. A., Valladares, B., Alonso, C., and Perez, J. M. (2004) Programmed cell death in trypanosomatids: a way to maximize their biological fitness? *Trends Parasitol* **20**, 375-380
 165. Debrabant, A., and Nakhasi, H. (2003) Programmed cell death in trypanosomatids: is it an altruistic mechanism for survival of the fittest? *Kinetoplastid Biol Dis* **2**, 7
 166. Li, F. J., and He, C. Y. (2014) Acidocalcisome is required for autophagy in *Trypanosoma brucei*. *Autophagy* **10**, 1978-1988

167. Li, F. J., and He, C. Y. (2017) Autophagy in protozoan parasites: *Trypanosoma brucei* as a model. *Future Microbiol* **12**, 1337-1340
168. Alvarez, V. E., Kosec, G., Sant'Anna, C., Turk, V., Cazzulo, J. J., and Turk, B. (2008) Autophagy is involved in nutritional stress response and differentiation in *Trypanosoma cruzi*. *J Biol Chem* **283**, 3454-3464
169. Figarella, K., and Uzcategui, N. L. (2014) What's the role of autophagy in trypanosomes? *Microb Cell* **1**, 6-8
170. Li, F. J., Shen, Q., Wang, C., Sun, Y., Yuan, A. Y., and He, C. Y. (2012) A role of autophagy in *Trypanosoma brucei* cell death. *Cell Microbiol* **14**, 1242-1256
171. Williams, R. A., Tetley, L., Mottram, J. C., and Coombs, G. H. (2006) Cysteine peptidases CPA and CPB are vital for autophagy and differentiation in *Leishmania mexicana*. *Mol Microbiol* **61**, 655-674
172. Teuliere, J., Bernard, G., and Baptiste, E. (2020) The Distribution of Genes Associated With Regulated Cell Death Is Decoupled From the Mitochondrial Phenotypes Within Unicellular Eukaryotic Hosts. *Front Cell Dev Biol* **8**, 536389
173. Kaczanowski, S., Sajid, M., and Reece, S. E. (2011) Evolution of apoptosis-like programmed cell death in unicellular protozoan parasites. *Parasit Vectors* **4**, 44
174. Proto, W. R., Coombs, G. H., and Mottram, J. C. (2013) Cell death in parasitic protozoa: regulated or incidental? *Nat Rev Microbiol* **11**, 58-66
175. Fulda, S., Gorman, A. M., Hori, O., and Samali, A. (2010) Cellular stress responses: cell survival and cell death. *Int J Cell Biol* **2010**, 214074
176. Li, L., Tan, H., Zou, Z., Gong, J., Zhou, J., Peng, N., Su, L., Maegele, M., Cai, D., and Gu, Z. (2020) Preventing necroptosis by scavenging ROS production alleviates heat stress-induced intestinal injury. *Int J Hyperthermia* **37**, 517-530
177. Mouratidis, P. X., Rivens, I., and Ter Haar, G. (2015) A study of thermal dose-induced autophagy, apoptosis and necroptosis in colon cancer cells. *Int J Hyperthermia* **31**, 476-488
178. Somero, G. N. (2020) The cellular stress response and temperature: Function, regulation, and evolution. *J Exp Zool A Ecol Integr Physiol* **333**, 379-397
179. Ikwegbue, P. C., Masamba, P., Oyinloye, B. E., and Kappo, A. P. (2017) Roles of Heat Shock Proteins in Apoptosis, Oxidative Stress, Human Inflammatory Diseases, and Cancer. *Pharmaceuticals (Basel)* **11**
180. Kennedy, D., Jager, R., Mosser, D. D., and Samali, A. (2014) Regulation of apoptosis by heat shock proteins. *IUBMB Life* **66**, 327-338
181. Lanneau, D., Brunet, M., Frisan, E., Solary, E., Fontenay, M., and Garrido, C. (2008) Heat shock proteins: essential proteins for apoptosis regulation. *J Cell Mol Med* **12**, 743-761
182. Hombach, A., Ommen, G., MacDonald, A., and Clos, J. (2014) A small heat shock protein is essential for thermotolerance and intracellular survival of *Leishmania donovani*. *J Cell Sci* **127**, 4762-4773
183. Urmenyi, T. P., Silva, R., and Rondinelli, E. (2014) The heat shock proteins of *Trypanosoma cruzi*. *Subcell Biochem* **74**, 119-135
184. Fernandez-Cortes, F., Serafim, T. D., Wilkes, J. M., Jones, N. G., Ritchie, R., McCulloch, R., and Mottram, J. C. (2017) RNAi screening identifies *Trypanosoma brucei* stress response protein kinases required for survival in the mouse. *Sci Rep* **7**, 6156

185. Muller, I. B., Domenicali-Pfister, D., Roditi, I., and Vassella, E. (2002) Stage-specific requirement of a mitogen-activated protein kinase by *Trypanosoma brucei*. *Mol Biol Cell* **13**, 3787-3799
186. Ridgley, E. L., Xiong, Z. H., and Ruben, L. (1999) Reactive oxygen species activate a Ca²⁺-dependent cell death pathway in the unicellular organism *Trypanosoma brucei*. *Biochem J* **340** (Pt 1), 33-40
187. Palmer, G., Horgan, D. J., Tisdale, H., Singer, T. P., and Beinert, H. (1968) Studies on the respiratory chain-linked reduced nicotinamide adenine dinucleotide dehydrogenase. XIV. Location of the sites of inhibition of rotenone, barbiturates, and piericidin by means of electron paramagnetic resonance spectroscopy. *J Biol Chem* **243**, 844-847
188. Li, N., Ragheb, K., Lawler, G., Sturgis, J., Rajwa, B., Melendez, J. A., and Robinson, J. P. (2003) Mitochondrial complex I inhibitor rotenone induces apoptosis through enhancing mitochondrial reactive oxygen species production. *J Biol Chem* **278**, 8516-8525
189. Radad, K., Rausch, W. D., and Gille, G. (2006) Rotenone induces cell death in primary dopaminergic culture by increasing ROS production and inhibiting mitochondrial respiration. *Neurochem Int* **49**, 379-386
190. Fang, J., Wang, Y., and Beattie, D. S. (2001) Isolation and characterization of complex I, rotenone-sensitive NADH: ubiquinone oxidoreductase, from the procyclic forms of *Trypanosoma brucei*. *Eur J Biochem* **268**, 3075-3082
191. Seitaj, B., Maull, F., Zhang, L., Wullner, V., Wolf, C., Schippers, P., La Rovere, R., Distler, U., Tenzer, S., Parys, J. B., Bultynck, G., and Methner, A. (2020) Transmembrane BAX Inhibitor-1 Motif Containing Protein 5 (TMBIM5) Sustains Mitochondrial Structure, Shape, and Function by Impacting the Mitochondrial Protein Synthesis Machinery. *Cells* **9**
192. Varecha, M., Potesilova, M., Matula, P., and Kozubek, M. (2012) Endonuclease G interacts with histone H2B and DNA topoisomerase II alpha during apoptosis. *Mol Cell Biochem* **363**, 301-307
193. Gannavaram, S., Vedvyas, C., and Debrabant, A. (2008) Conservation of the pro-apoptotic nuclease activity of endonuclease G in unicellular trypanosomatid parasites. *J Cell Sci* **121**, 99-109
194. Arnoult, D., Parone, P., Martinou, J. C., Antonsson, B., Estaquier, J., and Ameisen, J. C. (2002) Mitochondrial release of apoptosis-inducing factor occurs downstream of cytochrome c release in response to several proapoptotic stimuli. *J Cell Biol* **159**, 923-929
195. Kraeva, N., Horakova, E., Kostygov, A. Y., Koreny, L., Butenko, A., Yurchenko, V., and Lukes, J. (2017) Catalase in *Leishmaniinae*: With me or against me? *Infect Genet Evol* **50**, 121-127
196. Jockers-Scherubl, M. C., Schirmer, R. H., and Krauth-Siegel, R. L. (1989) Trypanothione reductase from *Trypanosoma cruzi*. Catalytic properties of the enzyme and inhibition studies with trypanocidal compounds. *Eur J Biochem* **180**, 267-272
197. Schlecker, T., Comini, M. A., Melchers, J., Ruppert, T., and Krauth-Siegel, R. L. (2007) Catalytic mechanism of the glutathione peroxidase-type tryparedoxin peroxidase of *Trypanosoma brucei*. *Biochem J* **405**, 445-454
198. Bogacz, M., and Krauth-Siegel, R. L. (2018) Tryparedoxin peroxidase-deficiency commits trypanosomes to ferroptosis-type cell death. *Elife* **7**

199. Garcia-Bermudez, J., and Birsoy, K. (2021) A mitochondrial gatekeeper that helps cells escape death by ferroptosis. *Nature* **593**, 514-515
200. Schlesinger, M., Vilchez Larrea, S. C., Haikarainen, T., Narwal, M., Venkannagari, H., Flawia, M. M., Lehtio, L., and Fernandez Villamil, S. H. (2016) Disrupted ADP-ribose metabolism with nuclear Poly (ADP-ribose) accumulation leads to different cell death pathways in presence of hydrogen peroxide in procyclic *Trypanosoma brucei*. *Parasit Vectors* **9**, 173

APPENDICES

Appendix A

Table 9 Putative homologs identified in trypanosomatid genomes and associated functions defined in other systems

Gene and synonyms	Protein	Function
VPS34	Phosphatidylinositol 3-kinase VPS34	cytoplasm to vacuole transport (Cvt) and VPS34 PI3-kinase complex I autophagy recruits ATG8-phosphatidylinositol conjugate and ATG12-ATG5 conjugate to autophagosomal structure
ATG1 (ULK1)	Serine/threonine-protein kinase ATG1	Cvt, required for formation of autophagosomes nucleophagy, mitophagy, endoplasmic reticulum (ER) degradation
VPS53	Vacuolar protein sorting-associated protein 53	part of the GARP complex involved in retrograde transport from early to late endosomes to the trans-Golgi network
ATG20, CVT20	Autophagy-related protein 20	Cvt, pexophagy, mitophagy survival of cells during severe ER stress
ATG24, SNX4, CVT13	Sorting nexin-4	mitophagy and pexophagy retrieval of late-Golgi SNARES from post-Golgi endosomes for Cvt
ATG3	Autophagy-related protein 3	E2 conjugating enzyme required for Cvt and autophagy, nucleophagy, mitophagy covalent binding activity of phosphatidylethanolamine to Gly of ATG8
ATG4	Cysteine protease ATG4	Cvt and autophagy, nucleophagy, mitophagy cleaves C-terminal AA of ATG8 ATG8-PE deconjugation
ATG7, CVT2	Ubiquitin-like modifier-activating enzyme ATG7	activating enzyme involved in 2 ubiquitin-like systems required for Cvt and autophagy activates ATG12 to conjugate with ATG5 and ATG8 to conjugate with phosphatidylethanolamine
ATG8, CVT5	Autophagy-related protein 8	Cvt and autophagosome formation, nucleophagy, mitophagy mediates delivery of vesicles and autophagosomes
ATG21, CVT21	Autophagy-related protein 21	-Cvt, vesicle formation, mitophagy binding phosphatidylethanolamine to ATG8 and

		recruiting ATG to pre-autophagosomal structure (PAS)
ATG26	Sterol 3-beta-glucotransferase	synthesis of sterol glucoside membrane lipids
ATG9, CVT7	Autophagy-related protein 9	Cvt vesicle formation, mitophagy organization of PAS, recruits ATG23
ATG18, CVT18	Autophagy-related protein 18	proper vacuole morphology osmotically-induced vacuole fragmentation Cvt vesicle formation, pexophagy
VPS15	Serine/threonine-protein kinase VPS15	Cvt and autophagy recruits ATG-phosphatidylinositol and ATG12-ATG5 conjugates to PAS
VPS30, ATG6	Beclin-1-like protein	limits pathogen-associated cell death response and autophagic activity vacuolar protein sorting
TOR1, TOR2	Serine/threonine-protein kinase TOR1, TOR2	regulates multiple cellular processes controlling cell growth in response to nutrients regulates nutrient transport and autophagy
TRAF2	TNF receptor-associated factor 2	regulates activation of NF-kappa-B and JNK and regulates cell survival and apoptosis inhibits necroptosis signaling
TRAF5	TNF receptor-associated factor 5	links TNF receptors to signaling pathways mediates NFkB and JNK inhibits necroptosis and protects from apoptosis
IF2B1, ZBP1	Insulin-like growth factor 2 mRNA-binding protein 1	senses endogenous Z-form nucleic acids and triggers RIPK3-dependend necroptosis
JNK, MAPK8	Mitogen-activated protein kinase 8	stimulated by extracellular cytokines or physical stress to activate the stress-associated/JNK pathway regulates expression of genes and pro- and anti-apoptotic proteins regulates TNF- and TLR's-mediated necroptosis
ERK2, MAPK1	Mitogen-activated protein kinase 1	essential part of MAP kinase signal transduction pathway and MAP/ERK cascade
ERK1, MAPK3	Mitogen-activated protein kinase 3	involved in the activation of necroptosis and the mediating necrostatin-1
P38, MAPK11	Mitogen-activated protein kinase 11	regulates a broad range of cellular processes including proliferation, differentiation, and cell cycle progression

		important modulators of gene expression and inflammatory responses
ZFP36, TTP	mRNA decay activator protein ZFP36	suppresses TNF-alpha by stimulated AU-rich element-mediated TNF-alpha mRNA decay stabilizes RIP1 and promotes ripoptosome assembly
YWHA, 1433	14-3-3 protein	inhibits apoptosis and alleviates cellular stress sequesters BAD and FKHRL1 to cytoplasm
MCA1	Metacaspase-1	mediates cell death triggered by oxygen stress, salt stress, and chronological age cysteine protease that cleaves after arginine or lysine
MCA2	Metacaspase-2	
MCA5	Metacaspase-5	
MCA3	Metacaspase-3	may play a role in cell cycle G1/S transition of parasites
MCA4	Metacaspase-4	plays a role in parasite bloodstream form growth and parasite virulence
ENDO G	Endonuclease G	fragments DNA during apoptosis
PHB	Prohibitin	broad range of cellular functions determined by subcellular localization translocates to mitochondrial or nucleus under apoptotic signals, important part of mitochondrial apoptotic pathway
TMBIM5, GHITM	Growth hormone-inducible transmembrane protein	mitochondrial tubular network and cristae organization apoptotic release of cytochrome c
DLC1, EF1A1	Rho GTPase-activating protein 7	terminates downstream signaling of small GTPases induces mitochondrial apoptosis
PARP	Poly ADP-ribose polymerase 1	mediates parthanatos when over-activated in response to genomic stress synthesizes PAR, causing nuclear translocation of AIF -involved in various functions, namely DNA repair
PARG	Poly ADP-ribose glycohydrolase	regulates PAR after synthesis by PARP
MIF	Macrophage migration inhibitory factor	PARP1-dependent AIF-associated nuclease that cleaves genomic DNA into fragments
GPX4	Phospholipid hydroperoxide glutathione peroxidase	antioxidant peroxidase that reduces phospholipid hydroperoxide protects cells from oxidative damage, required to prevent ferroptosis
FSP1, AIFM2	Ferroptosis suppressor protein 1	NAD(P)H-dependent oxidoreductase involved in oxidative stress response, prevents lipid oxidative damage, suppressing ferroptosis

DHODH, PYRD	Dihydroorotate dehydrogenase	mitochondrial protein associated with the ETC, responsible for regulating bioenergetics, cell proliferation, ROS production, and apoptosis
ACSL4	Long-chain-fatty-acid—CoA ligase 4	catalyzes conversion of long-chain fatty acids to acyl-CoA for synthesis of lipids and degradation via beta-oxidation, essential for ferroptosis execution
SLC7A11 xCT	Cystine/glutamate transporter	imports cystine for glutathione biosynthesis and antioxidant defense
PGAM5	Serine/threonine-protein phosphatase PGAM5	substrate for KEAP1-dependent ubiquitin ligase, forms tri-partite complex with KEAP1 and NRF2 key downstream effector of oxeriptosis pathway -dephosphorylates and activates MAP3K5 kinase
		central mediator for programmed necrosis by TNF, ROS, and calcium ionophore
NLRP3	NACHT, LRR, and PYD domains-containing protein 3	initiates formation of inflammasome polymeric complex in response to damage signals to initiate pyroptosis